Advanced Imaging of Inflammation in Knee Osteoarthritis

Bas de Vries

ISBN 978-94-6361-542-6

Lay-out and printing by Optima Grafische Communicatie (www.ogc.nl)

The author gratefully acknowledges financial support of this thesis by:

- Department of Radiology & Nuclear Medicine, Erasmus MC
- Guerbet
- Masimo

Advanced Imaging of Inflammation in Knee Osteoarthritis

Geavanceerde beeldvorming van inflammatie bij knieartrose

Proefschrift

ter verkrijging van de graad van doctor aan de
Erasmus Universiteit Rotterdam
op gezag van de
rector magnificus

Prof.dr. F.A. van der Duijn Schouten

en volgens besluit van het College voor Promoties.
De openbare verdediging zal plaatsvinden op

dinsdag 25 mei 2021 om 13:00 uur

door

Bastiaan Alexander de Vries
geboren te Haarlem

Erasmus University Rotterdam

Promotiecommissie:

Promotor:	Prof. dr. G.P. Krestin
Overige leden:	Prof. dr. G. Kloppenburg Prof. dr. J.A.N. Verhaar Dr. ir. T. van Walsum
Copromotor:	Dr. E.H.G. Oei

TABLE OF CONTENTS

CHAPTER 1

GENERAL INTRODUCTION

THE KNEE AND ITS ANATOMY

The knee joint is the largest synovial joint of the human body in which the femur and tibia articulate, and allows for flexion, extension, and a small degree of rotation around the vertical axis. These bones are fixated within the joint by muscles, ligaments, and tendons. Each bone end is covered with a layer of cartilage, which is, together with the meniscus, designed to absorb pressure during mechanical loading. The patella is the third bone within the knee joint. Synovial fluid is an important lubricant within the knee capsule, which also provides important nutrients to the cartilage. The synovial fluid is created by the joint's synovial membrane that lines the joint and seals it, together with the fibrous outer membrane, into a joint capsule.[1] Another shock absorber in the knee is the infrapatellar fat pad (IPFP), also known as 'Hoffa's fat pad', an intracapsular, extra-synovial structure in the anterior knee joint and one of several fat pads of the knee.

OSTEOARTHRITIS OF THE KNEE

Epidemiology

Osteoarthritis (OA) is the most prevalent joint disease causing a tremendous burden to patients and society that will further increase in next decades. Current worldwide estimates are that 9.6% of men and 18.0% of women aged over 60 years have symptomatic OA, which is likely to increase by 40% in the following decades.[2,3] OA is associated with ageing and develops progressively over several years.[4] OA was traditionally considered a degenerative disease of articular cartilage, but recent insights show that other processes also play an important role in the pathogenesis of OA. Nowadays, OA is recognized as a whole organ disease involving many joint tissues (Figure 1).[4,5] OA in the knee is characterized by degeneration of articular cartilage, (subchondral) bone deformation, and by osteophytes. In addition to degradation of joint tissues, other processes, in particular synovial inflammation and changes in the subchondral bone, play a crucial role in development of OA.[6]

Clinical presentation, diagnosis and therapy

OA patients typically present with complaints of progressive joint pain and stiffness. According to emerging evidence, this may be a result of synovitis.[7,8] The diagnosis of knee OA is based primarily on the clinical history and physical examination. This clinical assessment is generally unable to detect OA at an early stage, and therefore treatment often is initiated in the late phase of the disease. In most clinical guidelines, imaging is recommended to support the diagnosis.[9,10] The most common method to image OA is radiography, a technique primarily useful to evaluate bones, and not the soft tissues that play an important role in the development of OA. As a result, radiography shows alterations that appear late in the disease

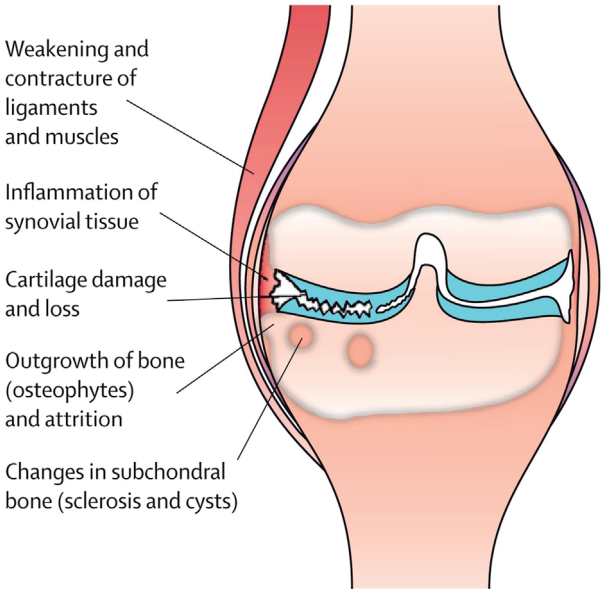

Figure 1: Knee OA as a whole organ disease (from Bijlsma *et al.*[4]).

course. Despite this drawback, radiography is still the gold standard for morphological assessment and staging of knee OA.[9]

Therapies for knee OA are mainly symptomatic and limited to pain control. There is still no disease-modifying medication to control or prevent OA disease progression. Currently, implantation of a knee prosthesis is the only option, when the disease is at an advanced stage. However, much research is performed to find a possible therapy for knee OA.[11–13] Some results are promising, but it is still too early to know how well these therapies work.

INFLAMMATION IN KNEE OA

Synovium

Joint inflammation, characterized by swelling of the synovium and joint effusion, also referred to as 'synovitis', is believed to be a key process and driver of symptoms in as many as in half of the knee OA patients.[14,15] The pathophysiological mechanisms leading to synovial inflammation are complex, but it is known that it plays an important role in the development of OA and the destruction of cartilage.[16–19] Synovitis can already occur in early OA and is clinically indicated by palpable joint swelling due to thickening of the synovium or from the accompanying joint effusion.[20] The synovium is a specialized connective tissue; it lines the inside of synovial joints and seals the synovial cavity and fluid from surrounding tissue. The

normal synovial layer is only 1-2 cells thick.[21] An important function of the synovium, is the supply of nutrients to cartilage through the synovial fluid which is produced by the synovial tissue. As a direct vascular or lymphatic supply to the cartilage is lacking, nutrition from the synovium and the subchondral bone is essential.[22]

Thickening of the richly innervated synovium due to inflammation has been associated with the severity of pain in knee OA.[7,8,23,24] Macrophages in the synovium possibly play an essential role in the cartilage damage via the production of matrix metalloproteinases, which suggests that synovial inflammation may be crucial for cartilage damage.[25]

Subchondral bone

One of the characteristic features of knee OA are subchondral bone changes, also referred to as bone marrow lesions (BMLs).[6] Animal studies have shown that cartilage damage is one of the effects of injury to the subchondral bone, and that subchondral bone injury precedes cartilage changes.[26,27] Changes in subchondral bone could be a marker of altered fluid dynamics, which are thought to affect cytokines excretion that regulate and accelerate bone remodeling and cartilage degeneration.[28] The altered fluid dynamics seems to be associated with inflammation.[29] A recent study in hip OA showed that BMLs detected on magnetic resonance imaging (MRI) are characterized by increased bone turnover and vascularity, which was confirmed by histopathology.[30] Moreover, subchondral bone changes in OA have been recognized as a key factor in the progression of OA and the perception of pain in OA patients.[31–33] Thus, increased tissue vascularity, accompanied by increased remodeling activity due to changes in the subchondral bone seem to act together in the process of OA.

Infrapatellar fat pad

The IPFP has been proposed as possible source of knee pain in patients suffering from OA and from the supposed precursor of knee OA, patellofemoral pain (PFP).[34–40] Changes, e.g. hypertrophy, in the IPFP are thought to be a manifestation of knee inflammation and are therefore classified as Hoffa synovitis on MRI.[40] The IPFP contains nociceptive nerve fibers, which play a possible role in the anterior knee pain in knee OA. These nerve fibers also play a role by inducing an inflammatory response within the knee and can cause vasodilation, which can lead to edema within the IPFP.[37]

IMAGING OF INFLAMMATION IN KNEE OA

As inflammation plays an important role within knee OA, there is increasing interest in imaging of inflammation. Inflamed tissues in the knee can be imaged with a variety of imaging techniques, each with advantages and disadvantages and varying degrees of invasiveness.

Magnetic Resonance Imaging

While radiography only provides an assessment of the bones, MRI can also visualize the soft tissues in and around the knee, such as the fat pads, tendons, muscles, etc.

A limitation of MRI when performed in the most common fashion, i.e. without contrast agent, is that it cannot visualize 'real synovitis'. Instead, only a surrogate measure of synovitis can be obtained, in which the assessment includes both the synovial membrane and the synovial fluid.

However, MRI can visualize synovitis when a contrast agent is administered, also referred to as contrast-enhanced MRI (CE-MRI), which currently is the gold standard for imaging of synovitis (Figure 2).[41] Yet, because of high costs, long scan time and potential health risks associated with the intravenous contrast agent in patients with renal insufficiency and allergies, it is often considered infeasible to implement synovitis imaging with CE-MRI in routine clinical MRI protocols and large clinical research studies.

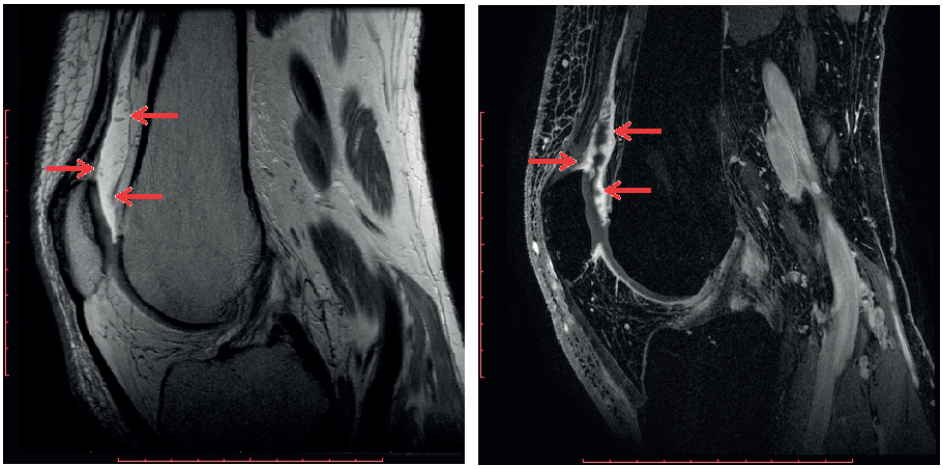

Figure 2: A sagittal MRI section of a T1 weighted MRI (left) and CE-MRI (right). Red arrows indicate location of inflamed synovial membrane.

A promising recent innovation in MRI of synovitis is by means of rapid diffusion weighted imaging with quantitative Dual Echo Steady State (qDESS) MRI without the need for a contrast agent. The qDESS technique can be used to generate images with an unique contrast, because it acquires images with both T1 and T2 weighting.[42]

T2-weighted fat-saturated ($T2_{FS}$) MRI can be used to depict lesions containing fluid, which include changes in subchondral bone and changes in the IPFP associated with knee OA. In subchondral bone marrow, $T2_{FS}$ MRI can be used to depict BMLs as areas of increased signal

intensity. Moreover, multiple studies have emphasized the importance of $T2_{FS}$-hyperintense IPFP regions on MRI, believed to represent inflammation, as a precursor for structural knee OA.[43–47]

While presence of fluid in a specific region in the subchondral bone or IPFP is not completely specific of inflammation, it is known that inflammation is associated with high blood perfusion. Perfusion in knee OA can be visualized and quantified with gadolinium-based dynamic contrast-enhanced MRI (DCE-MRI).[48] Increased blood perfusion, evaluated by DCE-MRI has been considered a surrogate measure of inflammation for a variety of musculoskeletal tissues.[49–54] Therefore, DCE-MRI holds promise to further characterize the role of subchondral bone, BMLs, and the IPFP, in the inflammatory cascade of OA. Pharmacokinetic models using DCE-MRI data enables quantitative measurement of physiological parameters such as blood flow, blood volume, and extravascular permeability. With quantitative DCE-MRI, the amount of contrast enhancement, based on signal intensity over time, is measured in a specific volume of interest. This analysis provides two important quantitative parameters (Figure 3): Ktrans, a measure of capillary permeability and flow into the tissue compartment, and Kep, which describes the rate constant back to the vascular compartment.[55]

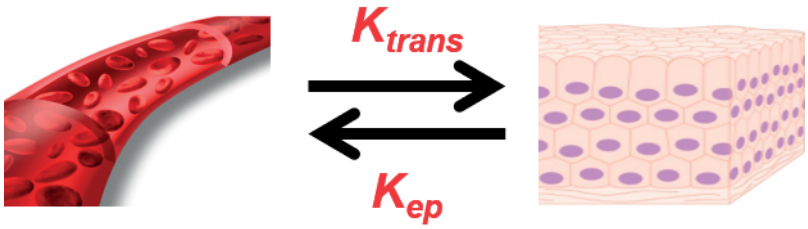

Figure 3: DCE-MRI perfusion parameters measured between vascular and tissue compartment.

Ultrasound

Despite the many advantages of MRI to comprehensively evaluate the osteoarthritic joint especially when no contrast agent is necessary, ultrasound (US) is another option that may be considered to visualize synovitis. Compared to MRI, US is more readily available, more practical, and less costly, reason why US is commonly used in clinical rheumatology practice and established methods have been described to image and grade synovitis with US in patients with rheumatoid arthritis.[56,57] For ultrasound, there is also a promising recent innovation for imaging synovitis, which is by using contrast-enhanced ultrasound (CEUS) with microbubbles, showing a correlation with CE-MRI.[58] A disadvantage of CEUS is that it does not offer a comprehensive joint assessment, but it may be potentially useful to triage

patients requiring more comprehensive joint assessment with MRI. In addition, (CE)US is observer dependent.

AIMS AND OUTLINE OF THIS THESIS

This thesis focuses on imaging methods to study the role of inflammation in knee OA. The aims of this thesis are I) to evaluate disturbed perfusion patterns in subchondral bone and the IPFP using perfusion MRI, and II) to assess new MR and US imaging methods for diagnosis of synovitis in knee OA.

The first part of this thesis focuses on quantitative DCE-MRI perfusion parameters within different tissues of the knee. In **Chapter 2,** perfusion within the subchondral bone in patients with knee OA is described, under the hypothesis that changes in subchondral bone could be a marker of altered fluid dynamics and inflammation. In **Chapter 3**, volume and blood perfusion are studied in the IPFP in healthy controls and patients with patellofemoral pain, a precursor of OA. In **Chapter 4,** the perfusion is studied within small IPFP regions with $T2_{FS}$-hyperintensity, which are believed to represent inflammation, in healthy controls, patients with PFP and OA patients.

The second part of this thesis focuses on diagnostic accuracy of imaging techniques for the visualization of synovitis in the knee, determined in a prospective study of patients with varying degrees of OA, the Diagnostic Imaging for Knee Osteoarthritis (DISKO) study. **Chapter 5** describes both the advantages and the disadvantages of using ultrasound for imaging synovitis in knee OA. In this study, common techniques are used such as gray scale, and power Doppler, but also a less commonly used technique, contrast-enhanced ultrasound. In **Chapter 6,** the implementation of a new MR imaging technique, qDESS for imaging synovitis without contrast agent, is discussed. CE-MRI was compared with qDESS in the diagnostic accuracy of imaging synovitis in knee OA.

The results of this thesis are further discussed and summarized in **Chapter 8 and 9**.

REFERENCES

1. Moore KL, Dalley AF, Agur AM. *Clinically Oriented Anatomy - Sixth Edition*. 6th ed. Lippincott Williams & Wilkins; Wolters Kluwer; 2009.
2. Brooks PM. The burden of musculoskeletal disease--a global perspective. *Clin Rheumatol*. 2006;25(6):778-781. doi:10.1007/s10067-006-0240-3
3. Zhang Y, Jordan JM. Epidemiology of osteoarthritis. *Clin Geriatr Med*. 2010;26(3):355-369. doi:10.1016/j.cger.2010.03.001
4. Bijlsma JWJ, Berenbaum F, Lafeber FPJG. Osteoarthritis: an update with relevance for clinical practice. *Lancet*. 2011;377(9783):2115-2126. doi:10.1016/S0140-6736(11)60243-2
5. Loeser RF, Goldring SR, Scanzello CR, Goldring MB. Osteoarthritis: a disease of the joint as an organ. *Arthritis Rheum*. 2012;64(6):1697-1707. doi:10.1002/art.34453
6. Berenbaum F. Osteoarthritis as an inflammatory disease (osteoarthritis is not osteoarthrosis!). *Osteoarthr Cartil*. 2013;21(1):16-21. doi:S1063-4584(12)01025-4 10.1016/j.joca.2012.11.012
7. Hill CL, Gale DG, Chaisson CE, *et al.* Knee effusions, popliteal cysts, and synovial thickening: association with knee pain in osteoarthritis. *J Rheumatol*. 2001;28(6):1330-1337.
8. Hill CL, Hunter DJ, Niu J, *et al.* Synovitis detected on magnetic resonance imaging and its relation to pain and cartilage loss in knee osteoarthritis. *Ann Rheum Dis*. 2007;66(12):1599-1603. doi:10.1136/ard.2006.067470
9. Zhang W, Doherty M, Peat G, *et al.* EULAR evidence-based recommendations for the diagnosis of knee osteoarthritis. *Ann Rheum Dis*. 2010;69(3):483-489. doi:10.1136/ard.2009.113100
10. Altman R, Asch E, Bloch D, *et al.* Development of criteria for the classification and reporting of osteoarthritis. Classification of osteoarthritis of the knee. Diagnostic and Therapeutic Criteria Committee of the American Rheumatism Association. *Arthritis Rheum*. 1986;29(8):1039-1049. doi:10.1002/art.1780290816
11. Takahashi T, Baboolal TG, Lamb J, Hamilton TW, Pandit HG. Is Knee Joint Distraction a Viable Treatment Option for Knee OA?—A Literature Review and Meta-Analysis. *J Knee Surg*. 2019;32(08):788-795. doi:10.1055/s-0038-1669447
12. Onakpoya IJ, Spencer EA, Perera R, Heneghan CJ. Effectiveness of curcuminoids in the treatment of knee osteoarthritis: a systematic review and meta-analysis of randomized clinical trials. *Int J Rheum Dis*. 2017;20(4):420-433. doi:10.1111/1756-185X.13069
13. Nasb M, Liangjiang H, Gong C, Hong C. Human adipose-derived Mesenchymal stem cells, low-intensity pulsed ultrasound, or their combination for the treatment of knee osteoarthritis: study protocol for a first-in-man randomized controlled trial. *BMC Musculoskelet Disord*. 2020;21(1):33. doi:10.1186/s12891-020-3056-4
14. Sellam J, Berenbaum F. The role of synovitis in pathophysiology and clinical symptoms of osteoarthritis. *Nat Rev Rheumatol*. 2010;6(11):625-635. doi:10.1038/nrrheum.2010.159
15. Rushton MD, Reynard LN, Barter MJ, *et al.* Characterization of the cartilage DNA methylome in knee and hip osteoarthritis. *Arthritis Rheumatol*. 2014;66(9):2450-2460. doi:10.1002/art.38713
16. Hayashi D, Roemer FW, Katur A, *et al.* Imaging of synovitis in osteoarthritis: current status and outlook. *Semin Arthritis Rheum*. 2011;41(2):116-130. doi:10.1016/j.semarthrit.2010.12.003
17. Roemer FW, Zhang Y, Niu J, *et al.* Tibiofemoral joint osteoarthritis: risk factors for MR-depicted fast cartilage loss over a 30-month period in the multicenter osteoarthritis study. *Radiology*. 2009;252(3):772-780. doi:10.1148/radiol.2523082197
18. Loeuille D, Chary-Valckenaere I, Champigneulle J, *et al.* Macroscopic and microscopic features of synovial membrane inflammation in the osteoarthritic knee: correlating magnetic resonance

imaging findings with disease severity. *Arthritis Rheum*. 2005;52(11):3492-3501. doi:10.1002/art.21373

19. Loeuille D, Rat A-C, Goebel J-C, *et al.* Magnetic resonance imaging in osteoarthritis: which method best reflects synovial membrane inflammation? Correlations with clinical, macroscopic and microscopic features. *Osteoarthr Cartil*. 2009;17(9):1186-1192. doi:10.1016/j.joca.2009.03.006
20. Benito MJ, Veale DJ, FitzGerald O, Van Den Berg WB, Bresnihan B. Synovial tissue inflammation in early and late osteoarthritis. *Ann Rheum Dis*. 2005;64(9):1263-1267. doi:10.1136/ard.2004.025270
21. D. Smith M. The Normal Synovium. *Open Rheumatol J*. 2012. doi:10.2174/1874312901105010100
22. Scanzello CR, Goldring SR. The role of synovitis in osteoarthritis pathogenesis. *Bone*. 2012. doi:10.1016/j.bone.2012.02.012
23. Lo GH, McAlindon TE, Niu J, *et al.* Bone marrow lesions and joint effusion are strongly and independently associated with weight-bearing pain in knee osteoarthritis: data from the osteoarthritis initiative. *Osteoarthr Cartil*. 2009;17(12):1562-1569. doi:10.1016/j.joca.2009.06.006
24. de Lange-Brokaar BJE, Ioan-Facsinay A, Yusuf E, *et al.* Association of pain in knee osteoarthritis with distinct patterns of synovitis. *Arthritis Rheumatol*. 2015;67(3):733-740. doi:10.1002/art.38965
25. Blom AB, van Lent PL, Libregts S, *et al.* Crucial role of macrophages in matrix metalloproteinase-mediated cartilage destruction during experimental osteoarthritis: involvement of matrix metalloproteinase 3. *Arthritis Rheum*. 2007;56(1):147-157. doi:10.1002/art.22337
26. Carlson CS, Loeser RF, Jayo MJ, Weaver DS, Adams MR, Jerome CP. Osteoarthritis in cynomolgus macaques: A primate model of naturally occurring disease. *J Orthop Res*. 1994;12(3):331-339. doi:10.1002/jor.1100120305
27. Radin EL, Martin RB, Burr DB, Caterson B, Boyd RD, Goodwin C. Effects of mechanical loading on the tissues of the rabbit knee. *J Orthop Res*. 1984;2(3):221-234. doi:10.1002/jor.1100020303
28. Lee JH, Dyke JP, Ballon D, Ciombor DM, Tung G, Aaron RK. Assessment of bone perfusion with contrast-enhanced magnetic resonance imaging. *Orthop Clin North Am*. 2009;40(2):249-257. doi:10.1016/j.ocl.2008.12.003
29. Scanzello CR, Loeser RF. Editorial: Inflammatory activity in symptomatic knee osteoarthritis: Not all inflammation is local. *Arthritis Rheumatol*. 2015;67(11):2797-2800. doi:10.1002/art.39304
30. Shabestari M, Vik J, Reseland JE, Eriksen EF. Bone marrow lesions in hip osteoarthritis are characterized by increased bone turnover and enhanced angiogenesis. *Osteoarthr Cartil*. 2016;24(10):1745-1752. doi:10.1016/j.joca.2016.05.009
31. Roemer FW, Guermazi A, Javaid MK, *et al.* Change in MRI-detected subchondral bone marrow lesions is associated with cartilage loss: The MOST Study. A longitudinal multicentre study of knee osteoarthritis. *Ann Rheum Dis*. 2009;68(9):1461-1465. doi:10.1136/ard.2008.096834
32. Felson DT, Niu J, Guermazi A, *et al.* Correlation of the development of knee pain with enlarging bone marrow lesions on magnetic resonance imaging. *Arthritis Rheum*. 2007;56(9):2986-2992. doi:10.1002/art.22851
33. Felson DT, McLaughlin S, Goggins J, *et al.* Bone Marrow Edema and Its Relation to Progression of Knee Osteoarthritis. *Ann Intern Med*. 2003;139(5 I). doi:10.7326/0003-4819-139-5_Part_1-200309020-00008
34. Draghi F, Ferrozzi G, Urciuoli L, Bortolotto C, Bianchi S. Hoffa's fat pad abnormalities, knee pain and magnetic resonance imaging in daily practice. *Insights Imaging*. 2016;7(3):373-383. doi:10.1007/s13244-016-0483-8

35. Felson DT. The sources of pain in knee osteoarthritis. *Curr Opin Rheumatol*. 2005;17(5):624-628. doi:10.1097/01.bor.0000172800.49120.97
36. Dye SF. The pathophysiology of patellofemoral pain: a tissue homeostasis perspective. *Clin Orthop Relat Res*. 2005;(436):100-110. doi:10.1097/01.blo.0000172303.74414.7d
37. Clockaerts S, Bastiaansen-Jenniskens YM, Runhaar J, *et al.* The infrapatellar fat pad should be considered as an active osteoarthritic joint tissue: a narrative review. *Osteoarthr Cartil*. 2010;18(7):876-882. doi:10.1016/j.joca.2010.03.014
38. Biedert RM, Sanchis-Alfonso V. Sources of anterior knee pain. *Clin Sports Med*. 2002;21(3):335-347, vii. doi:10.1016/S0278-5919(02)00026-1
39. Ioan-Facsinay A, Kloppenburg M. An emerging player in knee osteoarthritis: the infrapatellar fat pad. *Arthritis Res Ther*. 2013;15(6):225. doi:10.1186/ar4422
40. Hunter DJ, Guermazi A, Lo GH, *et al.* Evolution of semi-quantitative whole joint assessment of knee OA: MOAKS (MRI Osteoarthritis Knee Score). *Osteoarthr Cartil*. 2011;19(8):990-1002. doi:10.1016/j.joca.2011.05.004
41. Loeuille D, Sauliere N, Champigneulle J, Rat AC, Blum A, Chary-Valckenaere I. Comparing non-enhanced and enhanced sequences in the assessment of effusion and synovitis in knee OA: Associations with clinical, macroscopic and microscopic features. *Osteoarthr Cartil*. 2011;19(12):1433-1439. doi:10.1016/j.joca.2011.08.010
42. Staroswiecki E, Granlund KL, Alley MT, Gold GE, Hargreaves BA. Simultaneous estimation of T 2 and apparent diffusion coefficient in human articular cartilage in vivo with a modified three-dimensional double echo steady state (DESS) sequence at 3 T. *Magn Reson Med*. 2012;67(4):1086-1096. doi:10.1002/mrm.23090
43. Atukorala I, Kwoh CK, Guermazi A, *et al.* Synovitis in knee osteoarthritis: A precursor of disease? *Ann Rheum Dis*. 2016;75(2):390-395. doi:10.1136/annrheumdis-2014-205894
44. Han W, Aitken D, Zhu Z, *et al.* Signal intensity alteration in the infrapatellar fat pad at baseline for the prediction of knee symptoms and structure in older adults: a cohort study. *Ann Rheum Dis*. 2016;75(10):1783-1788. doi:10.1136/annrheumdis-2015-208360
45. Ruhdorfer A, Haniel F, Petersohn T, *et al.* Between-group differences in infra-patellar fat pad size and signal in symptomatic and radiographic progression of knee osteoarthritis vs non-progressive controls and healthy knees - data from the FNIH Biomarkers Consortium Study and the Osteoarthritis In. *Osteoarthr Cartil*. 2017;25(7):1114-1121. doi:10.1016/j.joca.2017.02.789
46. Wang K, Ding C, Hannon MJ, *et al.* Signal intensity alteration within infrapatellar fat pad predicts knee replacement within 5 years: data from the Osteoarthritis Initiative. *Osteoarthr Cartil*. 2018;26(10):1345-1350. doi:10.1016/j.joca.2018.05.015
47. Wang K, Ding C, Hannon MJ, Chen Z, Kwoh CK, Hunter DJ. Quantitative Signal Intensity Alteration in Infrapatellar Fat Pad Predicts Incident Radiographic Osteoarthritis: The Osteoarthritis Initiative. *Arthritis Care Res*. 2019;71(1):30-38. doi:10.1002/acr.23577
48. Aaron RK, Racine JR, Voisinet A, Evangelista P, Dyke JP. Subchondral bone circulation in osteoarthritis of the human knee. *Osteoarthr Cartil*. May 2018. doi:10.1016/j.joca.2018.04.003
49. Boesen M, Kubassova O, Bouert R, *et al.* Correlation between computer-aided dynamic gadolinium-enhanced MRI assessment of inflammation and semi-quantitative synovitis and bone marrow oedema scores of the wrist in patients with rheumatoid arthritis--a cohort study. *Rheumatol*. 2012;51(1):134-143. doi:10.1093/rheumatology/ker220
50. Axelsen MB, Stoltenberg M, Poggenborg RP, *et al.* Dynamic gadolinium-enhanced magnetic resonance imaging allows accurate assessment of the synovial inflammatory activity in rheumatoid

arthritis knee joints: a comparison with synovial histology. *Scand J Rheumatol*. 2012;41(2):89-94. doi:10.3109/03009742.2011.608375

51. Boesen M, Kubassova O, Sudol-Szopinska I, *et al.* MR Imaging of Joint Infection and Inflammation with Emphasis on Dynamic Contrast-Enhanced MR Imaging. *PET Clin*. 2018;13(4):523-550. doi:10.1016/j.cpet.2018.05.007
52. Riis RG, Gudbergsen H, Henriksen M, *et al.* Synovitis assessed on static and dynamic contrast-enhanced magnetic resonance imaging and its association with pain in knee osteoarthritis: A cross-sectional study. *Eur J Radiol*. 2016;85(6):1099-1108. doi:10.1016/j.ejrad.2016.03.017
53. Riis RG, Gudbergsen H, Simonsen O, *et al.* The association between histological, macroscopic and magnetic resonance imaging assessed synovitis in end-stage knee osteoarthritis: a cross-sectional study. *Osteoarthr Cartil*. 2017;25(2):272-280. doi:10.1016/j.joca.2016.10.006
54. Ballegaard C, Riis RG, Bliddal H, *et al.* Knee pain and inflammation in the infrapatellar fat pad estimated by conventional and dynamic contrast-enhanced magnetic resonance imaging in obese patients with osteoarthritis: a cross-sectional study. *Osteoarthr Cartil*. 2014;22(7):933-940. doi:10.1016/j.joca.2014.04.018
55. Sourbron SP, Buckley DL. Tracer kinetic modelling in MRI: estimating perfusion and capillary permeability. *Phys Med Biol*. 2012;57(2):R1-33. doi:10.1088/0031-9155/57/2/R1
56. Ohrndorf S, Backhaus M. Musculoskeletal ultrasonography in patients with rheumatoid arthritis. *Nat Rev Rheumatol*. 2013;9(7):433-437. doi:10.1038/nrrheum.2013.73
57. Hartung W, Kellner H, Strunk J, *et al.* Development and evaluation of a novel ultrasound score for large joints in rheumatoid arthritis: One year of experience in daily clinical practice. *Arthritis Care Res*. 2012;64(5):675-682. doi:10.1002/acr.21574
58. Song IH, Burmester GR, Backhaus M, *et al.* Knee osteoarthritis. Efficacy of a new method of contrast-enhanced musculoskeletal ultrasonography in detection of synovitis in patients with knee osteoarthritis in comparison with magnetic resonance imaging. *Ann Rheum Dis*. 2008;67(1):19-25. doi:10.1136/ard.2006.067462

PART I

QUANTITATIVE MRI PERFUSION PARAMETERS WITHIN DIFFERENT TISSUES OF THE KNEE

CHAPTER 2

Quantitative subchondral bone perfusion imaging in knee osteoarthritis using dynamic contrast- enhanced MRI

B.A. de Vries, R.A. van der Heijden, J. Verschueren, P.K. Bos, D.H.J. Poot, J. van Tiel, G. Kotek, G.P. Krestin, E.H.G Oei.

Semin Arthritis Rheum 2020 April; 50(2):177-182

ABSTRACT

INTRODUCTION

Subchondral bone changes, characterized by increased bone turnover and vascularity, are believed to stimulate progression and pain in knee osteoarthritis (OA). The objective of this study was to evaluate the bone perfusion in knee OA using quantitative dynamic contrast-enhanced MRI (DCE-MRI).

METHODS

Unicompartmental knee OA patients were included and underwent 3 Tesla DCE-MRI and T2-weighted MRI. Quantitative DCE-MRI analysis of Ktrans and Kep, representing perfusion parameters, was performed to evaluate differences between the most and least affected knee compartment. First, DCE-MRI parameter differences between epimetaphyseal and subchondral bone in both femur and tibia were assessed. Second, DCE-MRI parameters in subchondral bone marrow lesions (BMLs) were compared to surrounding subchondral bone without BMLs.

RESULTS

Twenty-three patients were analyzed. Median Ktrans and Kep in epimetaphyseal bone were significantly higher ($p<0.05$) in the most affected (Ktrans: 0.014; Kep: 0.054 min^{-1}) compared to least affected (Ktrans: 0.010; Kep: 0.016 min^{-1}) compartment. For subchondral bone, DCE-MRI parameters were significantly higher ($p<0.05$) in the most affected (Ktrans: 0.019; Kep: 0.091 min^{-1}) compared to least affected (Ktrans: 0.014; Kep: 0.058 min^{-1}) compartment as well. Subchondral BMLs detected on fat-saturated T2-weighted images were present in all patients. Median Ktrans (0.091 vs 0.000 min^{-1}) and Kep (0.258 vs 0.000 min^{-1}) were significantly higher within subchondral BMLs compared to surrounding subchondral bone without BMLs ($p<0.001$).

CONCLUSIONS

Increased perfusion parameters in epimetaphyseal bone, subchondral bone and BMLs are observed in unicompartmental knee OA. BMLs likely account for most of the effect of the higher bone perfusion in knee OA.

INTRODUCTION

Osteoarthritis (OA) is the most frequent form of arthritis and has major consequences for the individual patient and public health.[1] Recent insights show that OA is a whole organ disease in which many joint tissues are involved.[2] OA in the knee is characterized by degeneration of articular cartilage, synovial inflammation, and changes in the subchondral bone.[3] Animal studies showed that cartilage damage is one of the effects of injury to the subchondral bone, and that subchondral bone injury precedes cartilage changes.[4,5] Changes in subchondral bone could be a marker of altered fluid dynamics, which are thought to affect the excretion of cytokines that regulate and accelerate bone remodeling and cartilage degeneration.[6] The altered fluid dynamics seems to be associated with inflammation.[7] A recent study in hip OA showed that bone marrow lesions (BMLs) on magnetic resonance imaging (MRI) are characterized by increased bone turnover and vascularity, which was confirmed by histopathology.[8] Moreover, subchondral bone changes in OA have been recognized as a key factor in the progression of OA and the perception of pain in OA patients.[9–11] Increased tissue vascularity, accompanied by increased remodeling activity, due to changes in the subchondral bone are thus characteristic for the process of OA.

Changes in subchondral bone can be visualized using different MRI techniques. For example, T2-weighted fat-saturated MRI can be used to depict fluid containing areas in bone marrow as regions of increased signal intensity, which could indicate a BML. Subchondral bone perfusion in undifferentiated knee OA can also be visualized and quantified with gadolinium-based dynamic contrast-enhanced MRI (DCE-MRI).[12] Therefore, DCE-MRI holds promise to further characterize the role of subchondral bone and BMLs in the process of OA.

DCE-MRI combined with a pharmacokinetic model enables quantitative assessment of microvascular structure and function within a tissue, expressed by DCE-MRI parameters. Various pharmacokinetic compartment models have been described, for example Tofts[13] or Brix[14]. All models aim to estimate physiological parameters such as blood flow, blood volume, and extravascular permeability.[15] Tofts model is widely used and it has recently been demonstrated to be the most accurate model for bone.[16] An important physiological parameter is the volume transfer constant (Ktrans), which is a measure of the volume transfer constant between blood plasma and extracellular extravascular space (EES).[17] Another important parameter is Kep, which is the rate constant from the EES to the vascular component. Together, these two parameters provide robust quantitative outcome parameters of local tissue perfusion.[18]

The goal of this study was to evaluate perfusion in bone of the osteoarthritic knee with quantitative DCE-MRI. To this end, two objectives were defined. The first objective was to compare perfusion in epimetaphyseal and subchondral bone between osteoarthritic and less

osteoarthritic bone in patients with unicompartmental OA. The second objective was to evaluate perfusion in subchondral BMLs in comparison with surrounding bone tissue. Our hypothesis was that in both the osteoarthritic bone and in BMLs the DCE-MRI perfusion parameters are increased.

METHODS

Study population

DCE-MRI data was acquired for a study focusing on the validation of multiple quantitative MRI techniques in OA.[19] Patients aged 18 years or older with unicompartmental (either medial or lateral) knee OA were included from the outpatient clinic of the Department of Orthopedic Surgery of Erasmus University Medical Center Rotterdam. As all patients were suffering from unicompartmental knee OA, perfusion could be compared within the same knee for osteoarthritic bone (affected) and less-affected bone. All patients were scheduled for total knee replacement because of moderate to severe (K&L 3-4) radiographic knee OA according to Kellgren & Lawrence[20]. Patients were excluded in case of varus or valgus deformity in the knee above 10 degrees or chondrocalcinosis. Other exclusion criteria were contra-indications to undergo MRI, pregnancy, lactating women, renal insufficiency and allergy to contrast agents. The study was approved by the institutional review board of Erasmus MC (Rotterdam, The Netherlands), MEC-2012-218. Written informed consent was obtained from all subjects.

Image acquisition

Multisequence MRI was performed on a 3T MR system (Discovery MR750, General Electric Healthcare, Milwaukee, WI, USA) using a dedicated 8-channel knee transmit/receive coil. DCE-MRI was acquired in the sagittal plane, using a fat-suppressed 3D fast spoiled gradient echo (FSPGR) sequence with 35 phases of 10 seconds. Intravenous contrast (0.2 mmol/kg Magnevist (Bayer, Germany)) was administered using a power injector with a rate of 2 ml/s started after the first phase and followed by a saline flush. The field of view (FOV) was 22 x 22 cm, with an in-plane resolution of 0.85 x 1.20 mm and 5 mm slice thickness, a flip angle of 30° and repetition time of 9.3 ms was used. The protocol also included a fat-suppressed sagittal T2-weighted fast spin echo sequence with a FOV of 15 x 15 cm, 3 mm slice thickness, and an in-plane resolution of 0.36 x 0.59 mm. No B1+ field or T1 mapping sequences were included.

Image analysis

Quantitative DCE-MRI analysis was performed using Tofts pharmacokinetic model.[21] Accordingly, the DCE-MRI perfusion parameter maps of Ktrans and Kep were determined using the

DCETool in Horos.[22] The arterial input function (AIF) was determined by a region of interest in the popliteal artery. Ktrans reflects the volume transfer constant into the tissue compartment, while Kep describes the rate constant back into the vascular component.[13]

For the first objective, delineation of the epimetaphyseal and subchondral bone was performed on the DCE scans where the cortical and subchondral bone could be clearly discriminated. Epimetaphyseal bone was defined as the bone reaching from the articular bone surface to the metaphyseal/diaphyseal junction. For the femur and tibia, the bone regions of interest (ROIs) were drawn on three slices of both the most affected and least affected knee compartments, selecting the central slice within both femur condyles, as well as a slice directly medial and lateral of these central slices. This resulted in a total of twelve ROIs per knee for the epimetaphyseal bone. The subchondral bone ROIs were constructed by reducing the epimetaphyseal ROIs to 1 cm from the articular bone surface (Figure 1), again resulting in 12 ROIs. Both the epimetaphyseal and subchondral bone ROIs were divided into two groups, comprising the least and the most affected compartment of the knee. Subsequently, mean perfusion parameters were calculated for each compartment (femur and tibia combined) and also for the femur/tibia within compartment separately, by averaging over the ROIs in three adjacent slices. Epimetaphyseal and subchondral ROIs were delineated using the Horos software package (Horosproject.org, USA).

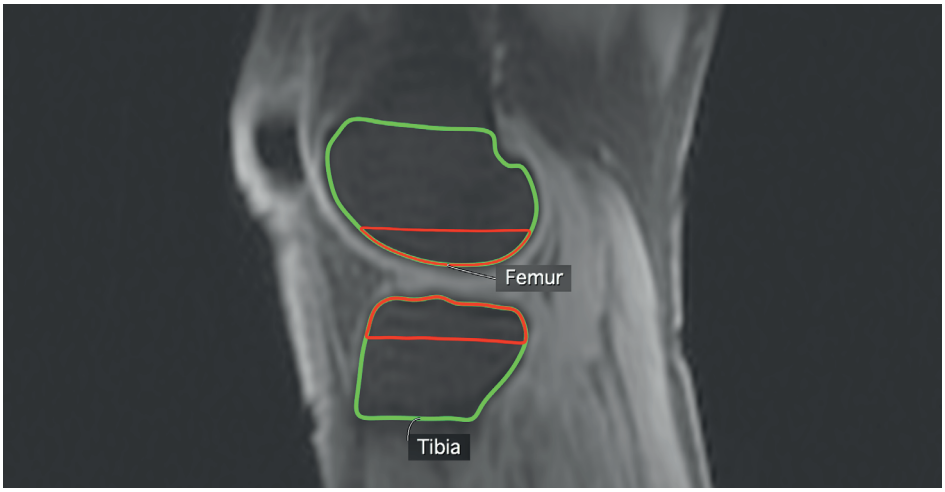

Figure 1: ROIs of epimetaphyseal bone of both femur and tibia (green) and subchondral bone ROI (red).

For the second objective, subchondral BMLs, seen as ill-defined areas of subchondral hyperintensity on fluid-sensitive sequences [23] were delineated on the fat-suppressed T2-weighted images. BMLs exhibit higher signal intensity than the surrounding bone on these T2-weighted acquisitions. Cystic or partially cystic lesions were not considered BMLs in this analysis. The

most clearly visible BML per patient was selected, independent of the most affected OA side. Accordingly, an elliptical shaped ROI was drawn within the maximum margins of the BML using Horos. The location of the BML could be in either the tibia or femur and one BML per patient was selected. For comparison, another ROI was drawn in subchondral bone with normal low signal intensity on the fat-suppressed T2-weighted images. Again, this resulted in two groups, comprising ROIs within BMLs and ROIs in normal bone marrow without BML and mean perfusion values over the ROIs were computed. All ROIs were drawn by a researcher with a technical medical degree and more than 3 years of experience in musculoskeletal imaging research (B.d.V.). Registration between the T2-weighted images and the DCE-scan was performed to propagate the ROIs to the DCE-scan. Analysis was performed using the DCETool in Horos. An example of a T2-image, DCE perfusion map and the fused image are shown in Figure 2. Before the perfusion parameters were calculated, the DCE-MR images were registered over time to correct for patient movement during the DCE-MRI acquisition, using an automated rigid registration tool.[24]

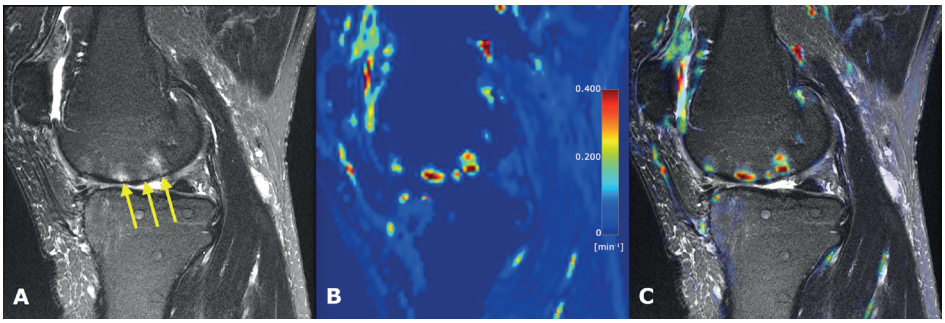

Figure 2: Examples of T2 and DCE-MRI. Sagittal T2-weighted MR image with fat saturation of an osteoarthritic knee showing BMLs in the subchondral bone of the femur (arrows) (A), Ktrans perfusion map of same region shows increased perfusion in the BMLs compared to surrounding bone (B) and T2 and perfusion images fused (C).

Statistical analysis

The image analysis results in mean Ktrans and Kep values for each region in each patient. Subsequently, for each region (femur, tibia or combination of femur and tibia) within each compartment (least affected or most affected) the median Ktrans and Kep over all patients were calculated, as well as the interquartile range (IQR) as a measure of variability. The Shapiro-Wilk test was used to evaluate the normal distribution of Ktrans and Kep. A paired Wilcoxon-signed-rank test was used to compare the Ktrans and Kep values of the most affected with the least affected bone compartment for both the epimetaphyseal and subchondral bone and to compare the Ktrans and Kep values in BML/non-BML. A non-parametric Levene's test was performed to verify the equality of variances in the samples (homogeneity of variance), i.e. to determine whether the variance between the two groups were significantly different

or assumed equal.[25,26] A *p* value of 0.05 was considered statistically significant. Statistical analysis was performed using SPSS v24 (IBM Corp., Armonk, NY, USA).

RESULTS

Twenty-three patients were included between December 2012 and June 2016. Data from all patients was suitable for analysis. The mean age was 63 years and the mean BMI was 29.8. The left knee was affected in 11 patients, and the right knee in 12 patients. For none of the patients a traumatic event as a direct cause of the knee OA was described in the medical records. All patient characteristics are shown in Table 1. Both the Ktrans and Kep values for all measurements showed a non-normal distribution (p value < 0.05).

Table 1: Patient characteristics.

Parameter	Value
No. of patients Males Females	23 8 15
Mean age, y (range)	63 (52 – 73)
Mean BMI (range)	29.8 (21 – 39)
Knee Left Right	 11 12
Most affected compartment Medial Lateral	 19 4
Most affected compartment (K&L grade)	
Grade 0	0
Grade 1	0
Grade 2	4
Grade 3	12
Grade 4	7
Least affected compartment (K&L grade)	
Grade 0	6
Grade 1	13
Grade 2	4
Grade 3	0
Grade 4	0

Table 2 shows the median and IQR values of DCE-MRI perfusion parameters of the most and least affected compartment in both epimetaphyseal and subchondral bone. These perfusion parameters were calculated in both the most affected and least affected compartment within the tibia and the femur and also for the combination of tibia and femur. Tests of the homogeneity of variances using the modified Levene's test did not reveal a violation of this assumption in the analyzed groups. Ktrans reflects the volume transfer constant into the tissue compartment, while Kep describes the rate constant back into the vascular compartment. In short, Ktrans reflects the supply of blood to bone tissue for Kep this is the opposite, i.e. perfusion from bone tissue back into the vasculature.[13] In the epimetaphyseal bone, significant differences ($p<0.05$) were found between the most affected and least affected compartment in the Ktrans values observed in the femur, tibia, and both combined. Also for the Kep values significant differences ($p<0.05$) between the most affected and least affected compartment were found in the tibia and both combined. For the subchondral bone, Kep and Ktrans showed statistically significant differences ($p<0.05$) between the most affected and least affected compartment in the tibia and when combining tibia and femur.

Table 2: DCE-MRI perfusion parameters of the knee bone. *p* values of the difference between least and most affected are reported. *p* values < 0.05 are indicated with *. IQR = interquartile range.

	K_{trans} (min^{-1})			K_{ep} (min^{-1})		
	Median	IQR	*p* value	Median	IQR	*p* value
Epimetaphyseal knee bone						
Femur						
Least affected compartment	0.010	[0.002 – 0.024]	0.013*	0.041	[0.012 – 0.108]	0.059
Most affected compartment	0.012	[0.005 – 0.039]		0.048	[0.020 – 0.163]	
Tibia						
Least affected compartment	0.009	[0.003 – 0.017]	0.018*	0.025	[0.008 – 0.081]	0.001*
Most affected compartment	0.017	[0.006 – 0.054]		0.061	[0.013 – 0.172]	
Femur and Tibia combined						
Least affected compartment	0.010	[0.003 – 0.022]	0.001*	0.016	[0.007 – 0.047]	<0.001*
Most affected compartment	0.014	[0.005 – 0.047]		0.054	[0.016 – 0.165]	
Subchondral knee bone						
Femur						
Least affected compartment	0.007	[0.002 – 0.023]	0.078	0.051	[0.011 – 0.087]	0.346
Most affected compartment	0.013	[0.004 – 0.044]		0.064	[0.019 – 0.200]	
Tibia						
Least affected compartment	0.016	[0.006 – 0.032]	0.045*	0.064	[0.024 – 0.234]	0.039*
Most affected compartment	0.025	[0.007 – 0.102]		0.155	[0.030 – 0.270]	
Femur and Tibia combined						
Least affected compartment	0.014	[0.003 – 0.028]	0.007*	0.058	[0.013 – 0.123]	0.025*
Most affected compartment	0.019	[0.005 – 0.074]		0.091	[0.027 – 0.253]	

Subchondral BMLs detected on fat-saturated T2-weighted images were present in all 23 patients. In total 23 BMLs were selected, one per patient, of which eighteen were located in the most affected compartment and five BMLs were located in the least affected compartment. Variance between subchondral bone with and without a BML was tested equal. Median Ktrans and Kep were significantly (p<0.001) higher within subchondral BMLs (Ktrans 0.091 IQR [0.058-0.158] and Kep 0.258 IQR [0.186-0.651] min^{-1}) compared to surrounding subchondral bone without BMLs (Ktrans 0.000 IQR [0.000-0.001] and Kep 0.000 IQR [0.000-0.004] min^{-1}). Both perfusion parameters, Ktrans and Kep, showed a median value of 0.000 in the normal subchondral bone. The IQR of both parameters was close to zero. Finally, no differences in Ktrans and Kep were observed between different locations of BMLs (tibial and femur, most affected and least affected compartment).

DISCUSSION

In this study, perfusion parameters in bone were measured with quantitative DCE-MRI in knees with unicompartmental knee OA. The most and least affected compartment of the knee, but also areas with and without BMLs, were compared in terms of perfusion parameters. As hypothesized, this study showed that Ktrans and Kep values of both epimetaphyseal and subchondral bone were significantly higher in the most affected compared to the least affect compartment in patients with unicompartmental knee OA. In addition, subchondral BMLs were associated with higher Ktrans and Kep compared to subchondral bone regions without BMLs. Both findings were consistent with our hypothesis.

Budzik *et al.* recently showed that perfusion parameters were higher in OA bone compared to non-OA bone in knee OA.[27] They also showed a positive correlation with the WORMS scoring of BMLs. In their study a model free DCE-MRI analysis method was applied, which only provides a generic AUC measurement, in contrast to the current study in which quantitative parameters based on a pharmacokinetic model were used as the outcome parameters.

Another recent study from Aaron *et al.*[12] studied OA bone perfusion in osteoarthritic bone in the human knee with DCE-MRI. Using in-house built software based on the Brix model, they found that the perfusion in normal and OA subchondral bone is different. Overall, they found a decrease in Kep and time-intensity-curve parameters, which is contrary to our results. Seah *et al.* [28] showed a correlation between the BML grade and Kel, which represents the washout of gadolinium contrast agent. Both studies did not evaluate the volume transfer constant Ktrans because they used the Brix pharmacokinetic model instead of Tofts that was used in our study. An important difference between Brix and Tofts is that in Brix there is no use of an AIF. Therefore the Ktrans parameter, a measure of the volume transfer constant

between blood plasma and extracellular extravascular space, cannot be calculated in Brix, while this is considered an important physiological parameter. In a prior study it has been demonstrated that Tofts renders better results than Brix in bone.[16] In that same study it was recommended to use a groupwise or an subject specific AIF, where we chose for the latter. A fixed AIF was not possible due to the difference of arrival time of the bolus. Since a groupwise AIF method was not available within the DCE Tool, we applied a subject specific method. All AIF curves were individually visually inspected and appeared to capture the bolus peak adequately. Moreover, accurate between-subject comparisons are precluded in the Brix model, which is considered another drawback of this analysis. Another, and possibly most important, difference is that Aaron *et al.* selected only one, mid-coronal, ROI of only the tibial bone in each patient and that no single patient demonstrated a BML in the selected ROI. In our study 12 ROIs per patient were drawn; six in each compartment, divided over tibia and femur. The fact that they found no BMLs is of concern, because it is known that in ~70% [29,30] of radiographic knee OA BMLs are seen. In addition, in our study BMLs were observed in all patients.

Another strength of our study is the inclusion of a homogeneous patient population with unicompartmental knee OA. This enabled the analysis of most affected bone compartment compared to least affected bone compartment within the same joint. As analysis was performed within the same patient, the influence from possible confounders such as BMI was low. In addition, not only the perfusion of small bone regions, but also of the whole epimetaphyseal area was analyzed.

A significant difference in DCE-MRI parameters in a BML compared to subchondral bone was seen, for example the median Ktrans in a BML was 0.091 min^{-1} [0.058-0.158] and 0.000 [0.000-0.001] in subchondral bone ($p<0.001$), even in our sample of one BML selected per patient. We chose to only analyze one BML per patient, although many patients had more than one BML in their knee. The other BMLs visually showed the same increase in perfusion parameters on the whole knee perfusion maps. Since subchondral BMLs were highly associated with increased perfusion parameters compared to subchondral bone regions without BMLs, BMLs likely account for most of the effect of the increased bone perfusion in knee OA. In fact, in bone marrow outside a BML the perfusion was almost unmeasurable in most of the subjects. An example can also be seen in Figure 2. It is thought that this increase in perfusion may be related to inflammation.[31]

As known from previous literature, also encountered in the current study, perfusion in the normal bone is low. Since the proportion of areas in which the perfusion was close to zero exceeded 50%, it was not considered meaningful to use median values within the ROI even

though these perfusion parameters within the ROI itself showed non-normal distribution. We therefore chose to calculate the mean values within the ROI.

For the analysis of the epimetaphyseal and subchondral regions, we did not use registration to register the T2 images to the DCE-MRI. The ROIs could be drawn directly on the DCE-MR images, because the cortical and subchondral bone could be clearly delineated. However, we did perform a rigid registration within these DCE-MR images to overcome patient movement during this dynamic scan.

A limitation of this study is the lack of longitudinal measurements. For this reason it is not possible to evaluate the effects of higher perfusion parameters in (subchondral) bone on the progression of OA. In future research, it would be very interesting to evaluate whether active BMLs with higher perfusion also show higher rates of cartilage degeneration over time in the overlying cartilage layer.

In this study we calculated Kep, which is dependent on the washout of the contrast agent. [21] Since it is possible that the end of the washout phase is not reached due to the duration of the DCE-MRI scan, we reviewed time intensity curves which demonstrated that the maximum contrast agent concentration was reached before the last phase of the DCE-MRI acquisition. Therefore, we believe Kep values to be a valid outcome parameter in our study. No B1+ and T1 correction was possible, as no B1+ or pre-contrast T1 map was acquired. A fixed T1(0) value of 1443 (standard value of the DCE Tool used in Horos) was used instead. Because of the large differences in DCE-MRI parameters observed in this study, particularly for BML versus surrounding bone marrow, we do not expect that these limitations would have changed the outcomes of this study. It is also worth noting that we used a dedicated transmit/receive knee coil with relatively homogeneous B1 field.

At the time of the MR acquisitions, linear gadolinium contrast agents, like gadopentetate dimeglumine, were commonly in use. Since then these have been withdrawn from the EU market and have been replaced by alternatives that carry less risks. As the perfusion kinetics of these alternatives is similar, we expect our results to be relevant for the newer generation contrast agents as well.

In conclusion, an increase in perfusion parameters in the epimetaphyseal bone, the subchondral bone and the BMLs is observed in unicompartmental knee OA. BMLs likely account for most of the effect of the higher bone perfusion in knee OA. This increased perfusion may be related to inflammation and might facilitate the targeted treatment for the inflammatory lesions in osteoarthritic knee bone.

ACKNOWLEDGMENTS

We would like to thank Melek Ekinci, BSc., for assistance in preliminary data analysis.

REFERENCES

1. Dillon CF, Rasch EK, Gu Q, Hirsch R. Prevalence of Knee Osteoarthritis in the United States: Arthritis Data from the Third National Health and Nutrition Examination Survey 1991-94. *J Rheumatol*. 2006;33(11):2271-2279. doi:06/13/1011
2. Loeser RF, Goldring SR, Scanzello CR, Goldring MB. Osteoarthritis: a disease of the joint as an organ. *Arthritis Rheum*. 2012;64(6):1697-1707. doi:10.1002/art.34453
3. Berenbaum F. Osteoarthritis as an inflammatory disease (osteoarthritis is not osteoarthrosis!). *Osteoarthr Cartil*. 2013;21(1):16-21. doi:S1063-4584(12)01025-4 10.1016/j.joca.2012.11.012
4. Carlson CS, Loeser RF, Jayo MJ, Weaver DS, Adams MR, Jerome CP. Osteoarthritis in cynomolgus macaques: A primate model of naturally occurring disease. *J Orthop Res*. 1994;12(3):331-339. doi:10.1002/jor.1100120305
5. Radin EL, Martin RB, Burr DB, Caterson B, Boyd RD, Goodwin C. Effects of mechanical loading on the tissues of the rabbit knee. *J Orthop Res*. 1984;2(3):221-234. doi:10.1002/jor.1100020303
6. Lee JH, Dyke JP, Ballon D, Ciombor DM, Tung G, Aaron RK. Assessment of bone perfusion with contrast-enhanced magnetic resonance imaging. *Orthop Clin North Am*. 2009;40(2):249-257. doi:10.1016/j.ocl.2008.12.003
7. Scanzello CR, Loeser RF. Editorial: Inflammatory activity in symptomatic knee osteoarthritis: Not all inflammation is local. *Arthritis Rheumatol*. 2015;67(11):2797-2800. doi:10.1002/art.39304
8. Shabestari M, Vik J, Reseland JE, Eriksen EF. Bone marrow lesions in hip osteoarthritis are characterized by increased bone turnover and enhanced angiogenesis. *Osteoarthr Cartil*. 2016;24(10):1745-1752. doi:10.1016/j.joca.2016.05.009
9. Roemer FW, Guermazi A, Javaid MK, *et al.* Change in MRI-detected subchondral bone marrow lesions is associated with cartilage loss: The MOST Study. A longitudinal multicentre study of knee osteoarthritis. *Ann Rheum Dis*. 2009;68(9):1461-1465. doi:10.1136/ard.2008.096834
10. Felson DT, Niu J, Guermazi A, *et al.* Correlation of the development of knee pain with enlarging bone marrow lesions on magnetic resonance imaging. *Arthritis Rheum*. 2007;56(9):2986-2992. doi:10.1002/art.22851
11. Felson DT, McLaughlin S, Goggins J, *et al.* Bone Marrow Edema and Its Relation to Progression of Knee Osteoarthritis. *Ann Intern Med*. 2003;139(5 I). doi:10.7326/0003-4819-139-5_Part_1-200309020-00008
12. Aaron RK, Racine JR, Voisinet A, Evangelista P, Dyke JP. Subchondral bone circulation in osteoarthritis of the human knee. *Osteoarthr Cartil*. May 2018. doi:10.1016/j.joca.2018.04.003
13. Tofts PS, Brix G, Buckley DL, *et al.* Estimating kinetic parameters from dynamic contrast-enhanced T(1)-weighted MRI of a diffusable tracer: standardized quantities and symbols. *J Magn Reson Imaging*. 1999;10(3):223-232. doi:10.1002/(sici)1522-2586(199909)10:3<223::aid-jmri2>3.0.co;2-s
14. Brix G, Semmler W, Port R, Schad LR, Layer G, Lorenz WJ. Pharmacokinetic parameters in cns gd-dtpa enhanced mr imaging. *J Comput Assist Tomogr*. 1991;15(4):621-628. doi:10.1097/00004728-199107000-00018
15. Sourbron SP, Buckley DL. Tracer kinetic modelling in MRI: estimating perfusion and capillary permeability. *Phys Med Biol*. 2012;57(2):R1-33. doi:10.1088/0031-9155/57/2/R1
16. Poot DHJ, van der Heijden RA, van Middelkoop M, Oei EHG, Klein S. Dynamic contrast-enhanced MRI of the patellar bone: How to quantify perfusion. *J Magn Reson Imaging*. 2018;47(3):848-858. doi:10.1002/jmri.25817

17. Chikui T, Obara M, Simonetti AW, *et al.* The principal of dynamic contrast enhanced MRI, the method of pharmacokinetic analysis, and its application in the head and neck region. *Int J Dent*. 2012. doi:10.1155/2012/480659
18. Zwick S, Kopp-schneider A. Simulation-based comparison of two approaches frequently used for dynamic contrast-enhanced MRI. 2010:432-442. doi:10.1007/s00330-009-1556-6
19. van Tiel J, Kotek G, Reijman M, *et al.* Is T1ρMapping an Alternative to Delayed Gadolinium-enhanced MR Imaging of Cartilage in the Assessment of Sulphated Glycosaminoglycan Content in Human Osteoarthritic Knees? An in Vivo Validation Study. *Radiology*. 2016;279(2):523-531. doi:10.1148/radiol.2015150693
20. Kellgren JH, Lawrence JS. Radiological assessment of osteo-arthrosis. *Ann Rheum Dis*. 1957;16(4):494-502. doi:10.1136/ard.16.4.494
21. Tofts PS, Kermode AG. Measurement of the blood-brain barrier permeability and leakage space using dynamic MR imaging. 1. Fundamental concepts. *Magn Reson Med*. 1991;17(2):357-367. doi:10.1002/mrm.1910170208
22. K. S. DCE Tool. http://kyungs.bol.ucla.edu/software/DCE_tool/DCE_tool.html. Published 2015. Accessed May 23, 2018.
23. Hunter DJ, Guermazi A, Lo GH, *et al.* Evolution of semi-quantitative whole joint assessment of knee OA: MOAKS (MRI Osteoarthritis Knee Score). *Osteoarthr Cartil*. 2011;19(8):990-1002. doi:10.1016/j.joca.2011.05.004
24. Klein S, Staring M, Murphy K, Viergever M a., Pluim J. Elastix: A Toolbox for Intensity-Based Medical Image Registration. *IEEE Trans Med Imaging*. 2010;29(1):196-205. doi:10.1109/TMI.2009.2035616
25. Nordstokke DW, Zumbo BD. A new nonparametric levene test for equal variances. *Psicologica*. 2010.
26. Nordstokke D, Zumbo B, Cairns SL, Saklofske D. The operating characteristics of the nonparametric Levene test for equal variances with assessment and evaluation data. *Pract Assessment, Res Eval*. 2011;16:1-8.
27. Budzik J-F, Ding J, Norberciak L, *et al.* Perfusion of subchondral bone marrow in knee osteoarthritis: A dynamic contrast-enhanced magnetic resonance imaging preliminary study. *Eur J Radiol*. 2017;88:129-134. doi:10.1016/j.ejrad.2016.12.023
28. Seah S, Wheaton D, Li L, *et al.* The relationship of tibial bone perfusion to pain in knee osteoarthritis. *Osteoarthr Cartil*. 2012;20(12):1527-1533. doi:10.1016/j.joca.2012.08.025
29. Goldsmith GM, Aitken D, Cicuttini FM, *et al.* Osteoarthritis bone marrow lesions at the knee and large artery characteristics. *Osteoarthritis Cartilage*. 2014;22(1):91-94. doi:10.1016/j.joca.2013.10.022
30. Ip S, Sayre EC, Guermazi A, *et al.* Frequency of bone marrow lesions and association with pain severity: Results from a population-based symptomatic knee cohort. *J Rheumatol*. 2011;38(6):1079-1085. doi:10.3899/jrheum.100587
31. Malemud CJ. The Biological Basis of Osteoarthritis : State of the Evidence. *Curr Opin Rheumatol*. 2015;27(3):289-294. doi:10.1097/BOR.0000000000000162

CHAPTER 3

Quantitative volume and dynamic contrast-enhanced MRI derived perfusion of the infrapatellar fat pad in patellofemoral pain

B.A. de Vries*, R.A. van der Heijden*, D.H.J. Poot, M. van Middelkoop, S.M.A. Bierma-Zeinstra, G.P. Krestin, E.H.G Oei.
*shared first authorship

Quant Imaging Med Surg 2021 January; 11(1):133-142.

ABSTRACT

INTRODUCTION

Patellofemoral pain (PFP) is a common knee condition and possible precursor of knee osteoarthritis. Inflammation, leading to an increased perfusion, or increased volume of the infrapatellar fat pad (IPFP) may induce knee pain. The aim of the study was to compare quantitative dynamic contrast-enhanced (DCE)-MRI parameters, as imaging biomarkers of inflammation, and volume of the IPFP between patients with PFP and controls and between patients with and without IPFP edema or joint effusion.

METHODS

Patients with PFP and healthy controls were included and underwent non-fat suppressed 3D fast-spoiled gradient-echo (FSPGR) and DCE-MRI. Image registration was applied to correct for motion. The IPFP was delineated on FSPGR using Horos software. Volume was calculated and quantitative perfusion parameters were extracted by fitting extended Tofts' pharmacokinetic model.

Differences in volume and DCE-MRI parameters between patients and controls were tested by linear regression analyses. IPFP edema and effusion were analyzed identically.

RESULTS

43 controls and 35 PFP patients were included. Mean (SD) IPFP volume was 26.04 (4.18) ml in control subjects and 27.52 (5.37) ml in patients. Median Ktrans was 0.0017 (0.0016) min^{-1} in control subjects and 0.0016 (0.0020) min^{-1} in patients. None of the differences in volume and perfusion parameters were statistically significant. Knees with effusion showed a higher perfusion of the IPFP compared to knees without effusion in patients only.

CONCLUSIONS

The IPFP has been implicated as source of knee pain, but higher DCE-MR blood perfusion, an imaging biomarker of inflammation, and larger volume are not associated with PFP. Patients' knees with effusion showed a higher perfusion, pointing towards inflammation.

INTRODUCTION

Patellofemoral pain (PFP) is a common knee disorder in active young individuals comprising pain in and around the kneecap. Symptoms commonly occur during knee loading activities, such as running and stair climbing, and during sitting with the knees bent.[1] Despite of a variety of treatment options, such as exercise therapy, patellar taping/bracing and foot orthoses, a large group of patients with persistent complaints remains.[2-5] PFP has been implicated as precursor of knee osteoarthritis (OA), but the exact pathophysiology remains unknown.[6-8]

Pathophysiologic processes of the infrapatellar fat pad (IPFP), also known as 'Hoffa's fat pad', have been proposed as a possible source of knee pain.[9-13] The IPFP is a richly innervated, highly vascularized, intracapsular, extra-synovial structure in the anterior knee joint between the patella and femur, where it plays a biomechanical role.[12,14-16] Structural changes of the IPFP, for example focal IPFP edema as sign of inflammation, have been pinpointed as precursor for structural knee OA, and a larger IPFP size was found in patients with patellofemoral OA.[17-19] IPFP size could increase as a result of low-grade inflammation due to repetitive mechanical overload, as for example in Hoffa disease[20] or, hypothetically, can also be larger to begin with and predispose to pain without any pathophysiologic cause. In a PFP population no differences in the presence of focal edema of the IPFP between healthy control subjects and patients with PFP was demonstrated[21]. IPFP size has been studied in OA[17,22], but has not been studied in PFP yet. Besides the biomechanical role, it is also suggested that the IPFP is an osteoarthritic joint tissue capable of modulating inflammatory responses in knee OA.[11] This might also apply to PFP.

Dynamic contrast-enhanced magnetic resonance imaging (DCE)-MRI enables non-invasive evaluation of inflammation by measuring blood perfusion, which is known to increase in the presence of inflammation. DCE-MRI derived increased blood perfusion parameters are therefore considered imaging biomarkers of inflammation in various musculoskeletal tissues.[23-28] To our knowledge, only one prior study applied semi-quantitative DCE-MRI in the IPFP of obese patients with knee OA and showed a correlation between knee pain and inflammation.[28] In a previous study including the same study population as the current study, quantitative DCE-MRI analysis of the patella identified an increased patellar perfusion, contrary to the decreased patellar perfusion based on vascular alterations that was expected.[29] Among the potential explanations of increased perfusion is the occurrence of an inflammatory process in which the IPFP plays an important modulating role.[12]

Therefore, the aim of this study was to compare quantitative DCE-MRI blood perfusion parameters, as imaging biomarkers of inflammation, and volume of the IPFP between patients with PFP and healthy control subjects. A second aim was to explore if specific perfusion

patterns exist in patients based on correlation of DCE-MRI perfusion parameters with clinical or MR imaging characteristics that potentially are related to inflammation or perfusion. Hypothetically, a larger IPFP volume and higher blood perfusion values are expected in patients with PFP than in healthy control subjects.

METHODS

Study population

In the current study, data was analyzed from a previously conducted cross sectional case-control study. Patients with minimum symptom duration of two months to a maximum of two years and healthy control subjects were included between January 2013 and September 2014. Patients who visited their general practitioner, physiotherapist or sports physician were included if diagnosed with PFP based on the presence of at least three of the following symptoms: pain while stair climbing; while squatting; while running; while cycling; while sitting for a prolonged period with the knee flexed, or crepitus. Exclusion criteria were: previous PFP episodes more than two years ago, onset after trauma, defined pathological condition of the affected knee at present, or previous surgery or injury of the affected knee. Healthy controls were recruited from patients' sports team members, friends, or colleagues. Exclusion criteria of controls were: history of PFP, surgery or injury of both knees, or first degree relatedness with patients. Other exclusion criteria for both groups were: contra-indications for contrast-enhanced MRI and insufficient knowledge of the Dutch language. Patients and controls were aimed to match for age, gender, body mass index (BMI), and activity level. Full details of this study haven been published elsewhere.[30] This study was approved by our institutional review board, is conducted in accordance with the Helsinki Declaration and written informed consent was obtained from all participants. All patients and controls, aged 18-40 years, with DCE-MRI data available were included in the current analysis.

Image acquisition

Participants underwent 3 Tesla MRI (Discovery MR750, GE Healthcare, USA) using a dedicated 8-channel knee coil (Invivo Inc., USA) at our institution. One knee, the (most) symptomatic knee of PFP patients was selected, or randomly chosen if both knees were equally painful or if both were asymptomatic (controls). The MRI protocol consisted of routine clinical proton density and T2-weighted fat-saturated sequences in three orthogonal planes, and a sagittal 3D spoiled non-fat-saturated fast-spoiled gradient-echo (non-FS FSPGR) sequence with a slice thickness of 0.5 mm.

DCE-MRI was acquired by a time-resolved imaging of contrast kinetics (TRICKS) sequence with anterior-posterior (AP) frequency encoding direction to avoid pulsation artifacts of the

popliteal artery into the region of interest. MRI parameters were: in-plane pixel resolution 1.5 mm, slice thickness 5 mm, field of view 380 × 380 × 70mm, acquisition matrix 256 × 128, 14 sagittal slices, 70% sampling in the phase direction, TE = 1.7 ms, TR = 9.3 ms, FA = 30°. The DCE-MRI protocol consisted of 35 phases of 10.30s ± 0.07s (constant within subject). Intravenous contrast administration of 0.2mmol/kg gadopentetate dimeglumine (Magnevist, Bayer, Berlin, Germany), at a rate of 2ml/s, was started after the first phase. Additionally, a non-fat-suppressed 3D FSPGR sequence with in-plane resolution of 0.3 mm × 0.3 mm and 0.5 mm slices was acquired before contrast administration for delineation of the patellar bone marrow.

In addition, participants completed a questionnaire on demographics, sports participation (yes/no) and knee complaints (Numerical rating score (NRS) pain score during rest and exercise, duration of symptoms, and function measured by the Anterior Knee Pain Scale (AKPS) 0-100[31]). Finally, a physical examination was performed in which the pressure pain threshold at the contralateral arm was tested as a measure of pain sensitization, according to a prior published method.[32,33]

Image analysis

IPFP edema located centrally and superolaterally and joint effusion were already assessed as part of the Magnetic Resonance Imaging Osteoarthritis Knee Score (MOAKS) with several additional scoring items in a prior study.[21,34]

The volume of interest (VOI) consisted of the whole IPFP with the following boundaries according to a recent study: the inferior patellar pole, femoral intercondylar notch, proximal patellar tendon, intermeniscal ligament, both menisci and the anterior tibia.[15] VOIs were delineated in correspondence with the DCE-MRI data on the non-FS FSPGR sequence, which has previously been reported to be superior to fat-saturated images (Figure 1).[35] All VOIs were drawn by a senior radiology resident subspecializing in musculoskeletal imaging (RH) after careful consideration of the boundaries in the first 10 subjects together with a senior musculoskeletal radiologist (EO). DCE-MRI time points were registered using an automated rigid body registration with Elastix.[36] Horos software (Horosproject.org, USA) was used to delineate the VOIs, register the non-FS FSPGR and DCE-maps, calculate the 3D volume and extract the perfusion parameters of the VOI with the DCE-tool.[37] Fitting a pharmacokinetic model to the data enables extraction of quantitative DCE-MRI parameters which (to a greater or lesser extent) reflect physiological phenomena such as blood flow, blood volume, and extravascular permeability.[38] Tofts' pharmacokinetic model has shown to be the most accurate model for patellar bone.[39] Tofts' extended model is more suitable for highly vascularized structures, such as the IPFP, by adding the vascular term Vp.[38] The arterial input function (AIF) was estimated in each participant using a ROI in the popliteal artery. All fitted AIF's were visually checked.

Quantitative DCE-MRI perfusion parameters Ktrans, Kep, Ve and Vp) were extracted by fitting the Tofts' extended pharmacokinetic model (Figure 2).[40] Ktrans reflects the volume transfer constant into the tissue compartment, Kep describes the rate constant back into the vascular component, Ve the extravascular extracellular space and Vp the vascular fraction.

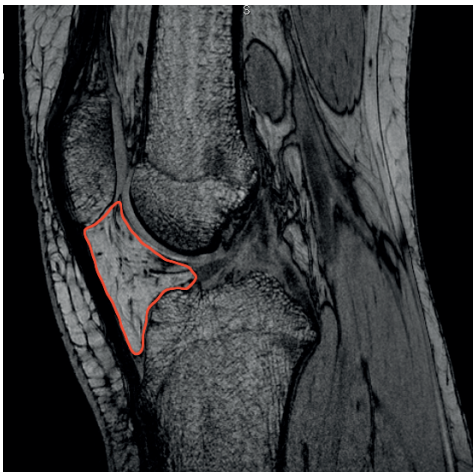

Figure 1: Delineation of the infrapatellar fat pad on the non-FS FSPGR sequence (red line).

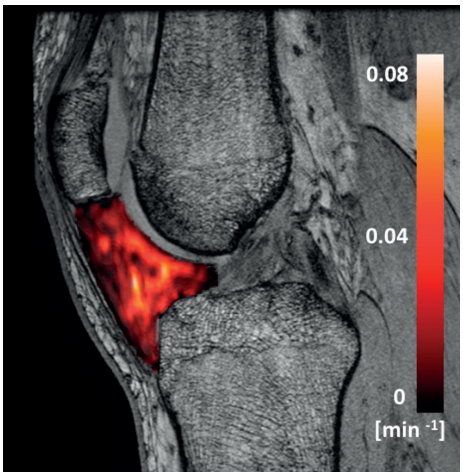

Figure 2: Overlay of a Ktrans map of the IPFP on the non-FS FSPGR sequence in a PFP patient.

Statistical analysis

The Shapiro-Wilk test was used to evaluate normality of the distribution of the parameters. Independent sample T-tests and chi-square tests, or Mann-Whitney U tests if data distribution was not normal, were applied to investigate differences in baseline characteristics between groups.

The DCE image analysis resulted in a mean value for the perfusion parameters within each VOI. The mean and standard deviation over all subjects were calculated for control subjects and PFP patients separately. Differences in variance of volume and perfusion parameters across subjects were tested with Levene's test. Volume followed a normal distribution. All perfusion parameters showed a normal distribution of residuals after logarithmic transformation and, accordingly, regression analyses could be performed. Differences in volume and perfusion parameters between groups were compared by linear regression analyses, adjusted for age, gender, BMI, and sports participation. Furthermore, possible patient subgroups were explored by multivariate linear regression analysis of the following variables: pain during rest and during exercise, duration of complaints, presence of sitting pain, function, pain pressure threshold contralateral arm as sensitization measure, presence of infrapatellar fat pad edema centrally and superolaterally and joint effusion. p values < 0.05 were considered to be statistically significant for the main linear regression analyses. Results are presented as mean differences with 95% confidence intervals. For the subgroup' analyses, a lower p value

of < 0.01 was applied due to multiple testing. All analyses were performed with SPSS v25 (IBM Corp., Armonk, NY, USA).

RESULTS

Population and patient characteristics

In a prior study 64 patients with PFP and 70 control subjects aged 14-40 years were included (Figure 3). DCE-MRI was only acquired in adults and image quality was sufficient in 35 adults PFP patients and 44 adult control subjects. Mean age was 26.1 (range 18-40, SD 5.0) years, mean BMI was 24.1 (SD 3.4) kg/m^2 and 49% (39) was female. The BMI was significantly higher in the patient group (Table 1). Patients reported a mean duration of complaints of 11.2 months and 45.7% (16) reported bilateral pain. Centrally located moderate to severe IPFP edema was present in 1 patient and 2 control subjects. Superolateral IPFP edema was present in 16 patients and 19 control subjects. Medium to large effusion (corresponding with MOAKS grade 2-3) was present in 4 patients and 7 control subjects. There were no significant differences in the presence of these features.

Table 1: Characteristics of study participants.

Characteristics	**Patients (n=35)**	**Controls (n=44)**	***p* value**
Female gender, n (%)	18 (51.4)	21 (47.7)	0.74
Age (years), mean (SD)	26.4 (5.6)	25.9 (4.6)	0.53
BMI (kg/m^2), mean (SD)	25.1 (3.8)	23.3 (2.8)	0.01
Sports participants, n (%)			
During inclusion	24 (68.6)	34 (77.3)	0.39
Before onset of pain	32 (91.4)	NA	NA
Pain (NRS), mean (SD)			
During rest	3.9 (2.7)	NA	NA
During strain	6.3 (2.4)	NA	NA
Duration of complaints, mean (SD)	11.2 (6.3)	NA	NA
Bilateral pain, n (%)	16 (45.7)	NA	NA
Sitting pain, n (%)	27 (77.1)	NA	NA
AKP function score, mean (SD)	68.6 (11.0)	NA	NA
Pain pressure threshold arm, mean (SD)	50.3 (13.8)	56.1 (14.3)	0.07
IPFP edema central (moderate to severe), n (%)	1 (2.9)	2 (4.5)	0.59
IPFP edema superolateral, n (%)	16 (45.7)	19 (43,2)	0.50
Effusion (medium to large), n (%)	4 (11.4)	7 (15.9)	0.50

BMI, body mass index; NRS, Numerical Rating Score; AKP, Anterior Knee Pain; IPFP, infrapatellar fat pad.

Volume and DCE-MRI parameters

Due to a lack of a plateau phase in the time intensity curve, the fitting algorithm might not provide valid values of Ve and subsequently Kep and therefore those parameters were not shown.

Mean IPFP volume was 26.04 (SD 4.18) ml in control subjects and 27.52 (5.37) ml in patients. Median Ktrans was 0.0017 (0.0016) min^{-1} in control subjects and 0.0016 (0.0020) min^{-1} in patients. Median Vp was remarkably higher in patients than control subjects, respectively 0.00037 (0.00039) and 0.00029 (0.00033), but this difference was not statistically significant (p=0.10). Mean volume and perfusion parameters did not differ between groups (Table 2, Figure 3).

Table 2: Mean and (SD) of the volume and median and (IQR) of the VOI mean for Ktrans and Vp and mean difference (95% CI) and adjusted p value in patients and controls.

Measures	Patients (n=35)	Controls (n=44)	Mean difference (95% CI)	Adjusted p value
Volume (mL)	27.52 (5.37)	26.04 (4.18)	1.48 (–0.66, 3.62)	0.07
Ktrans (min^{-1})	0.0016 (0.0020)	0.0017 (0.0016)	–1.12 (–13.47, 11.21)	0.98
Vp	0.00037 (0.00039)	0.00029 (0.00033)	1.10 (–0.65, 2.85)	0.10

VOI, volume of interest.

Vp was the only perfusion parameter for which Levene's test showed a significant difference in variance across groups (p=0.035). Further visual inspection of the boxplots showed two outliers in the patient group, which most likely account for the difference in variance (Figure S1: boxplot without the largest patient outlier).

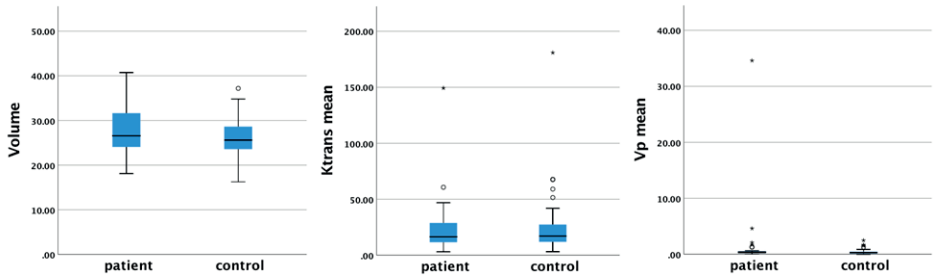

Figure 3: Boxplots of volume (ml) and perfusion parameters Ktrans (min^{-1}) and Vp (multiplied by 1000). The * indicates the outliers.

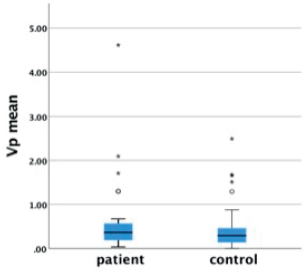

Figure S1: Boxplot of Vp mean (multiplied by 1000) with exclusion of the biggest patient outlier.

The patient subgroup analyses showed that presence of joint effusion was significantly associated with elevated Ktrans (p=0.002) and Vp (p=0.004), but not with volume (p=0.41). Remarkably, this association was not present in control subjects. None of the other subgroup analyses revealed significant associations for respectively volume/Ktrans/Vp: pain during rest p=0.76/0.74/0.31; during exercise p=0.07/0.25/0.51; duration of complaints p=0.78/0.30/0.14; presence of sitting pain p=0.29/0.23/0.24; function p=0.57/0.88/0.48; pain pressure threshold contralateral arm as sensitization measure p=0.82/0.54/0.27, presence of infrapatellar fat pad edema centrally p=0.11/0.44/0.56; presence of infrapatellar fat pad edema superolaterally p=0.82/0.75/0.54.

DISCUSSION

In this study, volume and quantitative DCE-MRI blood perfusion parameters Ktrans and Vp of the infrapatellar fat pad were compared between healthy control subjects and patients with patellofemoral pain. In contrast to our hypothesis, no significant differences were found in volume or DCE-MR blood perfusion parameters, as imaging biomarkers of inflammation, of the IPFP between healthy control subjects and patients with PFP. Furthermore, patient subgroups were explored in search of an association of DCE-MRI parameters with clinical characteristics and MR features potentially related to volume or perfusion/inflammation. Only effusion was significantly associated with higher Ktrans and Vp in patients with PFP.

In recent studies, inconsistent results were found in OA populations regarding IPFP volume. One study found an association between a larger volume and fewer structural abnormalities in patients with clinical knee OA, suggesting a protective role of a larger IPFP.[41] Two other studies did not find a correlation between IPFP volume and symptomatic or radiographic knee OA.[17,42] A fourth study, specifically focusing on patellofemoral osteoarthritis (PFOA), demonstrated that individuals with PFOA had a larger IPFP than controls, and a larger IPFP volume was directly related to pain.[43] Since age presumably influences fat pad volume in

patient with OA, the current volumes cannot be directly compared with the prior study including an older population of patients with PF OA.[44]

The single prior study that applied DCE-MRI, in a semi-quantitative manner, to investigate IPFP inflammation found a relation between their perfusion derived inflammation marker and knee pain in obese patients with knee OA.[28] DCE-MRI had not yet been applied in the IPFP of patients with PFP and healthy control subjects.

The lack of a difference between patients with PFP and control subjects might be explained by a still preserved tissue homeostasis in PFP without induced inflammatory response. In order to determine if a certain patient subgroup with explicit inflammation could be identified, additional exploratory subgroup analyses were conducted focusing on clinical characteristics and MR features potentially related inflammation. For instance, a larger size and higher perfusion of the IPFP could be expected in patients with other proposed signs of inflammation, such as Hoffa edema or effusion. Furthermore, we hypothesized that low-grade inflammation resulting in higher perfusion and/or increased volume would be associated with more pain and worse function or would have a more systemic effect resulting in longer symptom duration or presence of sensitization. Finally, an increase in size or vascular changes could also have been the answer to the enigma of patients with PFP, which explicitly exhibit pain during sitting with the knees bent.[29,45,46] In the end, none of these variables were significantly associated with volume or perfusion parameters besides effusion. Effusion was significantly associated with Ktrans and Vp, indicating a larger vascular fraction and more blood inflow in patients. Further evaluation revealed that these associations were not present in control subjects.

This implies that joint effusion is only associated with inflammation and neovascularization in patients with PFP. These results are only speculative, though, due to the low number of subjects per group. A potential explanation for the difference between groups might lie in a different mechanism of effusion, implying an inflammatory pathway in patients only. In control subjects one possible explanation might be a mechanical pathway.

In this study, for the first time, the IPFP volume and IPFP blood perfusion were quantitatively analyzed by DCE-MRI in order to unravel the role of the IPFP in the pathophysiology of PFP. A strength of this study is the inclusion of healthy control subjects next to patients with PFP. Furthermore, the current study applied quantitative assessment of DCE-MRI perfusion values, which offers more robust parameters that directly represent the microvasculature physiology, in contrast to semi-quantitative analysis.

A potential limitation might be the lack of B1+ or pre-contrast T1 map, which led to the use of a literature based fixed T1(0) value of 1443 ms. We do not expect this to have affected the outcome, since no differences in native T1 variability were expected between groups. Furthermore, a dedicated transmit/receive knee coil with relatively homogeneous B1 field was used. Second, quality of DCE-MRI imaging data was not sufficient in 9 patients and 6 control subjects due to artifacts at the beginning of the study. We do not expect this to have influenced our conclusions, as the baseline characteristics of these participants did not differ from the participants in which the DCE-MRI was sufficient. Due to time constraints in our MR protocol, DCE-MRI acquisition did not last long enough for the time intensity curve to reach plateau phase. As this might potentially lead to unreliable estimates of Ve and subsequently also of Kep, only the robust parameters Ktrans and Vp were presented. This is sufficient for our research purpose as these two are the most important parameters to identify increased perfusion.

ROI delineation was done by a single observer only, which leaves the variability introduced by having an alternative observer unknown. A previous study stated that the inter-observer variability is low when a large ROI is used.[47] This was done in quantitative MRI of cartilage, but given our experience in both cartilage and other structures like the fat pad we found these comparable. Furthermore, the boundaries of the ROI were discussed in depth with a senior musculoskeletal radiologist (EO).

Since a group-wise AIF is not available within the DCE-tool, we used a subject-specific AIF, despite the probability of not capturing the arterial bolus given the low temporal resolution of 10 seconds. Therefore, all AIF curves were visually checked and appeared to capture the bolus peak adequately. Another point to notice is that small, yet significant differences could have been left undetected due to the large inter-subject variability. Power analysis was not feasible in advance, due to the lack of knowledge regarding effect sizes. In future research including a larger number of subjects would be advised in order to be able to draw firm conclusions. With regard to our results, we do not think this would affect the main outcome as inter-subject variability is equally present in both groups and the variance was not statistically significantly different between groups, except for Vp. The clinical relevance of these potentially missed small differences would also be questionable given the small effect sizes and the fact that patients had a lower mean of Ktrans and Vp, which does not concur with the suspected increased blood perfusion accompanying inflammation. Finally, some of the subgroup analyses were theoretically underpowered due to the low prevalence of features. If these would have been the key features for the incidence of PFP, though, a higher prevalence would have been expected to start with. In general, due to the cross-sectional design no causal relations could be studied, but only associations. Future research might try to achieve

a complete picture of the perfusion in the knee joint. For now, this is quite challenging, because different tissues require different pharmacokinetic models.

In conclusion, patients with PFP and healthy control subjects do not demonstrate a significantly different volume or blood perfusion of the IPFP. Thus it seems that higher IPFP blood perfusion measured by DCE-MRI, as imaging biomarker of inflammation, and larger volume are not associated with PFP.

ACKNOWLEDGEMENTS

We would like to acknowledge Kyung Hyun Sung for the development of the DCE tool in Horos.

REFERENCES

1. Crossley KM, Stefanik JJ, Selfe J, Collins NJ, Davis IS, Powers CM, *et al.* 2016 Patellofemoral pain consensus statement from the 4th International Patellofemoral Pain Research Retreat, Manchester. Part 1: Terminology, definitions, clinical examination, natural history, patellofemoral osteoarthritis and patient-reported outcome measures. *Br J Sports Med*. 2016;50(14):839-43.
2. van der Heijden RA, Lankhorst NE, van Linschoten R, Bierma-Zeinstra SM, van Middelkoop M. Exercise for treating patellofemoral pain syndrome. *Cochrane Database Syst Rev* 2015;1:CD010387.
3. Callaghan MJ, Selfe J. Patellar taping for patellofemoral pain syndrome in adults. *Cochrane Database Syst Rev* 2012;4:CD006717.
4. Barton CJ, Munteanu SE, Menz HB, Crossley KM. The efficacy of foot orthoses in the treatment of individuals with patellofemoral pain syndrome: a systematic review. *Sports Med* 2010;40:377-395.
5. Swart NM, van Linschoten R, Bierma-Zeinstra SM, van Middelkoop M. The additional effect of orthotic devices on exercise therapy for patients with patellofemoral pain syndrome: a systematic review. Br J *Sports Med* 2012;46:570-577.
6. Thomas MJ, Wood L, Selfe J, Peat G. Anterior knee pain in younger adults as a precursor to subsequent patellofemoral osteoarthritis: a systematic review. *BMC Musculoskelet Disord* 2010;11:201.
7. Eijkenboom JFA, Waarsing JH, Oei EHG, Bierma-Zeinstra SMA, van Middelkoop M. Is patellofemoral pain a precursor to osteoarthritis?: Patellofemoral osteoarthritis and patellofemoral pain patients share aberrant patellar shape compared with healthy controls. *Bone Joint Res* 2018;7:541-547.
8. Crossley KM, Hinman RS. The patellofemoral joint: the forgotten joint in knee osteoarthritis. *Osteoarthritis Cartilage* 2011;19:765-767.
9. Biedert RM, Sanchis-Alfonso V. Sources of anterior knee pain. *Clin Sports Med* 2002;21:335-347, vii.
10. Dye SF. The pathophysiology of patellofemoral pain - A tissue homeostasis perspective. *Clinical Orthopaedics and Related Research* 2005:100-110.
11. Felson DT. The sources of pain in knee osteoarthritis. *Curr Opin Rheumatol* 2005;17:624-628.
12. Clockaerts S, Bastiaansen-Jenniskens YM, Runhaar J, Van Osch GJ, Van Offel JF, Verhaar JA, *et al.* The infrapatellar fat pad should be considered as an active osteoarthritic joint tissue: a narrative review. *Osteoarthritis Cartilage* 2010;18:876-882.
13. Ioan-Facsinay A, Kloppenburg M. An emerging player in knee osteoarthritis: the infrapatellar fat pad. *Arthritis Res Ther* 2013;15:225.
14. Dragoo JL, Johnson C, McConnell J. Evaluation and treatment of disorders of the infrapatellar fat pad. Sports Med 2012;42:51-67.
15. Stephen JM, Sopher R, Tullie S, Amis AA, Ball S, Williams A. The infrapatellar fat pad is a dynamic and mobile structure, which deforms during knee motion, and has proximal extensions which wrap around the patella. *Knee Surg Sports Traumatol Arthrosc* 2018;26:3515-3524.
16. Pan F, Han W, Wang X, Liu Z, Jin X, Antony B, *et al.* A longitudinal study of the association between infrapatellar fat pad maximal area and changes in knee symptoms and structure in older adults. *Ann Rheum Dis* 2015;74:1818-1824.
17. Ruhdorfer A, Haniel F, Petersohn T, Dorrenberg J, Wirth W, Dannhauer T, *et al.* Between-group differences in infra-patellar fat pad size and signal in symptomatic and radiographic progression of knee osteoarthritis vs non-progressive controls and healthy knees - data from the

FNIH Biomarkers Consortium Study and the Osteoarthritis Initiative. *Osteoarthritis Cartilage* 2017;25:1114-1121.

18. Han W, Aitken D, Zhu Z, Halliday A, Wang X, Antony B, *et al.* Signal intensity alteration in the infrapatellar fat pad at baseline for the prediction of knee symptoms and structure in older adults: a cohort study. *Ann Rheum Dis* 2016;75:1783-1788.
19. Wang K, Ding C, Hannon MJ, Chen Z, Kwoh CK, Hunter DJ. Quantitative Signal Intensity Alteration in Infrapatellar Fat Pad Predicts Incident Radiographic Osteoarthritis: The Osteoarthritis Initiative. *Arthritis Care Res* 2019;71:30-38.
20. Roemer FW, Jarraya M, Felson DT, Hayashi D, Crema MD, Loeuille D, *et al.* Magnetic resonance imaging of Hoffa's fat pad and relevance for osteoarthritis research: a narrative review. *Osteoarthritis Cartilage* 2016;24:383-397.
21. van der Heijden RA, de Kanter JL, Bierma-Zeinstra SM, Verhaar JA, van Veldhoven PL, Krestin GP, *et al.* Structural Abnormalities on Magnetic Resonance Imaging in Patients With Patellofemoral Pain: A Cross-sectional Case-Control Study. *Am J Sports Med* 2016;44:2339-2346.
22. Burda B, Steidle-Kloc E, Dannhauer T, Wirth W, Ruhdorfer A, Eckstein F. Variance in infra-patellar fat pad volume: Does the body mass index matter?-Data from osteoarthritis initiative participants without symptoms or signs of knee disease. *Ann Anat 2017*;213:19-24.
23. Boesen M, Kubassova O, Bouert R, Axelsen MB, Ostergaard M, Cimmino MA, *et al.* Correlation between computer-aided dynamic gadolinium-enhanced MRI assessment of inflammation and semi-quantitative synovitis and bone marrow oedema scores of the wrist in patients with rheumatoid arthritis--a cohort study. *Rheumatology (Oxford)* 2012;51:134-143.
24. Axelsen MB, Stoltenberg M, Poggenborg RP, Kubassova O, Boesen M, Bliddal H, *et al.* Dynamic gadolinium-enhanced magnetic resonance imaging allows accurate assessment of the synovial inflammatory activity in rheumatoid arthritis knee joints: a comparison with synovial histology. *Scand J Rheumatol* 2012;41:89-94.
25. Boesen M, Kubassova O, Sudol-Szopinska I, Maas M, Hansen P, Nybing JD, *et al.* MR Imaging of Joint Infection and Inflammation with Emphasis on Dynamic Contrast-Enhanced MR Imaging. *PET Clin* 2018;13:523-550.
26. Riis RG, Gudbergsen H, Henriksen M, Ballegaard C, Bandak E, Rottger D, *et al.* Synovitis assessed on static and dynamic contrast-enhanced magnetic resonance imaging and its association with pain in knee osteoarthritis: A cross-sectional study. *Eur J Radiol* 2016;85:1099-1108.
27. Riis RG, Gudbergsen H, Simonsen O, Henriksen M, Al-Mashkur N, Eld M, *et al.* The association between histological, macroscopic and magnetic resonance imaging assessed synovitis in end-stage knee osteoarthritis: a cross-sectional study. *Osteoarthritis Cartilage* 2017;25:272-280.
28. Ballegaard C, Riis RG, Bliddal H, Christensen R, Henriksen M, Bartels EM, *et al.* Knee pain and inflammation in the infrapatellar fat pad estimated by conventional and dynamic contrast-enhanced magnetic resonance imaging in obese patients with osteoarthritis: a cross-sectional study. *Osteoarthritis Cartilage* 2014;22:933-940.
29. van der Heijden RA, Poot DHJ, Ekinci M, Kotek G, van Veldhoven PLJ, Klein S, *et al.* Blood perfusion of patellar bone measured by dynamic contrast-enhanced MRI in patients with patellofemoral pain: A case-control study. *J Magn Reson Imaging* 2018;48:1344-1350.
30. van der Heijden RA, de Kanter JL, Bierma-Zeinstra SM, Verhaar JA, van Veldhoven PL, Krestin GP, *et al.* Structural Abnormalities on Magnetic Resonance Imaging in Patients With Patellofemoral Pain: A Cross-sectional Case-Control Study. *Am J Sports Med 2016*.
31. Kujala UM, Jaakkola LH, Koskinen SK, Taimela S, Hurme M, Nelimarkka O. Scoring of patellofemoral disorders. *Arthroscopy* 1993;9:159-163.

32. van der Heijden RA, Vollebregt T, Bierma-Zeinstra SM, van Middelkoop M. Strength and Pain Threshold Handheld Dynamometry Test Reliability in Patellofemoral Pain. *Int J Sports Med* 2015;36:1201-1205.
33. van der Heijden RA, Rijndertse MM, Bierma-Zeinstra SMA, van Middelkoop M. Lower Pressure Pain Thresholds in Patellofemoral Pain Patients, Especially in Female Patients: A Cross-Sectional Case-Control Study. *Pain Med* 2018;19:184-192.
34. Hunter DJ, Guermazi A, Lo GH, Grainger AJ, Conaghan PG, Boudreau RM, *et al.* Evolution of semi-quantitative whole joint assessment of knee OA: MOAKS (MRI Osteoarthritis Knee Score). *Osteoarthritis Cartilage* 2011;19:990-1002.
35. Steidle-Kloc E, Wirth W, Ruhdorfer A, Dannhauer T, Eckstein F. Intra- and inter-observer reliability of quantitative analysis of the infra-patellar fat pad and comparison between fat- and non-fat-suppressed imaging--Data from the osteoarthritis initiative. *Ann Anat* 2016;204:29-35.
36. Klein S, Staring M, Murphy K, Viergever MA, Pluim JP. elastix: a toolbox for intensity-based medical image registration. *IEEE Trans Med Imaging* 2010;29:196-205.
37. K. S. DCE Tool. http://kyungs.bol.ucla.edu/software/DCE_tool/DCE_tool.html. (2015) Accessed 23 May 2018.
38. Sourbron SP, Buckley DL. Tracer kinetic modelling in MRI: estimating perfusion and capillary permeability. *Phys Med Biol* 2012;57:R1-33.
39. Poot DHJ, van der Heijden RA, van Middelkoop M, Oei EHG, Klein S. Dynamic contrast-enhanced MRI of the patellar bone: How to quantify perfusion. *J Magn Reson Imaging* 2018;47:848-858.
40. Tofts PS, Kermode AG. Measurement of the blood-brain barrier permeability and leakage space using dynamic MR imaging. 1. Fundamental concepts. *Magn Reson Med* 1991;17:357-367.
41. Cai J, Xu J, Wang K, Zheng S, He F, Huan S, *et al.* Association Between Infrapatellar Fat Pad Volume and Knee Structural Changes in Patients with Knee Osteoarthritis. *J Rheumatol 2015*;42:1878-1884.
42. Steidle-Kloc E, Culvenor AG, Dorrenberg J, Wirth W, Ruhdorfer A, Eckstein F. Relationship Between Knee Pain and Infrapatellar Fat Pad Morphology: A Within- and Between-Person Analysis From the Osteoarthritis Initiative. *Arthritis Care Res* 2018;70:550-557.
43. Cowan SM, Hart HF, Warden SJ, Crossley KM. Infrapatellar fat pad volume is greater in individuals with patellofemoral joint osteoarthritis and associated with pain. *Rheumatol Int* 2015;35:1439-1442.
44. Chuckpaiwong B, Charles HC, Kraus VB, Guilak F, Nunley JA. Age-associated increases in the size of the infrapatellar fat pad in knee osteoarthritis as measured by 3T MRI. *J Orthop Res* 2010;28:1149-1154.
45. Collins NJ, Vicenzino B, van der Heijden RA, van Middelkoop M. Pain During Prolonged Sitting Is a Common Problem in Persons With Patellofemoral Pain. *J Orthop Sports Phys Ther* 2016;46:658-663.
46. Naslund J, Walden M, Lindberg LG. Decreased pulsatile blood flow in the patella in patellofemoral pain syndrome. *Am J Sports Med* 2007;35:1668-1673.
47. Tiderius CJ, Tjornstrand J, Akeson P, Sodersten K, Dahlberg L, Leander P. Delayed gadolinium-enhanced MRI of cartilage (dGEMRIC): Intra- and interobserver variability in standardized drawing of regions of interest. *Acta Radiologica* 2004;45:628-634.

CHAPTER 4

Quantitative DCE-MRI demonstrates increased blood perfusion in Hoffa's fat pad signal abnormalities in knee osteoarthritis, but not in patellofemoral pain

B.A. de Vries*, R.A. van der Heijden*, D.H.J. Poot, M. van Middelkoop, D.E. Meuffels, G.P. Krestin, E.H.G Oei.
**shared first authorship*

European Radiology 2020 June;30(6):3401-3408.

ABSTRACT

INTRODUCTION

Infrapatellar fat pad (IPFP) fat-suppressed T2 ($T2_{FS}$) hyperintense regions on MRI are an important imaging feature of knee osteoarthritis (OA) and are thought to represent inflammation. These regions are also common in non-OA subjects, and may not always be linked to inflammation. Our aim was to evaluate quantitative blood perfusion parameters, as surrogate measure of inflammation, within $T2_{FS}$-hyperintense regions in patients with OA, with patellofemoral pain (PFP), supposed OA precursor, and control subjects.

METHODS

Twenty-two knee OA patients, 35 PFP patients and 43 healthy controls were included and underwent MRI, comprising T2 and DCE-MRI sequences. $T2_{FS}$-hyperintense IPFP regions were delineated and a reference region was drawn in adjacent IPFP tissue with normal signal intensity. After fitting the extended Tofts pharmacokinetic model, quantitative DCE-MRI perfusion parameters were compared between the two regions within subjects in each subgroup, using a paired Wilcoxon signed-rank test.

RESULTS

$T2_{FS}$-hyperintense IPFP regions were present in 16 of 22 (73%) OA patients, 13 of 35 (37%) PFP patients and 14 of 43 (33%) controls. DCE-MRI perfusion parameters were significantly different between regions with and without a $T2_{FS}$-hyperintense signal in OA patients, demonstrating higher Ktrans compared to normal IPFP tissue (0.039 min^{-1} versus 0.025 min^{-1}, p=0.017) and higher Ve (0.157 versus 0.119, p=0.010). For PFP patients and controls no significant differences were found.

CONCLUSIONS

IPFP $T2_{FS}$-hyperintense regions are associated with higher perfusion in knee OA patients in contrast to identically appearing regions in PFP patients and controls, pointing towards an inflammatory pathogenesis in OA only.

INTRODUCTION

The infrapatellar fat pad (IPFP), also known as 'Hoffa's fat pad', is an intracapsular, extra-synovial structure in the anterior knee joint and is one of several fat pads of the knee. This structure has been proposed as possible source of knee pain in patients suffering from osteoarthritis (OA) and from the supposed precursor of knee OA: patellofemoral pain (PFP).[1–6] In OA research, the MRI Osteoarthritis Knee Score (MOAKS) is one of the most commonly used scoring systems for knee OA on MRI.[7] In this method the presence and size of hyperintense signal within the IPFP is scored on unenhanced fat-suppressed MR images. These hyperintense lesions are thought to be a manifestation of knee inflammation and are therefore classified as Hoffa synovitis.[7] Moreover, multiple studies have emphasized the importance of $T2_{FS}$-hyperintense IPFP regions as a precursor for structural knee OA.[8–12]

A recent study that included patients with PFP and healthy controls subjects showed that $T2_{FS}$-hyperintense regions in the IPFP are rather common.[13] The question arises whether this identically appearing feature, commonly encountered in daily clinical practice and considered an 'early OA' feature, has a different pathophysiology across populations. A hyperintense $T2_{FS}$ signal may be caused by edema due to inflammatory induced vasodilatation, but a prior study by Roemer *et al.* suggested that this feature may not always be linked to inflammation.[14] Other causative effects of a fluid signal might be edema due to mechanical friction/impingement, or increased vascularity due to neo-angiogenesis, necrosis or cellular infiltration.[15,16]

Dynamic contrast-enhanced (DCE) MRI enables further evaluation of the pathophysiology of IPFP $T2_{FS}$-hyperintense lesions. Fitting a pharmacokinetic model to the DCE-MRI data enables quantitative surrogate measurement of physiological parameters such as blood flow, blood volume, and extravascular permeability.[17] Increased blood perfusion, evaluated by DCE-MRI, has been considered a surrogate measure of inflammation for a variety of musculoskeletal tissues.[18–23] To the best of our knowledge, the only research with regard to DCE-MRI in the IPFP was performed by Ballegaard *et al.*[23] They studied obese patients with knee OA using a heuristic DCE-MRI analysis approach and found a positive correlation between knee pain and their DCE-MRI-derived inflammation marker and between knee pain and Hoffa-synovitis assessed by MOAKS, thereby stipulating the importance of the IPFP and the potential of DCE-MRI as a biomarker of inflammation.[23] So far, DCE-MRI has not been applied for studying the pathogenesis of $T2_{FS}$-hyperintense IPFP regions in an OA and non-OA population.

Therefore, the aim of this study was to evaluate differences in quantitative DCE-MRI blood perfusion parameters between a $T2_{FS}$-hyperintense region of the IPFP and adjacent IPFP tissue with normal signal intensity within patients with knee OA, patients with PFP, and healthy

control subjects. Our hypothesis was that $T2_{FS}$-hyperintense IPFP regions demonstrate different DCE-MRI perfusion parameters in patients with OA, patients with PFP and healthy control subjects, with the highest degree of perfusion expected in patients with OA.

METHODS

Study population

In the current study, we analyzed data from two previous studies in order to include both patients with OA and patients with PFP, the supposed precursor of OA. In the first study, patients with unicompartmental radiographic knee OA with a severity of KL (Kellgren & Lawrence[24]) grade 2 and higher, aged 52 to 75 years, scheduled to undergo knee replacement surgery, were included. Patients were excluded when the glomerular filtration rate was <60mL/min. In the second study healthy controls and patients with PFP, aged between 18 and 40 years, were included. Patients were excluded if they had other defined pathological conditions of the knee such as patellar tendinopathy or osteoarthritis, if the onset of PFP occurred after trauma, if they had previous knee injuries or surgery or previous episodes of PFP that occurred more than two years ago, or if they had contraindications for MRI scanning with contrast administration. Patients of both studies were included between 2013 and 2017 at the Erasmus University Medical Center Rotterdam (Rotterdam, The Netherlands); details of each study have been published elsewhere[13,25]. Both studies were approved by the institutional review board of Erasmus MC and written informed consent was obtained from all subjects.

MR imaging acquisition

In both studies, all subjects underwent MRI using the same MRI scanner and an identical MRI protocol. Multisequence MRI was performed using a 3T MRI system (Discovery MR750, General Electric Healthcare) and a dedicated 8-channel transmit/receive knee coil (Invivo). DCE-MRI was acquired in the sagittal plane, using a fat-suppressed 3D fast spoiled gradient echo (FSPGR) sequence with 35 phases of 10 s. Contrast agent 0.2 mmol/kg gadopentetate dimeglumine (Magnevist, Bayer) was administrated intravenously with a power injector at a rate of 2 ml/s started after the first phase and followed by a saline flush. The field-of-view (FOV) was 22 × 22 cm, with an in-plane resolution of 0.85 × 1.20 mm and 5 mm slice thickness, a flip angle of 30° and repetition time of 9.3 ms was used. T2 mapping was performed using a iMSDE prepared 3D fast spin echo (FSE) sequence with a FOV of 15 × 15 cm, 3 mm slice thickness, and an in-plane resolution of 0.52 ×0.78 mm, using 5 different echo times in the preparation module (3.1, 13.4, 27.0, 40.7, 68.1 ms). The protocol also included a fat-suppressed sagittal T2-weighted FSE sequence with a FOV of 15 × 15 cm, 3 mm slice thickness, and an in-plane resolution of 0.36 × 0.59 mm.

Image analysis

To correct for patient movement, all 35 time points of the DCE-MRI were registered using an automated rigid body registration with Elastix.[26] We first assessed the fat-saturated T2-weighted images for the presence of $T2_{FS}$-hyperintense regions in the IPFP. Subsequently, detected $T2_{FS}$-hyperintense regions were delineated on the quantitative T2 maps. The delineation of ROIs was performed on T2 maps as these images were scanned in the same part of the scan session as the DCE-MRI, in contrast to the $T2_{FS}$-weighted images, and thus the regions of interest (ROIs) could be copied to the DCE-maps. ROIs were placed within the borders of the hyperintense regions using the Horos software package (Horosproject.org). When multiple hyperintense regions were found in the IPFP, the ROI was placed in only one, the largest region. Two ROIs were drawn in the IPFP, one within the $T2_{FS}$-hyperintense region and the second in an adjacent area without T2-hyperintensity (Figure 1). All ROIs were drawn by a researcher with a technical medical degree and more than three years of experience in musculoskeletal imaging research (B.d.V). The same ROIs from the T2-maps were copied to the registered DCE-MR images to extract quantitative DCE measures from the same regions. These quantitative DCE parameters (Ktrans, Kep, Ve, Vp) were calculated by fitting the extended Tofts pharmacokinetic model to the DCE-MRI data, using the DCETool in Horos.[27,28]. Subsequently, mean T2 value and mean perfusion parameter values of the ROIs were calculated. The Tofts pharmacokinetic model is widely used for this purpose and has shown to be the most accurate model for patellar bone.[29] For highly vascularized tissues, like the IPFP, the extended Tofts pharmacokinetic model is more suitable due to the addition of the vascular term Vp; therefore in this study, we used the extended Tofts pharmacokinetic model.[30] Ktrans reflects the volume transfer constant into the tissue compartment, Kep describes the rate constant back into the vascular component, Ve is the extravascular extracellular space and Vp is the vascular fraction of the region.[31] The arterial input function (AIF) was estimated using a ROI in the popliteal artery. All fitted AIFs were visually checked.

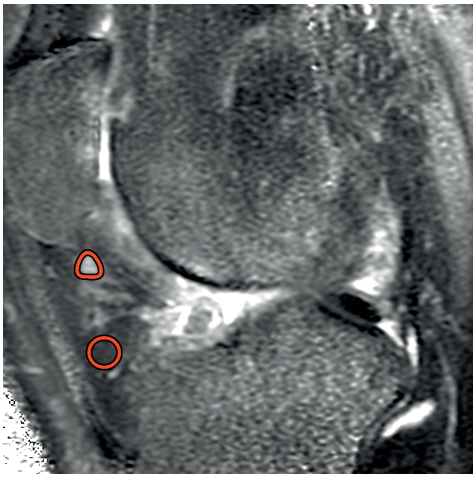

Figure 1: Two ROIs were drawn in the IPFP, one within the $T2_{FS}$-hyperintense region and the second in an adjacent area without T2-hyperintensity.

Statistical analysis

The image analyses result in a mean value for the T2 and perfusion parameters within each region. For each region, the median T2 and perfusion parameters over all subjects in a certain group were calculated, as well as the interquartile range (IQR) as a measure of variability. Since all DCE-MRI variables showed a non-normal distribution, using the Shapiro-Wilk test, a paired Wilcoxon signed-rank test was used to compare perfusion parameter values of the $T2_{FS}$-hyperintense region with the adjacent region with normal signal intensity within the different subject groups. A Mann-Whitney U test was used to evaluate the location distribution of $T2_{FS}$-hyperintense IPFP regions over the groups as well as differences in DCE-MRI perfusion parameters of a central versus a peripheral $T2_{FS}$-hyperintense region. Statistical analysis was performed using SPSS v25 (IBM Corp., Armonk, NY, USA). p values < 0.05 were considered to be statistically significant.

RESULTS

In total, 100 participants were included from both studies: 22 patients with knee OA, 35 patients with PFP, and 43 healthy controls. The mean BMI was higher in the OA group (30.6 kg/m^2) in comparison to the PFP and the control group with a mean BMI of 24.6 and 22.3 kg/m^2, respectively. The Knee Injury and Osteoarthritis Outcome Score (KOOS) indicated that pain symptoms were most severe in the OA group. Characteristics of all participants are shown in Table 1.

Table 1: Characteristics of participants with T2 regions within IPFP.

Groups Parameter	OA Patients N = 16	PFP patients N = 13	Controls N = 14	Total N = 43
Sex male (%)	5 (31%)	8 (62%)	7 (50%)	20 (47%)
Age in years	63.3 ± 6.3 [a.]	27.0 ± 5.6 [a.]	25.8 ± 4.4 [a.]	29.6 [b.] [24.0-60.0]
BMI in kg/m^2	30.6 ± 5.2 [a.]	24.6 ± 3.5 [a.]	22.3 ± 2.2 [a.]	24.3 [b.] [21.9-29.1]
KOOS pain subscale	40.5 ± 11.0 [a.]	71.6 ± 17.9 [a.]	100.0 [b.] [100.0-100.0]	66.7 [b.] [44.4-100.0]

[a.] Mean ± SD, [b.] Median [IQR]. SD: standard deviation, IQR: interquartile range.

$T2_{FS}$-hyperintense IPFP regions were present in 43 subjects. The prevalence of the $T2_{FS}$-hyperintense IPFP regions was different between the groups: 16 of 22 (73%) knee OA patients, 13 of 35 (37%) PFP patients, and 14 of 43 (33%) controls. Of the 16 knee OA patients, three had a radiographic OA severity of Kellgren and Lawrence grade 2, eight had KL grade 3, and five patients had KL grade 4.

The median T2 value in IPFP tissue without T2-hyperintensity was 36.4, 33.9, and 32.7 ms in OA patients, PFP patients and controls, respectively. For the $T2_{FS}$-hyperintense regions, these values were 61.4, 52.3, and 53.7 ms, respectively (Table 2).

Table 2: T2 and DCE-MRI perfusion parameters in the IPFP. *p* values of the difference between T2-hyperintense region and tissue with normal signal intensity are reported. *p* values < 0.05 are indicated with *. IQR = interquartile range.

	T2 relaxation time (ms)		Ktrans x 1000 (min^{-1})			Kep x 1000 (min^{-1})			Ve x 1000 (unit-less)			Vp x 1000 (unit-less)		
	Median	IQR	Median	IQR	*p* value †	Median	IQR	*p* value †	Median	IQR	*p* value †	Median	IQR	*p* value †
OA patients														
T2-hyperintense region	61.40	31.27	39.03	65.79	0.017*	197.57	198.66	0.079	157.19	259.45	0.010*	2.09	6.15	0.363
Normal signal intensity	36.39	6.15	24.73	22.76		163.49	131.83		119.18	151.43		1.03	5.98	
PFP patients														
T2-hyperintense region	52.30	10.66	11.07	13.49	0.552	173.41	198.61	0.552	143.00	128.37	0.917	0.22	0.52	0.477
Normal signal intensity	33.85	4.62	13.61	10.09		112.86	181.96		143.95	125.33		0.11	0.39	
Controls														
T2-hyperintense region	53.67	15.49	9.84	17.28	0.363	91.00	97.38	0.778	160.62	255.09	0.510	0.13	0.70	0.075
Normal signal intensity	32.71	4.74	14.36	23.02		122.28	117.59		181.53	116.12		0.01	0.18	

† Wilcoxon signed-rank test

Most hyperintense regions were located centrally (n = 30) in the IPFP whereas 13 were located more peripherally. We observed no significant difference in location distribution between groups as well as no difference in all DCE-MRI perfusion parameters of a central versus a peripheral $T2_{FS}$ hyperintense region.

In knee OA patients, the $T2_{FS}$-hyperintense IPFP regions demonstrated significantly higher values of Ktrans (see Figure 2) and Ve compared to tissue with normal signal intensity (0.039 min^{-1} vs. 0.025 min^{-1} for Ktrans and 0.157 vs. 0.119 for Ve). Kep and Vp were higher within $T2_{FS}$-hyperintense lesions in OA patients compared to tissue with normal signal intensity (median Kep 0.198 min^{-1} vs. 0.163 min^{-1} and median Vp 0.002 vs. 0.001, respectively). However, these differences were not statistically significant for both Kep (p = 0.079) and Vp (p = 0.363). In both controls and PFP patients, all DCE-MRI perfusion parameters were not significantly different between IPFP tissue with and without a $T2_{FS}$-hyperintensity. In PFP-patients a Ktrans of 0.014 min^{-1} and Kep 0.113 min^{-1} in IPFP tissue with normal signal

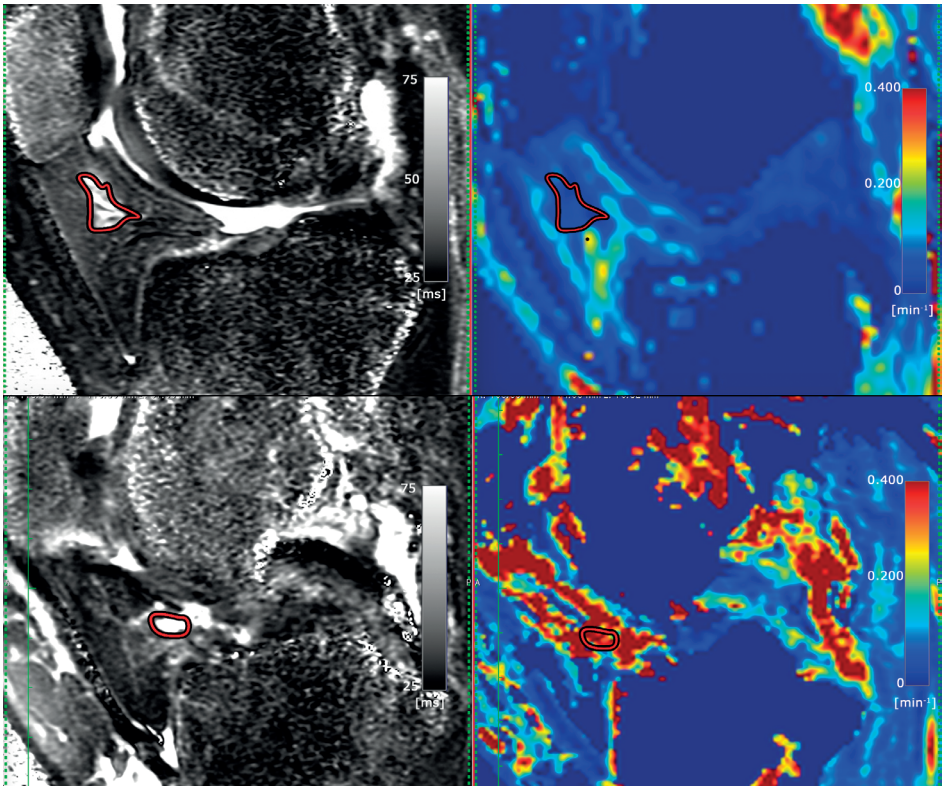

Figure 2: Delineated T2-hyperintense region within IPFP on T2 map (left) and corresponding Ktrans map (values in min^{-1}) (right) in patient with PFP (upper row) and patient with OA (lower row). Higher values of Ktrans are depicted in red.

intensity and a Ktrans of 0.011 min^{-1} and Kep 0.173 min^{-1} in tissue with $T2_{FS}$-hyperintensity was found. In controls, the median Ktrans was 0.014 min^{-1} and median Kep was 0.122 min^{-1} in IPFP tissue with normal signal intensity and in tissue with $T2_{FS}$ -hyperintensity these values were 0.010 and 0.091 min^{-1}, respectively. Moreover, all DCE-MRI perfusion parameters were higher in both the hyperintense lesions and normal IPFP tissue in the OA group. All DCE-MRI results are shown in Table 2.

DISCUSSION

In this study, quantitative DCE-MRI perfusion parameters were measured within $T2_{FS}$-hyperintense regions and adjacent IPFP tissue with normal signal intensity of patients with knee OA, patients with PFP and in healthy controls. Our hypothesis was that identically appearing $T2_{FS}$-hyperintense IPFP regions in patients with OA, PFP, and control subjects demonstrate different degrees of increased perfusion measured with quantitative DCE-MRI compared to adjacent IPFP tissue with normal signal intensity. We expected the highest perfusion in patients with OA, in which term Hoffa synovitis has been coined to describe such regions. Indeed, we found that $T2_{FS}$-hyperintense regions showed significantly increased perfusion compared to adjacent IPFP tissue with normal signal intensity in OA patients only, in contrast to both patients with PFP and healthy controls. This finding suggests an inflammatory pathogenesis of such regions in OA patients, but not in patients with PFP and healthy control subjects. Our observation that knee OA patients demonstrated, in general, higher DCE-MRI perfusion parameters than PFP patients and healthy controls, irrespective of the presence of a $T2_{FS}$-hyperintense region, also indicate that the entire IPFP may be affected by inflammation in OA and possibly also by neo-angiogenesis, based on the elevated Vp, which represents the vascular fraction within the ROI. Our observation of this phenomenon in the IPFP is of interest, as from previous literature it is known that OA is not a simple 'wear and tear' disease of cartilage and bone, but a whole organ disease, including several soft tissues such as the IPFP.[32] Accordingly, there is an increasing focus on systemic treatment approaches for OA, such as anti-inflammatory and anti-angiogenic medication.[33] In future trials, it will be a prerequisite to identify OA subtypes, in which advanced MR imaging, such as DCE-MRI, could potentially play a major role.

The different results for PFP found in this study are not consistent with current insights in PFP, which is supposed to be a precursor of OA.[34,35] A possible explanation might be that tissue homeostasis is not yet as disturbed in PFP and inflammatory cytokines are not yet released. Thus, even though T2-hyperintense IPFP regions appear identically on unenhanced T2-weighted fat-saturated MR images in OA and PFP patients as well as healthy controls, the results of our DCE-MRI analysis show that there are different degrees of perfusion within the

IPFP of controls, PFP patients, and OA patients, which may point towards different pathophysiologies. This knowledge will help the practicing radiologist who is confronted with an increased application of sensitive knee MRI to appraise these lesions in the context of the patient's age and concurrent abnormalities.

In this study, the IPFP was quantitatively analyzed by T2 mapping and DCE-MRI in order to investigate the pathophysiology of T2 signal alterations in the IPFP within OA and PFP. The single prior study that applied DCE-MRI to investigate the IPFP by Ballegaard *et al.* [23] used a different approach in the definition of the region of interest, as they focused on the entire IPFP in 3D rather than $T2_{FS}$-hyperintensities within the fat pad. Furthermore, only obese patients with knee OA were included and a heuristic DCE-MRI analysis method without pharmacokinetic modeling was performed.

A strength of the current study is the quantitative assessment of DCE-MRI perfusion values, which offers more robust parameters that directly represent the microvasculature physiology, in contrast to semi-quantitative analysis. Furthermore, the inclusion of different patient groups from two studies offered the possibility to determine the nature of $T2_{FS}$-hyperintense IPFP regions across different disease entities, one of which (PFP) has been suggested as a precursor to the each other (OA). We were able to directly compare the results of the quantitative DCE-MRI analysis from both studies because the exact same MRI scanner was used with identical scan and image post processing for both studies. Additionally, statistical analyses were performed within subjects of each subgroup, and thus possible differences in confounding variables between the subgroups will not have influenced our results.

A potential limitation was that no $B1^+$ inhomogeneity assessment and T1 correction was possible, due to the lack of $B1^+$ or pre-contrast T1 map. A fixed T1(0) value of 1443 ms (standard value of the DCE Tool used in Horos) was used instead. We expect that differences that may have arisen as a result of ignoring region T1 variability will not change the outcome of this study, as the observed differences in perfusion were large and substantially larger than any differences that we would expect due to T1 variability. Furthermore, we used a dedicated transmit/receive knee coil with relatively homogeneous B1 field. At the time of the MR acquisitions, linear gadolinium contrast agents, like gadopentetate dimeglumine, were commonly in use. Since then, these have been withdrawn from the EU market and have been replaced by alternatives that carry less risk for nephrogenic systemic fibrosis. As the perfusion kinetics of these alternatives are similar, we expect our results to be relevant for the newer generation contrast agents as well. Another limitation is that the OA group comprised patients referred for knee arthroplasty because of end-stage clinical OA, although the radiographic OA severity ranged from KL grade 2 to 4, with grade 4 relatively underrepresented. Furthermore, ROIs were drawn on one slice only. Finally, $T2_{FS}$-hyperintense lesions

were found only in 43 subjects, and the OA group was relatively small. However, all these subjects underwent an extensive MRI protocol including the administration of an intravenous contrast agent. In future research, it would be interesting to examine the perfusion of $T2_{FS}$-hyperintense lesions in a population with a wider range of clinical OA severity, to evaluate the diagnostic value of $T2_{FS}$-hyperintense lesions and their perfusion characteristics in classifying patients with unknown OA status, and to study the relationship of perfusion parameters with clinical symptoms.

In conclusion, $T2_{FS}$-hyperintense regions of the IPFP demonstrated higher quantitative DCE-MRI blood perfusion parameters compared to adjacent tissue with normal signal intensity in patients with knee OA, but not in patients with PFP and healthy control subjects. This suggests different pathophysiology of IPFP $T2_{FS}$-hyperintense regions across patient subgroups, in which an inflammatory pathogenesis is only present in OA.

ACKNOWLEDGEMENTS

We would like to acknowledge Kyung Hyun Sung for the development of the DCE tool in Horos.

REFERENCES

1. Draghi F, Ferrozzi G, Urciuoli L, Bortolotto C, Bianchi S. Hoffa's fat pad abnormalities, knee pain and magnetic resonance imaging in daily practice. *Insights Imaging*. 2016;7(3):373-383. doi:10.1007/s13244-016-0483-8
2. Felson DT. The sources of pain in knee osteoarthritis. *Curr Opin Rheumatol*. 2005;17(5):624-628. doi:10.1097/01.bor.0000172800.49120.97
3. Dye SF. The pathophysiology of patellofemoral pain: a tissue homeostasis perspective. *Clin Orthop Relat Res*. 2005;(436):100-110. doi:10.1097/01.blo.0000172303.74414.7d
4. Clockaerts S, Bastiaansen-Jenniskens YM, Runhaar J, *et al.* The infrapatellar fat pad should be considered as an active osteoarthritic joint tissue: a narrative review. *Osteoarthr Cartil*. 2010;18(7):876-882. doi:10.1016/j.joca.2010.03.014
5. Biedert RM, Sanchis-Alfonso V. Sources of anterior knee pain. *Clin Sports Med*. 2002;21(3):335-347, vii. doi:10.1016/S0278-5919(02)00026-1
6. Ioan-Facsinay A, Kloppenburg M. An emerging player in knee osteoarthritis: the infrapatellar fat pad. *Arthritis Res Ther*. 2013;15(6):225. doi:10.1186/ar4422
7. Hunter DJ, Guermazi A, Lo GH, *et al.* Evolution of semi-quantitative whole joint assessment of knee OA: MOAKS (MRI Osteoarthritis Knee Score). *Osteoarthr Cartil*. 2011;19(8):990-1002. doi:10.1016/j.joca.2011.05.004
8. Atukorala I, Kwoh CK, Guermazi A, *et al.* Synovitis in knee osteoarthritis: A precursor of disease? *Ann Rheum Dis*. 2016;75(2):390-395. doi:10.1136/annrheumdis-2014-205894
9. Han W, Aitken D, Zhu Z, *et al.* Signal intensity alteration in the infrapatellar fat pad at baseline for the prediction of knee symptoms and structure in older adults: a cohort study. *Ann Rheum Dis*. 2016;75(10):1783-1788. doi:10.1136/annrheumdis-2015-208360
10. Ruhdorfer A, Haniel F, Petersohn T, *et al.* Between-group differences in infra-patellar fat pad size and signal in symptomatic and radiographic progression of knee osteoarthritis vs non-progressive controls and healthy knees - data from the FNIH Biomarkers Consortium Study and the Osteoarthritis In. *Osteoarthr Cartil*. 2017;25(7):1114-1121. doi:10.1016/j.joca.2017.02.789
11. Wang K, Ding C, Hannon MJ, *et al.* Signal intensity alteration within infrapatellar fat pad predicts knee replacement within 5 years: data from the Osteoarthritis Initiative. *Osteoarthr Cartil*. 2018;26(10):1345-1350. doi:10.1016/j.joca.2018.05.015
12. Wang K, Ding C, Hannon MJ, Chen Z, Kwoh CK, Hunter DJ. Quantitative Signal Intensity Alteration in Infrapatellar Fat Pad Predicts Incident Radiographic Osteoarthritis: The Osteoarthritis Initiative. *Arthritis Care Res*. 2019;71(1):30-38. doi:10.1002/acr.23577
13. van der Heijden RA, de Kanter JL, Bierma-Zeinstra SM, *et al.* Structural Abnormalities on Magnetic Resonance Imaging in Patients With Patellofemoral Pain: A Cross-sectional Case-Control Study. *Am J Sport Med*. 2016;44(9):2339-2346. doi:10.1177/0363546516646107
14. Roemer FW, Guermazi A, Zhang Y, *et al.* Hoffa's Fat Pad: Evaluation on Unenhanced MR Images as a Measure of Patellofemoral Synovitis in Osteoarthritis. *AJR Am J Roentgenol*. 2009;192(6):1696-1700. doi:10.2214/AJR.08.2038
15. Subhawong TK, Eng J, Carrino JA, Chhabra A. Superolateral Hoffa's fat pad edema: Association with patellofemoral maltracking and impingement. *Am J Roentgenol*. 2010. doi:10.2214/AJR.10.4668
16. Link TM, Li X. Bone marrow changes in osteoarthritis. *Semin Musculoskelet Radiol*. 2011;15(3):238-246. doi:10.1055/s-0031-1278423

17. Sourbron SP, Buckley DL. Tracer kinetic modelling in MRI: estimating perfusion and capillary permeability. *Phys Med Biol*. 2012;57(2):R1-33. doi:10.1088/0031-9155/57/2/R1
18. Boesen M, Kubassova O, Bouert R, *et al.* Correlation between computer-aided dynamic gadolinium-enhanced MRI assessment of inflammation and semi-quantitative synovitis and bone marrow oedema scores of the wrist in patients with rheumatoid arthritis--a cohort study. *Rheumatol*. 2012;51(1):134-143. doi:10.1093/rheumatology/ker220
19. Axelsen MB, Stoltenberg M, Poggenborg RP, *et al.* Dynamic gadolinium-enhanced magnetic resonance imaging allows accurate assessment of the synovial inflammatory activity in rheumatoid arthritis knee joints: a comparison with synovial histology. *Scand J Rheumatol*. 2012;41(2):89-94. doi:10.3109/03009742.2011.608375
20. Boesen M, Kubassova O, Sudol-Szopinska I, *et al.* MR Imaging of Joint Infection and Inflammation with Emphasis on Dynamic Contrast-Enhanced MR Imaging. *PET Clin*. 2018;13(4):523-550. doi:10.1016/j.cpet.2018.05.007
21. Riis RG, Gudbergsen H, Henriksen M, *et al.* Synovitis assessed on static and dynamic contrast-enhanced magnetic resonance imaging and its association with pain in knee osteoarthritis: A cross-sectional study. *Eur J Radiol*. 2016;85(6):1099-1108. doi:10.1016/j.ejrad.2016.03.017
22. Riis RG, Gudbergsen H, Simonsen O, *et al.* The association between histological, macroscopic and magnetic resonance imaging assessed synovitis in end-stage knee osteoarthritis: a cross-sectional study. *Osteoarthr Cartil*. 2017;25(2):272-280. doi:10.1016/j.joca.2016.10.006
23. Ballegaard C, Riis RG, Bliddal H, *et al.* Knee pain and inflammation in the infrapatellar fat pad estimated by conventional and dynamic contrast-enhanced magnetic resonance imaging in obese patients with osteoarthritis: a cross-sectional study. *Osteoarthr Cartil*. 2014;22(7):933-940. doi:10.1016/j.joca.2014.04.018
24. Kellgren JH, Lawrence JS. Radiological assessment of osteo-arthrosis. *Ann Rheum Dis*. 1957;16(4):494-502. doi:10.1136/ard.16.4.494
25. van Tiel J, Kotek G, Reijman M, *et al.* Is T1ρMapping an Alternative to Delayed Gadolinium-enhanced MR Imaging of Cartilage in the Assessment of Sulphated Glycosaminoglycan Content in Human Osteoarthritic Knees? An in Vivo Validation Study. *Radiology*. 2016;279(2):523-531. doi:10.1148/radiol.2015150693
26. Klein S, Staring M, Murphy K, Viergever M a., Pluim J. Elastix: A Toolbox for Intensity-Based Medical Image Registration. *IEEE Trans Med Imaging*. 2010;29(1):196-205. doi:10.1109/TMI.2009.2035616
27. Tofts PS, Kermode AG. Measurement of the blood-brain barrier permeability and leakage space using dynamic MR imaging. 1. Fundamental concepts. *Magn Reson Med*. 1991;17(2):357-367. doi:10.1002/mrm.1910170208
28. K. S. DCE Tool. http://kyungs.bol.ucla.edu/software/DCE_tool/DCE_tool.html. Published 2015. Accessed May 23, 2018.
29. Poot DHJ, van der Heijden RA, van Middelkoop M, Oei EHG, Klein S. Dynamic contrast-enhanced MRI of the patellar bone: How to quantify perfusion. *J Magn Reson Imaging*. 2018;47(3):848-858. doi:10.1002/jmri.25817
30. Sourbron SP, Buckley DL. On the scope and interpretation of the Tofts models for DCE-MRI. *Magn Reson Med*. 2011;66(3):735-745. doi:10.1002/mrm.22861
31. Tofts PS, Brix G, Buckley DL, *et al.* Estimating kinetic parameters from dynamic contrast-enhanced T(1)-weighted MRI of a diffusable tracer: standardized quantities and symbols. *J Magn Reson Imaging*. 1999;10(3):223-232. doi:10.1002/(sici)1522-2586(199909)10:3<223::aid-jmri2>3.0.co;2-s

32. Loeser RF, Goldring SR, Scanzello CR, Goldring MB. Osteoarthritis: a disease of the joint as an organ. *Arthritis Rheum*. 2012;64(6):1697-1707. doi:10.1002/art.34453
33. Ghouri A, Conaghan PG. Update on novel pharmacological therapies for osteoarthritis. *Ther Adv Musculoskelet Dis*. 2019. doi:10.1177/1759720x19864492
34. Thomas MJ, Wood L, Selfe J, Peat G. Anterior knee pain in younger adults as a precursor to subsequent patellofemoral osteoarthritis: A systematic review. *BMC Musculoskelet Disord*. 2010. doi:10.1186/1471-2474-11-201
35. Eijkenboom JFA, Waarsing JH, Oei EHG, Bierma-Zeinstra SMA, van Middelkoop M. Is patellofemoral pain a precursor to osteoarthritis? *Bone Joint Res*. 2018. doi:10.1302/2046-3758.79.bjr-2018-0112.r1

PART II

DIAGNOSTIC ACCURACY OF IMAGING TECHNIQUES FOR THE VISUALIZATION OF SYNOVITIS IN THE KNEE

CHAPTER 5

Diagnostic accuracy of grayscale, power Doppler and contrast-enhanced ultrasound compared with contrast-enhanced MRI in the visualization of synovitis in knee osteoarthritis

B.A. de Vries, S.J. Breda, D.E. Meuffels, D.F. Hanff, M.G.M. Hunink, G.P. Krestin, E.H.G Oei.

Europ J Radiol 2020 Dec; 133

ABSTRACT

INTRODUCTION

To assess the diagnostic accuracy of grayscale (GSUS), power Doppler (PDUS) and contrast-enhanced ultrasound (CEUS) for detecting synovitis in knee osteoarthritis (OA).

METHODS

Patients with different degrees of radiographic knee OA were included prospectively. All underwent GSUS, PDUS, CEUS, and contrast-enhanced magnetic resonance imaging (CE-MRI), on which synovitis was assessed semi-quantitatively. Correlations of synovitis severity on ultrasound based techniques with CE-MRI were determined. Receiver operating characteristic (ROC) analysis was performed to assess diagnostic performance of GSUS, PDUS, and CEUS, for detecting synovitis, using CE-MRI as reference-standard.

RESULTS

In the 31 patients included, synovitis scoring on GSUS and CEUS was significantly correlated (ρ=0.608, p<0.001 and ρ=0.391, p=0.033) with CE-MRI. For detecting mild synovitis, the area under the curve (AUC) was 0.781 (95% CI 0.609-0.953) for GSUS, 0.788 (0.622-0.954) for PDUS, and 0.653 (0.452-0.853) for CEUS. Sensitivity and specificity were 0.667 (0.431-0.845) and 0.700 (0.354-0.919) for GSUS, 0.905 (0.682-0.983) and 0.500 (0.201-0.799) for PDUS, and 0.550 (0.320-0.762) and 0.700 (0.354-0.919) for CEUS, respectively. The AUC of GSUS increased to 0.862 (0.735-0.989), 0.823 (0.666-0.979), and 0.885 (0.767-1.000), when combined with PDUS, CEUS, or both, respectively. For detecting moderate synovitis, the AUC of GSUS was higher (0.882 (0.750-1.000)) and no added value of PDUS and CEUS was observed.

CONCLUSIONS

GSUS has limited overall accuracy for detecting synovitis in knee OA. When GSUS is combined with PDUS or CEUS, overall diagnostic performance improves for detecting mild synovitis, but not for moderate synovitis.

INTRODUCTION

Osteoarthritis (OA) is the most frequent form of arthritis and has major consequences for the individual patient and for public health. Joint inflammation, characterized by swelling of the synovium and joint effusion, also referred to as synovitis, is a key process in half of all OA patients.[1] Even in the early stages of OA, synovitis plays an important role in the perception of symptoms[2] and it is an important predictor of OA progression.[3] As the prominent role of synovitis in OA and the importance of identifying patients with synovitis for targeted anti-inflammatory treatment are increasingly recognized, the interest in imaging of synovitis in OA is growing.

The accepted reference standard for visualizing synovitis is MRI after intravenous administration of a contrast agent, also referred to as contrast-enhanced MRI (CE-MRI).[4] CE-MRI, however, incurs high costs, long scan times, and potential health issues in high-risk patients related to the use of contrast agents. Therefore, there is reluctance to implement synovitis imaging with CE-MRI routinely in clinical practice and in large clinical research studies on OA.

Despite the many advantages of MRI for a comprehensive evaluation of the osteoarthritic joint, ultrasound (US) is a suitable alternative to image the soft tissues of the knee and is therefore commonly used in clinical rheumatology practice.[5] Compared with MRI, US is more readily available, more practical, and less costly. Among the various methods that have been proposed for imaging synovitis with US, there are three methods that stand out. The most commonly used method is grayscale ultrasound (GSUS), although differentiating the synovium from joint fluid is difficult, since both synovial tissue and fluid generally appear hypoechoic on a grayscale image. In addition to GSUS, the extent of vascularization, which is expected to be increased in synovitis, can be visualized using power Doppler ultrasound (PDUS). PDUS has been shown to enhance diagnostic accuracy in conditions associated with increased vascularity such as arthritis, tendinitis, tumors, and in monitoring of healing processes.[6] Contrast-enhanced ultrasound (CEUS) constitutes a promising, relatively novel tool for imaging synovitis. CEUS makes use of contrast agents composed of microbubbles, that allow assessment of perfusion, based on enhanced ultrasound reflections in tissues where blood flow is increased. CEUS has been adopted especially in the abdomen, to be implemented on various organs such as liver, spleen, kidneys, and pancreas.[7,8]

We hypothesized that ultrasound is an accurate diagnostic tool for imaging synovitis in knee OA compared with CE-MRI, and that the diagnostic performance of GSUS is potentially enhanced by PDUS and CEUS. The aim of this study was to determine the diagnostic accuracy of GSUS, PDUS and CEUS for detecting synovitis in knee osteoarthritis compared with CE-MRI as reference standard.

METHODS

Study population

Patients were included in this prospective observational diagnostic accuracy study from the outpatient clinic of the Department of Orthopedic Surgery of the Department of Orthopedic Surgery of the Erasmus Medical Center (Rotterdam, the Netherlands). Patients eligible for this study were aged over 18 years, were diagnosed with radiographic knee OA with a Kellgren & Lawrence (KL) grade of at least grade 1 and had clinical suspicion of synovitis, based on of palpable joint effusion. Exclusion criteria were: previous knee replacement surgery, knee trauma in the preceding six months, absolute and relative contra-indications to undergo MRI; pregnancy, renal insufficiency (GFR < 60 mL/min/1.73m^2) and known allergy to MR or US contrast agents. The institutional ethics review board approved the study (protocol number MEC-2016-322). Both oral and written informed consent was obtained from all subjects.

MR imaging

MRI was performed using a 3T MRI scanner (Discovery MR750, GE Healthcare, Milwaukee, WI, USA) with a dedicated 8-channel knee coil. The MRI protocol included proton density weighted and fat-saturated T2-weighted sequences in three orthogonal planes to morphologically assess the knee. For CE-MRI, we applied a 3D T1-weighted sequence with fat suppression obtained after the intravenous administration of 0.2 mmol/kg of gadoterate meglumine (Dotarem®, Guerbet, Aulnay-sous-Bois, France). This double dose of gadolinium agent was used for delayed gadolinium enhanced MRI of cartilage (dGEMRIC), the analysis of which is beyond the scope of this article.

Synovitis on CE-MR images was scored independently by two experienced musculoskeletal radiologists (EO, DH), with discrepancies resolved in consensus, using a semiquantitative scoring method described by Guermazi *et al.*[9] according to this method, synovitis was scored at 11 different sites throughout the knee (Table 1). At each site, the maximal thickness of the enhanced synovium was graded as follows: grade 0 if <2 mm, grade 1 if 2–4 mm and grade 2 if >4 mm. These scores were subsequently summed to generate a whole-knee synovitis score and this sum score was finally categorized into 0–4 (normal or equivocal synovitis); 5–8 (mild synovitis); 9–12 (moderate synovitis) and ≥13 (severe synovitis).

Table 1: Sites scored for synovitis on CE-MRI according to Guermazi *et al.*[9]

1. Medial parapatellar recess	7. Lateral perimeniscal
2. Lateral parapatellar recess	8. Adjacent to the anterior cruciate ligaments
3. Suprapatellar	9. Adjacent to the posterior cruciate ligaments
4. Infrapatellar	10. Baker's cysts
5. Intercondylar	11. Loose bodies
6. Medial perimeniscal	

Ultrasound imaging

Ultrasound imaging was performed on the same day, directly following the MRI examination using an ultrasound machine (LOGIQ E9, GE Healthcare, Milwaukee, WI, USA),equipped with a linear 5-15 MHz transducer (ML6-15, GE Healthcare, Milwaukee, WI, USA). US was performed by one trained examiner (SB, radiologist-in-training with 5 years' experience).

GSUS was performed using standardized protocols, with musculoskeletal program presets, which were kept unchanged for all examinations. GSUS was used to assess the extent of synovitis, based on joint fluid and synovial hypertrophy in the longitudinal scan plane at three locations (suprapatellar, medial and lateral), as described by Hartung *et al.*[10] synovial hypertrophy was defined as abnormal hypoechoic (relative to subcutaneous fat) intraarticular tissue that is nondisplaceable and poorly compressible, and which may exhibit Doppler signal.[11] At the three evaluated locations, synovitis visualized by GSUS was graded semi-quantitatively, based on the joint capsule distension, with scores ranging from 0–3 at each site (grade 0 (absent); grade 1 (mild): small hypoechoic/anechoic line beneath joint capsule; grade 2 (moderate): joint capsule elevated parallel to joint area; grade 3 (severe): strong convex distension of the joint).[10]

PDUS was performed at the same locations as GSUS, using a frequency of 10 MHz with a pulse repetition frequency of 1.0kHz. All settings including the color box size were standardized. PDUS activity in the synovium was scored semi-quantitatively with scores ranging from 0–3 at each site (grade 0: no intra-articular color signal; grade 1: up to 3 single color signals or 2 single color signals and 1 confluent color signal representing only low flow; grade 2: 1 to 50% of the intraarticular area filled with color signals representing clear flow; grade 3: > 50% of the intraarticular area filled with color signals).[10]

GSUS and PDUS scores were summed for all three locations resulting in a sum score ranging from 0-9 for each US technique.

The site with the highest degree of synovitis on GSUS and PDUS was imaged using CEUS (Figure 1). CEUS was performed using 2.4 ml sulphur hexafluoride (SonoVue, Bracco, Milan, Italy), a second-generation ultrasound contrast agent, administered intravenously in the antecubital vein, followed by a saline bolus injection. The contrast inflow was imaged for 2 minutes. Synovial thickness on CEUS was scored semi-quantitatively, based on the maximal thickness on any slice, and graded as follows: grade 0 if < 2 mm, grade 1 if 2–4 mm, grade 2 if 5-10 mm, grade 3 if > 10 mm.[12]

The scoring of ultrasound images was performed by two persons in consensus who were blinded to the CE-MRI scores, one radiologist-in-training with 5 years' experience (SB) and a researcher with a technical medical degree and more than 3 years' experience in musculoskeletal imaging research (BdV).

Statistical analysis

Correlations were assessed between synovitis sum scores on GSUS, PDUS and CEUS and the whole-knee synovitis sum score on CE-MRI using Spearman's rank correlation, where < 0.3 indicates little or no correlation; 0.3-0.7 moderate correlation; > 0.7 strong correlation. Interobserver reliability between the two readers was assessed by calculating the intraclass correlation coefficient for summed synovitis scores and weighted Kappa statistics for each individual site and all sites pooled on CE-MRI. Receiver operating characteristic (ROC) analysis was performed to determine the diagnostic performance of GSUS, PDUS and CEUS. These were analyzed separately and combined, for the detection of synovitis with a severity of mild or higher, and moderate or higher, based on CE-MRI as the reference standard. Sensitivity, specificity, positive predictive value (PPV) and negative predictive value (NPV) were calculated along with 95% confidence intervals. For this purpose, sum scores of GSUS, PDUS and CEUS were converted to binomial data (presence or absence). In the absence of clearly reported sum score cut-off values for any of the ultrasound techniques, Youden's index was used to define the threshold value that optimized the differentiating ability of GSUS, PDUS and CEUS.[13] A p value of <0.05 was considered statistically significant. Statistical analysis was performed using SPSS v25 (IBM Corp., Armonk, NY, USA).

RESULTS

Thirty-one patients (14 females and 17 males; mean age 58 years) were included in this study. In one patient, CEUS was not acquired due to temporary license problems on the ultrasound machine, therefore, analyses on CEUS were performed in 30 patients. Baseline characteristics are shown in Table 2.

Imaging findings

On CE-MRI, 10 (32.3%) patients had no synovitis, while 9 (29.0%), 7 (22.6%) and 5 (16.1%) had mild, moderate and severe synovitis, respectively. We found good interobserver reliability for the summed synovitis score on CE-MRI, with an ICC of 0.81 (95% CI 0.64-0.90). The weighted Kappa value per individual site was variable and ranged from 0.22 to 0.78, whereas interobserver reliability for all sites pooled was moderate (weighted Kappa 0.56; 95% CI 0.47-0.64). With GSUS, the median sum score over the 3 locations assessed, was 4 (IQR 3-5, range 1-8), while for PDUS the median sum score was 2 (IQR 2-3, range 0-6). With CEUS, 16 of 30 patients (53.3%) were scored with grade 0, 6 (20.0%) with grade 1 (slight thickening), 7 (23.3%) with grade 2 (moderate), and 1 (3.3%) with grade 3. Table 3 describes the distribution of KL grades and ultrasound sum scores per grade of synovitis severity based on CE-MRI. Figure 1 shows an example of US and CE-MRI findings in a representative patient.

Table 2: Baseline patient characteristics.

Parameter	Value
No. of patients Males Females	31 14 17
Mean age, y (range)	58 (33 – 81)
Mean BMI (range)	27.5 (20.6 – 39.9)
Symptomatic knee Left Right	 15 16
Mean Knee injury and Osteoarthritis Outcome Score (KOOS), pain subscale (95% CI)	51.7 (42.8 – 60.6)
Radiographic OA severity (K&L grade)	
Grade 0	0
Grade 1	6
Grade 2	10
Grade 3	8
Grade 4	7

Table 3: Distribution of KL grade and ultrasound sum scores per grade of synovitis severity based on CE-MRI.

Synovitis severity on CE-MRI	Median KL (IQR)	Median GSUS sum score (IQR)	Median PDUS sum score (IQR)	Median CEUS sum score (IQR)
No synovitis (sum score 0-4) (n=10)	2 (1-2)	3.0 (1.8-4)	1.5 (1-2.3)	0 (0-1)
Mild synovitis (sum score 5-8) (n=9)	3 (1-3.5)	3.0 (3-4)	3.0 (2-4)	0 (0-1.5)
Moderate synovitis (sum score 9-12) (n=7)	3 (2-4)	5.0 (3-8)	3.0 (2-3)	1.0 (0-2)
Severe synovitis (sum score ≥13) (n=5, CEUS n=4)	3 (3-4)	5.0 (5-7)	2.0 (1-4.5)	2.0 (0.5-2)

Correlation between US and CE-MRI

A moderate, statistically significant, correlation was observed between the GSUS sum score and CE-MRI whole-knee sum score (Spearman's $\rho = 0.608$, $p < 0.001$). The correlation between PDUS sum score and CE-MRI whole-knee sum score was weak ($\rho = 0.299$, $p = 0.102$) and not statistically significant, whereas the correlation between CEUS sum score and CE-MRI sum score was moderate and statistically significant ($\rho = 0.391$, $p < 0.033$).

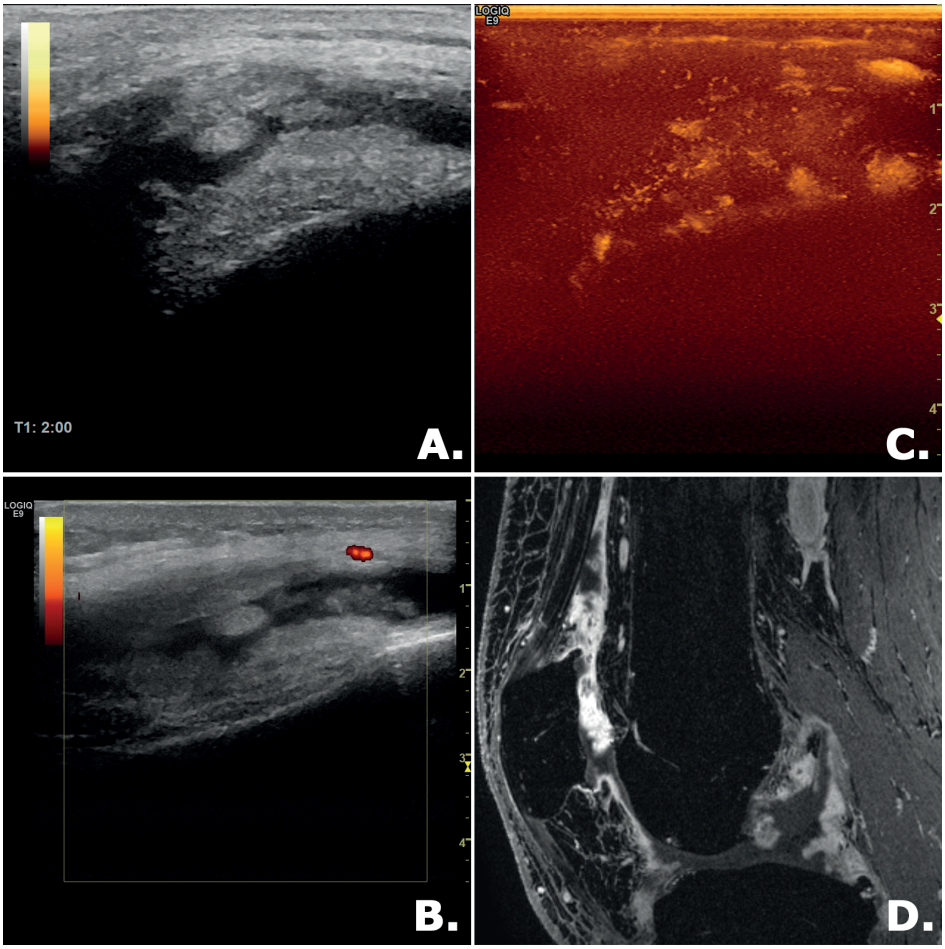

Figure 1: US and CE-MRI findings in a representative patient with KL grade 3 radiographic OA and severe synovitis. A: longitudinal GSUS image of the suprapatellar recess, reveals convex distention of the joint capsule by synovial fluid and hyperechoic synovial tissue. B: corresponding PDUS image of same patient, revealing less than 3 color signals. C: corresponding CEUS image, depicting a summed representation of the detected contrast microbubbles. D: sagittal image from CE-MRI showing severe synovitis in the same patient.

Receiver operating characteristic (ROC) analysis

Table 4 describes the results of the receiver operating characteristic (ROC) analysis for the detection of synovitis with a severity of mild or higher, and moderate or higher, based on CE-MRI. When the ultrasound techniques were analyzed separately, the areas under the curve (AUC) were 0.781 for GSUS, 0.788 for PDUS, and 0.653 for CEUS, for the detection of synovitis with a severity of mild or higher. The sensitivity of GSUS was moderate (0.667) similar to the specificity (0.700) (Table 4). PDUS showed a high sensitivity (0.905) but a substantially lower specificity (0.500), CEUS demonstrated moderate sensitivity (0.550) and specificity (0.700).

Table 4: Results of receiver operating characteristic (ROC) analysis and diagnostic performance statistics.

	AUC ROC (95% CI)	Cut-off based on Youden's index	Sensitivity (95% CI)	Specificity (95% CI)	PPV (95% CI)	NPV (95% CI)	FP	TP	TN	FN
Mild, moderate, or severe synovitis										
GSUS	0.781 (0.609-0.953)	4	0.667 (0.431-0.845)	0.700 (0.354-0.919)	0.824 (0.558-0.953)	0.500 (0.240-0.760)	3	14	7	7
PDUS	0.788 (0.622-0.954)	2	0.905 (0.682-0.983)	0.500 (0.201-0.799)	0.792 (0.573-0.921)	0.714 (0.303-0.949)	5	19	5	2
CEUS	0.653 (0.452-0.853)	1	0.550 (0.320-0.762)	0.700 (0.354-0.919)	0.786 (0.488-0.943)	0.438 (0.208-0.694)	3	11	7	9
GSUS+PDUS	0.862 (0.735-0.989)	7	0.619 (0.387-0.810)	1.000 (0.655-1.000)	1.000 (0.717-1.000)	0.556 (0.313-0.776)	0	13	10	8
GSUS+CEUS	0.823 (0.666-0.979)	5	0.650 (0.409-0.837)	0.900 (0.541-0.994)	0.929 (0.642-0.996)	0.563 (0.306-0.792)	1	13	9	7
GSUS+PDUS+CEUS	0.885 (0.767-1.000	7	0.909 (0.571-0.995)	0.789 (0.539-0.930)	0.714 (0.420-0.904)	0.938 (0.677-0.997)	1	15	9	5
Moderate or severe synovitis										
GSUS	0.882 (0.750-1.000)	5	0.750 (0.428-0.933)	0.947 (0.719-0.997)	0.900 (0.541-0.995)	0.857 (0.626-0.962)	1	9	18	3
PDUS	0.592 (0.387-0.797)	2	0.917 (0.598-0.996)	0.316 (0.136-0.565)	0.458 (0.262-0.668)	0.857 (0.420-0.992)	13	11	6	1
CEUS	0.708 (0.510-0906)	1	0.727 (0.393-0.927)	0.684 (0.435-0.864)	0.571 (0.296-0.812)	0.813 (0.537-0.950)	6	8	13	3
GSUS+PDUS	0.787 (0.621-0.953)	7	0.667 (0.354-0.887)	0.737 (0.486-0.899)	0.615 (0.322-0.849)	0.778 (0.519-0.926)	5	8	14	4
GSUS+CEUS	0.895 (0.770-1.000)	5	0.909 (0.571-0.995)	0.789 (0.539-0.930)	0.714 (0.420-0.904)	0.938 (0.677-0.997)	4	10	15	1
GSUS+PDUS+CEUS	0.844 (0.706-0.983)	7	0.909 (0.571-0.995)	0.684 (0.435-0.864)	0.625 (0.359-0.837)	0.929 (0.642-0.996)	6	10	13	1

AUC: Area Under the Curve; PPV: Positive Predictive Value; NPV: Negative Predictive Value; FP: False Positive; TP: True Positive; TN: True Negative; FN: False Negative

When combinations of ultrasound techniques were analyzed, the AUC of GSUS increased from 0.781 to 0.862 when it was combined with PDUS and to 0.823 when it was combined with CEUS, largely explained by substantially increased specificity. When all three US techniques were combined, the AUC was 0.885 with a substantially higher sensitivity (0.909) and NPV (0.938) than for the combinations of two techniques. However, the specificity (0.789) was substantially lower than for two techniques combined, as was the PPV (0.714).

For the detection of moderate or severe synovitis, the AUC for GSUS was 0.882, while the AUCs for PDUS and CEUS were substantially lower, 0.592 and 0.708, respectively. The sensitivity of GSUS was moderate (0.750) while specificity was very high (0.947). The trend for PDUS was opposite (sensitivity 0.917; specificity 0.316), while CEUS demonstrated moderate sensitivity (0.727) and specificity (0.684). The combination of PDUS with GSUS did not increase diagnostic performance compared to GSUS alone, whereas the addition of CEUS increased the AUC marginally (0.882 to 0.895), with increased sensitivity and NPV, but decreased specificity and PPV. Finally, combining all three ultrasound techniques resulted in a sensitivity of 0.909, but specificity was substantially lower than for GSUS alone or combined with either PDUS or CEUS.

DISCUSSION

This study demonstrated that, even under optimized conditions, the combination of GSUS, PDUS and CEUS shows only limited overall diagnostic accuracy for the assessment of synovitis compared to CE-MRI as the gold standard. We found that GSUS showed the highest overall diagnostic performance compared to PDUS and CEUS when analyzed separately. Nevertheless, although GSUS has high PPV, it has limited sensitivity, specificity, and NPV for the detection of synovitis with a severity of mild or higher based on CE-MRI. Thus, the application of GSUS alone for detection of mild synovitis is insufficient, and, accordingly, our results indicate that adding PDUS or CEUS increases overall diagnostic performance for detecting mild synovitis. From a practical perspective, the application of CEUS involves the intravenous administration of a contrast agent, which results in longer examination times and higher costs. Since the addition of CEUS to GSUS/PDUS only increased sensitivity and NPV, but substantially decreased specificity and PPV, we believe that CEUS is less likely to be useful in most clinical practices.

For the detection of synovitis with a severity of moderate or higher, no added value of PDUS and CEUS was observed compared to GSUS alone. The increased sensitivity associated with the combination of GSUS and CEUS or all three ultrasound techniques combined was accompanied by a greater reduction in specificity.

Synovitis plays a key role in pain perception in OA patients[14] and has been identified as an important factor for OA progression.[3] Therefore, according to recent insights, identifying patients with synovitis through imaging is crucial in order to initiate targeted anti-inflammatory therapy and prevent progression of OA.[15] Ideally, the diagnosis of synovitis is made at an early stage of OA before structural joint damage is evident on radiography, and when the severity of synovitis may be still mild. However, large-scale evaluation of OA patients with the reference standard for synovitis imaging, CE-MRI, is not feasible since CE-MRI requires the use of a gadolinium-based contrast agent and a long scan time and incurs high costs. Because ultrasound theoretically remains an attractive alternative to CE-MRI that is more readily available, less costly and faster, further study is needed to better understand and improve upon the reasons for its limited diagnostic accuracy demonstrated in this study. One previous study by Song *et al.*[16] evaluated GSUS, PDUS and CEUS in comparison with CE-MRI in a population of 36 patients with painful knee OA. In their study, only the superior and lateral recess were systematically evaluated, MRI was performed on a low-field dedicated extremity scanner precluding the assessment of obese patients, 4.8 ml instead of 2.4 ml Sulphur hexafluoride was used for CEUS, the focus of analysis was mainly on sensitivity and percentage positive findings, and no combinations of ultrasound techniques were evaluated[16] Our finding that PDUS has higher sensitivity than GSUS, with an opposite trend for specificity, is in agreement with their study.

In a study among patients with rheumatoid arthritis, Rednic *et al.*[17] found that synovial thickness measured with CEUS might be related to the 'active' state of synovitis. Our finding that CEUS and CE-MRI only correlated moderately in OA patients may point towards a higher degree of 'active' synovitis in rheumatoid arthritis.

All patients included in this study had clinical signs of synovitis, with palpable effusion documented on clinical examination. Although this was an inclusion criterion for our study, not all patients showed synovitis on CE-MRI. As many as 11 out of 31 patients were classified as having no or equivocal synovitis on CE-MRI (sum score 0-4). This may be explained by a high false-positive rate of detecting effusion on clinical examination, as well as the fact that imaging for this study was not performed at the time of the clinical diagnosis of synovitis. Moreover, OA is characterized by so-called 'flare-ups', sudden and temporary increases in symptoms along with exacerbations of synovitis[18,19], and it is possible that the degree of synovitis at the time of imaging was lower than during clinical examination. However, since our analyses focused on comparison of imaging techniques within the same patient exactly at the same time point, we expect that this will not have affected our results.

Overall, our study showed that US, in any combination of the evaluated US techniques, is inferior to CE-MRI for the assessment of synovitis in knee OA. The most plausible explanation

for this, is the intrinsic difference between US as a 2D imaging tool that only assesses distinct superficial knee joint areas, and MRI that provides a comprehensive 3D visualization of all areas in the knee. In addition, pressure applied on the skin might also affect the assessment in US imaging, where areas of synovitis could be displaced outside of the imaging plane, although in our study we applied minimal pressure. Finally, using CE-MRI, the enhanced synovium can be clearly distinguished from joint effusion, which in our experience is more difficult with US.

The strengths of our study are that we included patients with all severities of radiographic OA (KL grade 1 to 4), and that we were able to perform a comprehensive range of ultrasound and MRI techniques, including two different contrast-enhanced methods with two different contrast agents on the same day, within a few hours, in as many as 30 patients. Another strength of our study is that we used standardized protocols for the ultrasound acquisition, although we realize that adapted protocols might be more suitable for specific patient groups, e.g. the use of a curved US transducer in patients with a very high BMI. The main limitation of this study is the small sample size from the perspective of statistical analysis, resulting in a small number of patients in each category of synovitis severity, and large measures of variability associated with US grades and diagnostic performance statistics. The low number of subjects per KL grade also precluded subgroup analysis by severity of radiographic OA. However, due to the extensive imaging protocol with two contrast administrations, a larger number of subjects was not feasible. In view of the limited statistical power, our results suggests that, if a sonographic diagnosis of synovitis is necessary, the individual sonographic techniques may only be used complementarily and not as alternatives.

Specifically for CEUS, another limitation was that we were only able to assess one location within the knee for one contrast injection. Furthermore, we did not always detect synovitis with CEUS in cases which were diagnosed with synovitis using GSUS and CE-MRI, although the assumption is that the microbubbles flow through inflamed tissue with increased vascularity. Factors that may possibly account for this are low flow, small size of the vessels and obesity. Another limitation is that we used a double dose of gadolinium contrast agent for the purpose of dGEMRIC, but we believe that this did not affect appearance of synovitis on CE-MRI compared to a single dose of gadolinium. A final limitation is that the scoring of all ultrasound images was performed during the same session, whereas for CE-MRI this was performed independently.

In conclusion, ultrasound has only limited accuracy in detecting synovitis in knee osteoarthritis compared to CE-MRI. When GSUS is combined with PDUS or CEUS, overall diagnostic performance is improved for detecting synovitis with a severity of mild or higher, but not for

synovitis with severity of moderate or higher. From a practical perspective, GSUS is most feasibly combined with PDUS, whereas CEUS is less likely to be useful in most clinical practices.

ACKNOWLEDGMENTS

We would like to thank the ReumaNederland (Dutch Arthrits Foundation, the Netherlands, grant ID: 15-1-205) for the funding provided for this study and GE Healthcare for providing the ultrasound equipment.

REFERENCES

1. Sellam J, Berenbaum F. The role of synovitis in pathophysiology and clinical symptoms of osteoarthritis. *Nat Rev Rheumatol*. 2010;6(11):625-635. doi:10.1038/nrrheum.2010.159
2. Benito MJ, Veale DJ, FitzGerald O, Van Den Berg WB, Bresnihan B. Synovial tissue inflammation in early and late osteoarthritis. *Ann Rheum Dis*. 2005;64(9):1263-1267. doi:10.1136/ard.2004.025270
3. Atukorala I, Kwoh CK, Guermazi A, *et al.* Synovitis in knee osteoarthritis: A precursor of disease? *Ann Rheum Dis*. 2016;75(2):390-395. doi:10.1136/annrheumdis-2014-205894
4. Loeuille D, Sauliere N, Champigneulle J, Rat AC, Blum A, Chary-Valckenaere I. Comparing non-enhanced and enhanced sequences in the assessment of effusion and synovitis in knee OA: Associations with clinical, macroscopic and microscopic features. *Osteoarthr Cartil*. 2011;19(12):1433-1439. doi:10.1016/j.joca.2011.08.010
5. Ohrndorf S, Backhaus M. Musculoskeletal ultrasonography in patients with rheumatoid arthritis. *Nat Rev Rheumatol*. 2013;9(7):433-437. doi:10.1038/nrrheum.2013.73
6. Paczesny Ł, Kruczyński J. Ultrasound of the knee. *Semin Ultrasound CT MR*. 2011;32(2):114-124. doi:10.1053/j.sult.2010.11.002
7. Battaglia V, Cervelli R. Liver investigations: Updating on US technique and contrast-enhanced ultrasound (CEUS). *Eur J Radiol*. 2017;96:65-73. doi:10.1016/j.ejrad.2017.08.029
8. Nicolau C, Ripollés T. Contrast-enhanced ultrasound in abdominal imaging. *Abdom Imaging*. 2012;37(1):1-19. doi:10.1007/s00261-011-9796-8
9. Guermazi A, Roemer FW, Hayashi D, *et al.* Assessment of synovitis with contrast-enhanced MRI using a whole-joint semiquantitative scoring system in people with, or at high risk of, knee osteoarthritis: the MOST study. *Ann Rheum Dis*. 2011;70(5):805-811. doi:10.1136/ard.2010.139618
10. Hartung W, Kellner H, Strunk J, *et al.* Development and evaluation of a novel ultrasound score for large joints in rheumatoid arthritis: One year of experience in daily clinical practice. *Arthritis Care Res (Hoboken)*. 2012;64(5):675-682. doi:10.1002/acr.21574
11. Wakefield RJ, Balint P V., Szkudlarek M, *et al.* Musculoskeletal ultrasound including definitions for ultrasonographic pathology. *J Rheumatol*. 2005;32(12):2485-2487.
12. Klauser A, Franz M, Bellmann Weiler R, *et al.* Contrast-Enhanced Ultrasonography for the Detection of Joint Vascularity in Arthritis – Subjective Grading Versus Computer-Aided Objective Quantification. *Ultraschall der Medizin - Eur J Ultrasound*. 2011;32(S 02):E31-E37. doi:10.1055/s-0031-1281671
13. Youden WJ. Index for rating diagnostic tests. *Cancer*. 1950;3(1):32-35. doi:10.1002/1097-0142(1950)3:1<32::aid-cncr2820030106>3.0.co;2-3
14. de Lange-Brokaar BJE, Ioan-Facsinay A, Yusuf E, *et al.* Association of pain in knee osteoarthritis with distinct patterns of synovitis. *Arthritis Rheumatol*. 2015;67(3):733-740. doi:10.1002/art.38965
15. Philp AM, Davis ET, Jones SW. Developing anti-inflammatory therapeutics for patients with osteoarthritis. *Rheumatology (Oxford)*. 2017;56(6):869-881. doi:10.1093/rheumatology/kew278
16. Song IH, Burmester GR, Backhaus M, *et al.* Knee osteoarthritis. Efficacy of a new method of contrast-enhanced musculoskeletal ultrasonography in detection of synovitis in patients with knee osteoarthritis in comparison with magnetic resonance imaging. *Ann Rheum Dis*. 2008;67(1):19-25. doi:10.1136/ard.2006.067462
17. Rednic N, Tamas M, Fodor D, *et al.* Contrast-Enhanced Ultrasound in Knee Joint Synovitis Measurement (Abstract). In: ESSR Congress; 2012. doi:10.1594/essr2012/P-0063

18. Parry EL, Thomas MJ, Peat G. Defining acute flares in knee osteoarthritis: a systematic review. *BMJ Open*. 2018;8(7):e019804. doi:10.1136/bmjopen-2017-019804
19. Parry EL, Ogollah R, Peat G. "Acute flare-ups" in patients with, or at high risk of, knee osteoarthritis: a daily diary study with case-crossover analysis. *Osteoarthr Cartil*. 2019;27(8):1124-1128. doi:10.1016/j.joca.2019.04.003

CHAPTER 6

Detection of knee synovitis using non-contrast-enhanced qDESS compared with contrast-enhanced MRI

B.A. de Vries, S.J. Breda, B. Sveinsson, E.J. McWalter, D.E. Meuffels, G.P. Krestin, B.A. Hargreaves, G.E. Gold, E.H.G. Oei.

Arthritis Res Ther 2021 Feb; 23(55)

ABSTRACT

INTRODUCTION

To assess diagnostic accuracy of quantitative Double Echo in Steady State (qDESS) MRI for detecting synovitis in knee osteoarthritis (OA).

METHODS

Patients with different degrees of radiographic knee OA were included prospectively. All underwent MRI with both qDESS and contrast-enhanced T1-weighted magnetic resonance imaging (CE-MRI). A linear combination of the two qDESS images can be used to create an image that displays contrast between synovium and the synovial fluid. Synovitis on both qDESS and CE-MRI was assessed semi-quantitatively, using a whole-knee synovitis sum score, indicating no/equivocal, mild, moderate, and severe synovitis. The correlation between sum scores of qDESS and CE-MRI (reference standard) were determined using Spearman's rank correlation coefficient and intraclass correlation coefficient for absolute agreement.

Receiver operating characteristic analysis was performed to assess the diagnostic performance of qDESS for detecting different degrees of synovitis, with CE-MRI as reference standard.

RESULTS

In the 31 patients included, very strong correlation was found between synovitis sum scores on qDESS and CE-MRI (ρ=0.96, p<0.001), with high absolute agreement (0.84 (95% CI 0.14-0.95)). Mean sum score (SD) values on qDESS 5.16 (3.75) were lower than on CE-MRI 7.13 (4.66), indicating systematically underestimated synovitis severity on qDESS. For detecting mild synovitis or higher, high sensitivity and specificity were found for qDESS (1.00 (95% CI 0.80-1.00) and 0.909 (0.571-1.00), respectively). For detecting moderate synovitis or higher, sensitivity and specificity were good (0.727 (95% CI 0.393-0.927) and 1.00 (0.800-1.00), respectively).

CONCLUSIONS

qDESS MRI is able to, however with an underestimation, detect synovitis in patients with knee OA.

INTRODUCTION

Osteoarthritis (OA) is the most common joint disease. In men and women over 60 years, 10% and 13% respectively suffer from symptomatic knee OA.[1] Joint inflammation, characterized by swelling of the synovium and joint effusion, is believed to be a key process of knee OA in half of all OA patients.[2] Synovial inflammation, also referred to as synovitis, already occurs in early OA[3] and plays an important role in OA symptom perception, with odds ratios (ORs) varying between 3.2 and 10.0 for effusion/synovitis.[4,5] Pain is the most prevalent symptom of OA, and is associated with inflammation.[5] Synovitis is also an important predictor of OA progression.[6] Hence, synovitis is considered a potential tissue-specific target for novel anti-inflammatory treatments[7]. In addition, synovitis has been suggested as a predictive factor of knee OA progression in worsening of cartilage damage, with accompanying ORs up to 3.11 for progression of pain on a visual analog scale (VAS) after one year.[8] As the prominent role of synovitis in OA is increasingly recognized, there is growing interest in identifying OA patients with synovitis by means of imaging for the purpose of personalized prognostication and therapy.

The most common method to image OA in routine patient care and large clinical studies consists of radiography, but this primarily only visualizes bony structures and cannot assess synovitis. Magnetic resonance imaging (MRI) is a very suitable method for imaging OA, because it offers a comprehensive assessment of multiple joint tissues involved in OA[9], including direct visualization of articular cartilage, subchondral bone, menisci, ligaments, and joint effusion as a surrogate marker of inflammation. Furthermore, MRI can directly visualize synovitis when an intravenous contrast agent is administered, also referred to as contrast-enhanced MRI (CE-MRI).[10] CE-MRI is currently considered the reference standard for imaging of synovitis, because the direct visualization of thickened synovium is preferred over the assessment of joint effusion and these findings should be treated as two separate entities.[11] Thus, MRI complemented with CE-MRI is an excellent technique to study relationships between synovitis and other OA manifestations. However, because of high costs, longer examination times, and potential health risks associated with the intravenous contrast agent or undergoing repeated examinations, especially in patients with renal insufficiency and allergies, there is reluctance to implement synovitis imaging with CE-MRI in routine clinical MRI protocols and large clinical research studies.[12] These disadvantages of CE-MRI highlight the need for an imaging technique without the use of a contrast agent.

A promising recent innovation in MRI of synovitis is diffusion-weighted imaging with quantitative double-echo in steady-state (qDESS) MRI without the need for a contrast agent, which has higher resolution than conventional diffusion weighted techniques, without off-resonance-induced distortion. qDESS is a 3D gradient-spoiled steady-state sequence, acquiring an echo before and after a spoiler gradient, which are usually combined to one

image in the qDESS and used in the Osteoarthritis Initiative. The advantage of qDESS is that next to the diffusion image it can also be used to get a comprehensive image of an OA knee within 5 minutes.[13] In the 1980s several groups[14–16] showed that the different contrasts of the two echoes is useful, and this was more recently demonstrated by Welsch *et al.*[17] Further modification to[18,19] qDESS by increasing the magnitude of the spoiler gradient between the two echoes and acquiring separate echoes, synovitis can be detected without the need for an intravenous contrast agent, as shown previously by McWalter *et al.*[20] The images have different levels of diffusion weighting, enabling good separation of fluid and surrounding tissues. This work demonstrates the feasibility of visualizing synovitis using qDESS MRI[20]; specifically that qDESS MRI correlates well with CE-MRI in patients with moderate to advanced clinical synovitis.

Therefore, the purpose of this study was to assess the diagnostic performance of qDESS MRI for the assessment of knee synovitis in patients with a varying degree of radiographic knee OA, using CE-MRI as the reference standard. Based on our pilot study, we hypothesized that qDESS MRI has high diagnostic performance, and that the addition of qDESS MRI to clinical scan protocols can be feasibly implemented on a larger scale in prospective clinical studies, in order to assess the prognostic value of synovitis and the response to interventions.

METHODS

Study population

Patients with knee OA were included consecutively from the outpatient clinic of the Department of Orthopedic Surgery. The institutional review board approved the study and informed consent was obtained from all subjects. Patients included for this study were aged over 18 years, with a severity of at least Kellgren & Lawrence (K&L)[21] grade 1 and had clinical suspicion of synovitis based on palpable joint effusion. Exclusion criteria were: previous knee replacement surgery, knee trauma in the preceding six months, absolute and relative contraindications to undergo MRI, pregnancy, renal insufficiency (GFR < 60 mL/min/1.73m^2) and a known allergy to MR gadolinium containing contrast agents.

MR image acquisition

A 3T MR system (Discovery MR750, General Electric Healthcare, Milwaukee, WI, USA) was used with a dedicated 8-channel knee coil (Invivo, Gainesville, FL, USA). For CE-MRI, we applied a sagittal 3D T1-weighted spoiled gradient-echo sequence (SPGR) with fat saturation obtained after the intravenous administration of 0.2 mmol/kg of gadoterate meglumine (Dotarem®, Guerbet, Aulnay-sous-Bois, France). The T1-weighted scan was performed 6 minutes after the intravenous administration of the contrast agent. Scan parameters of the

T1-weighted scan were TR/TE = 10.8/5.4 ms; flip angle = 20°; FOV = 20 × 20cm; slice thickness = 0.5mm; matrix = 512 × 512; receiver bandwidth= ± 62.5 kHz.

qDESS scans were performed directly before CE-MRI, using the sagittal 3D qDESS sequence[18] with TE1 = 9ms and TE2 = 46.7 ms for echoes before and after the spoiler gradient, respectively, TR = 26.0 ms; matrix size 256 x 256; flip angle = 25°; FOV = 20 cm, a slice thickness of 3 mm, and using water-only excitation. Typically, S+ denotes the signal at the first echo, before the spoiler, which mostly has a T1/T2 contrast, while S– denotes the signal at second echo, after the spoiler, which additional T2 and diffusion weighting.[18] The sequence was run with a spoiler gradient of duration 3.4 ms on the slice axis and a gradient area of 15660 μs*G/cm (156 ms*mT/m), providing strong diffusion weighting. This area corresponds to a gradient inducing a phase difference of 20 cycles over the slice. Scan time was approximately 5 minutes. This gave a total of two images per slice (Figure 1).

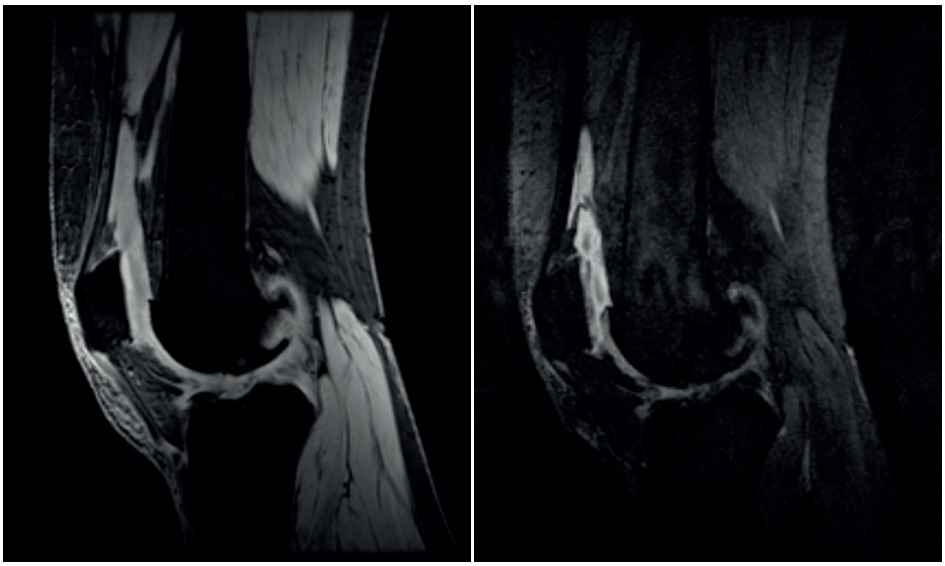

Figure 1: Sagittal qDESS images at the level of the patella, T2 effects dominate the contrast difference between the two echoes S+ (left) and S- (right).

Image processing

CE-MR images were evaluated qualitatively according to the synovitis grading, while the qDESS scans required image processing after acquisition. This image processing was performed using custom software (The MathWorks, Natick, MA, USA) created by McWalter et al[20]. The qDESS images were processed to optimize the contrast between the synovial membrane and synovial fluid. The resulting images was created as a linear combination of the echo 1 (S^+) and echo 2 (S^-) images according to the equation: *Synovitis Image* = $S^+ - \beta S^-$

where S+ and S- are the images on echoes 1 and 2 respectively. The image processing software uses a subtraction ratio, where a coefficient β is used to null the synovial fluid accordingly. Simulations were used to determine β that nulled the fluid signal, using the Extended Phase Graph (EPG) model[22] of the qDESS sequence and known values of T_1 and T_2 relaxation times and diffusivity for synovial fluid (3620 ms, 767 ms and 2.6 μm^2/ms, respectively).[19,23] We found a ratio of β = 2.49, based on EPG calculation with our scan parameters mentioned earlier. Using this ratio and the equation above, synovitis images were created for each patient.

Image grading

Synovitis on both CE-MRI and qDESS images was scored by a musculoskeletal radiologist with 16 years of experience in reading clinical and research knee MRI scans (EO) using the semi-quantitative scoring method described by Guermazi *et al.*[24]. Synovitis was scored at 11 different sites throughout the knee (Table 1), and at each location the synovial membrane was scored based on the maximal thickness on any slice using the following cut-offs: grade 0 if < 2 mm, grade 1 if 2–4 mm and grade 2 if > 4 mm. Subsequently, a whole-knee synovitis sum score was calculated by summing the scores of all 11 sites. The diagnosis of synovitis was based on the whole-knee synovitis sum score, as follows: normal or equivocal synovitis (sum score 0–4); mild synovitis (sum score 5–8); moderate synovitis (sum score 9–12); and severe synovitis (sum score ≥ 13). Scoring of qDESS and CE-MRI images was performed independently and in random order, blinded for patient details. Scans were scored on all scan planes, using reformatted images from the 3D sequences.

Table 1: Sites scored for synovitis according to Guermazi *et al.*[24]

1. Medial parapatellar recess	7. Lateral perimeniscal
2. Lateral parapatellar recess	8. Adjacent to the anterior cruciate ligaments
3. Suprapatellar	9. Adjacent to the posterior cruciate ligaments
4. Infrapatellar	10. Baker's cysts
5. Intercondylar	11. Loose bodies
6. Medial perimeniscal	

Statistical analysis

The correlation between whole-joint synovitis sum scores of qDESS MRI and CE-MRI (reference standard) were determined using Spearman's rank correlation coefficient. Correlation alone is illustrative, therefore more exploratory the intraclass correlation coefficient (ICC) was measured for absolute agreement. A correlation coefficient of 0.40-0.59 is considered as moderate, 0.6-0.79 as strong and 0.8-1 as very strong. Site-specific correlations were also evaluated for all 11 sites separately. Receiver operating characteristic (ROC) analysis was performed to determine the diagnostic performance of the whole-joint synovitis sum score of qDESS MRI, using CE-MRI as the reference standard. Both qDESS and CE-MRI

scores were categorized into two categories using the previously published cut-offs[24] and then a tabulation of these two categorized scores was done. Sensitivity, specificity, positive predictive value (PPV) and negative predictive value (NPV) were calculated along with 95% confidence intervals (CI). First, ROC analyses were performed for the diagnosis of synovitis with severity of mild or higher, moderate or higher, and severe using the original cut-off values as described.[24] Finally, the ROC analysis was repeated with adjusted cut-off values of the qDESS whole-joint sum score, based on Youden's index.[25] A p value of <0.05 was considered statistically significant. Statistical analysis was performed using SPSS (version 25, IBM Corp., Armonk, NY, USA).

RESULTS

Thirty-one patients (14 females and 17 males; mean age 58 years) were included in this study, of which 6 (19%) had radiographic OA with a severity of K&L grade 1, 10 (32%) had K&L grade 2, 8 (26%) had K&L grade 3, and 7 (23%) had end-stage grade 4 radiographic OA. Baseline characteristics are presented in Table 2.

Table 2: Baseline patient characteristics.

Parameter	Value
No. of patients Males Females	31 14 17
Mean age in years ± SD	58 ± 10
Mean BMI in kg/m^2 ± SD	27.5 ± 4.4
Symptomatic knee Left Right	 15 16
Radiographic OA severity (K&L grade)	
Grade 0	0
Grade 1	6
Grade 2	10
Grade 3	8
Grade 4	7

Imaging findings

On CE-MRI, 11 (35.5%) patients had no synovitis, 9 (29.0%) had mild synovitis, 6 (19.4%) had moderate synovitis and 5 (16.1%) had severe synovitis. On qDESS MRI, 10 out of 31 patients (32.3%) had no synovitis, 13 (41.9%) had mild synovitis, 8 (25.8%) had moderate

synovitis and none had severe synovitis, when the cut-off values of the whole-joint synovitis sum scores were used as defined by Guermazi *et al.*[24]. qDESS MRI whole-knee sum score showed a mean (SD) of 5.16 (3.75) compared to 7.13 (4.66) for CE-MRI whole-knee. Representative qDESS and CE-MRI images are shown in Figure 2 and Figure 3.

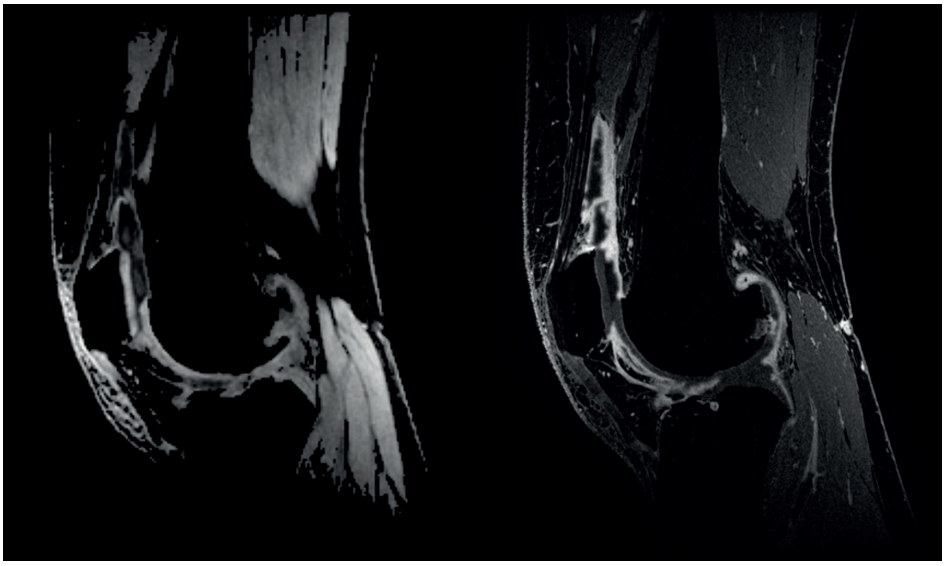

Figure 2: Sagittal qDESS hybrid difference image (left) and CE-MRI (right), both at the level of the patella.

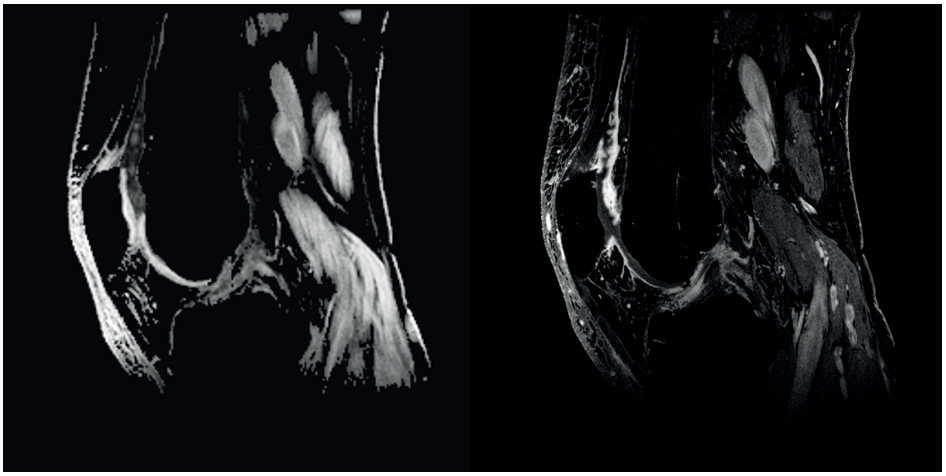

Figure 3: Sagittal qDESS hybrid difference image (left) and CE-MRI (right), both at the level of the origin of anterior cruciate ligament.

Correlation analysis

Very strong correlation was found between whole-joint synovitis sum scores of qDESS and CE-MRI (Spearman's rank correlation coefficient 0.96 (95% CI 0.91-0.98), $p < 0.001$)). The scatterplot of all datapoints can be found in Figure 4. The ICC for absolute agreement was 0.84 (95% CI 0.14-0.95) (Table 3).

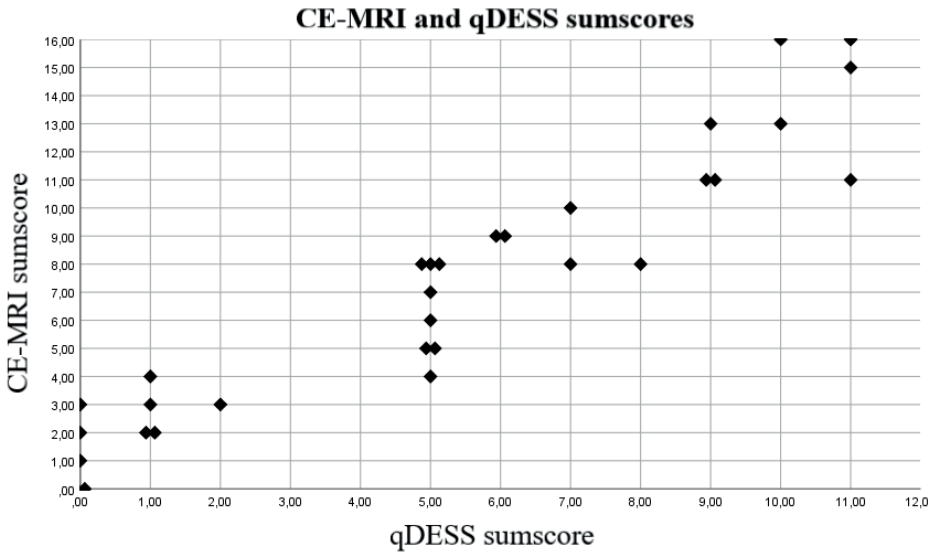

Figure 4: Scatterplot of Guermazi sumscores from both CE-MRI and qDESS.

Table 3: Site-specific correlations.

	Spearman's correlation (*p* value)	ICC absolute agreement (95% CI)
1. Medial parapatellar recess	0.74 (<0.001)	0.70 (0.45-0.84)
2. Lateral parapatellar recess	0.82 (<0.001)	0.81 (0.65-0.91)
3. Suprapatellar	0.89 (<0.001)	0.85 (0.71-0.93)
4. Infrapatellar	0.60 (<0.001)	0.49 (0.09-0.74)
5. Intercondylar	0.41 (0.022)	0.30 (-0.02-0.57)
6. Medial perimeniscal	0.52 (0.003)	0.44 (0.08-0.69)
7. Lateral perimeniscal	0.67 (<0.001)	0.58 (0.22-0.78)
8. Adjacent to the anterior cruciate ligaments	0.65 (<0.001)	0.59 (0.30-0.78)
9. Adjacent to the posterior cruciate ligaments	0.84 (<0.001)	0.83 (0.68-0.92)
10. Baker's cysts	0.95 (<0.001)	0.97 (0.93-0.98)
11. Loose bodies	not applicable	not applicable
Whole-joint synovitis sum score	0.96 (<0.001)	0.84 (0.14-0.95)

When each of the 11 regions was analyzed individually, the highest correlations (> 0.8) were observed for the lateral parapatellar recess, suprapatellar, adjacent to the posterior cruciate ligament, and in Baker's cyst. Correlation was low for the intercondylar site (Table 3). There were no patients who had synovial thickening around a loose body.

ROC analysis

The results of the ROC analyses are shown in Table 4. The diagnostic performance of qDESS MRI for detecting mild or higher degree of synovitis showed an AUC (std. error) of 0.98 (0.02), using the original cut-off values, with an accompanying sensitivity and specificity of 1.00 (95% CI 0.80-1.00) and 0.91 (95% CI 0.57-1.00), respectively. For detection of severe synovitis, however, a sensitivity of 0 (95% CI 0-0.537) was found and a specificity of 1.00 (0.84-1.00). After adjusting the cut-off values, the cut-off values changed from 5 to 4, 9 to 6, and 13 to 9, for mild or higher, moderate or higher, and severe synovitis, respectively. Also, the sensitivity and specificity changed after cut-off adjustment, especially for severe synovitis, where the sensitivity increased to 1.00 (95% CI 0.46-1.00) and specificity increased to 0.89 (95% CI 0.69-0.97). The results of the ROC analysis after optimization are shown in Table 5.

DISCUSSION

Our findings have shown that the qDESS synovitis images can differentiate between the synovial membrane and joint effusion, with high correlation for mild and moderate synovitis. While the contrast between the synovial fluid and membrane for the qDESS synovitis images are visually not as good as the T1-weighted contrast-enhanced sequence images, the synovial membrane is clearly distinguishable. qDESS systematically underestimated synovitis severity compared to CE-MRI. Adjustment of the cut-off values increased the agreement of qDESS, especially for severe synovitis.

In this study we included patients with knee OA ranging from K&L 1-4, whereas in a previous pilot study[20] data of patients with knee OA K&L 2 or 3 was analyzed. We believe that, because of its non-contrast properties, DESS ultimately holds promise as an (early) OA imaging biomarker that can be applied routinely in clinical patient care and research. It can be implemented widely in existing MRI protocols, and become a useful addition to the multi-tissue capability of MRI for OA assessment. The inclusion of a technique capable of visualizing synovitis in MRI protocols may facilitate identification of patients with an 'inflammatory' OA phenotype who may benefit from targeted anti-inflammatory treatment.

Lower synovial scores were found using qDESS than using CE-MRI. A possible explanation for this could be that diffusion parameters measured by qDESS on the edges of synovial

Table 4: Diagnostic performance of qDESS MRI for mild, moderate and severe synovitis.

Synovitis grade based on CE-MRI	AUC (std. error)	Cut-off value of whole-joint synovitis sum score[24]	TP	TN	FP	FN	Sensitivity (95% CI)	Specificity (95% CI)	PPV (95% CI)	NPV (95% CI)
Mild or higher (n=20)	0.98 (0.02)	=>5	20	10	1	0	1.00 (0.80-1.00)	0.91 (0.57-1.00)	0.95 (0.74-1.00)	1.00 (0.66-1.00)
Moderate or higher (n=11)	0.98 (0.02)	=>9	8	20	0	3	0.73 (0.39-0.93)	1.00 (0.80-1.00)	1.00 (0.60-1.00)	0.87 (0.65-0.97)
Severe (n=5)	0.96 (0.03)	=>13	0	26	0	5	0 (0-0.54)	1.00 (0.84-1.00)	-	0.84 (0.66-0.94)

AUC: Area Under the Curve; TP: True Positive; TN: True Negative; FP: False Positive; FN: False Negative; PPV: Positive Predictive Value; NPV: Negative Predictive Value

Table 5: Diagnostic performance of qDESS MRI for mild, moderate and severe synovitis using adapted cut-offs values of whole-joint synovitis sum score.

Synovitis grade based on CE-MRI	AUC (std. error)	Optimized cut-off value of whole-joint synovitis sum score	TP	TN	FP	FN	Sensitivity (95% CI)	Specificity (95% CI)	PPV (95% CI)	NPV (95% CI)
Mild or higher (n=20)	0.98 (0.02)	=>4	20	10	1	0	1.00 (0.80-1.00)	0.91 (0.57-1.00)	0.95 (0.74-1.00)	1.00 (0.66-1.00)
Moderate or higher (n=11)	0.98 (0.02)	=>6	11	18	2	0	1.00 (0.68-1.00)	0.90 (0.67-0.98)	0.85 (0.54-0.97)	1.00 (0.78-1.00)
Severe (n=5)	0.96 (0.03)	=>9	5	23	3	0	1.00 (0.46-1.00)	0.89 (0.69-0.97)	0.63 (0.26-0.90)	1.00 (0.82-1.00)

AUC: Area Under the Curve; TP: True Positive; TN: True Negative; FP: False Positive; FN: False Negative; PPV: Positive Predictive Value; NPV: Negative Predictive Value

tissue are almost equal to synovial fluid, which makes the synovial tissue look smaller on qDESS than on CE-MRI. Further optimization of the qDESS technique, both with regard to the acquisition and image processing may in future reduce the systematic underestimation of synovitis severity.

There are other non-CE-MRI scoring methods, such as WORMS[26], KOSS[27], BLOKS[28], and MOAKS[29], that do not require a contrast agent. However, all these methods score synovitis indirectly based on a combination of both effusion and synovial hypertrophy.

Diffusion Tensor Imaging (DTI) is another technique that can image synovitis in knee OA non-invasively, without using a contrast agent. It is used to study the structure of biological tissue. The idea of using DTI for knee synovitis is based on previous experience in brain imaging, where high Fractional Anisotropy (FA) is positively correlated with pro-inflammatory cytokines. Agarwal *et al.*[30] found that the synovium showed higher FA values compared to surrounding tissue. Double inversion recovery (DIR) MRI is another method, which enables the evaluation of inflamed synovium by simultaneously suppressing fat signal and water signal intensity of the joint effusion.[31–33] Also, a recent study showed that using fluid attenuation inversion recovery (FLAIR) MRI, by nullifying the fluid signal, inflamed synovium was detectable without using a contrast agent.[34] Ultrasound is an alternative imaging modality to assess synovitis. However, although ultrasound may be particularly useful to diagnose synovitis, it has limitations with regard to quantitative assessment. Also, while MRI allows the evaluation of all potential locations of synovitis in the knee joint, both superficial and deep, ultrasound can only visualize superficial areas.

The strengths of our study are that we included patients with all severities of radiographic OA (K&L grade 1 to 4), and that we were able to perform different MRI sequences, including contrast-enhanced MRI in as many as 31 patients. 31 patients can also be seen as a low amount, however in this study it is enough as it is mostly exploratory. There are certain other limitations to our study. First, the data presented in this manuscript is cross-sectional; therefore, no link regarding disease progression could be made. Second, to create the qDESS synovitis images, some minor post processing is required. However, we believe that these are technical issues can be addressed relatively easily, and we expect that the demonstration of good diagnostic performance by this and other studies may accelerate the translation of the adapted qDESS sequence and post processing algorithms. No histology was assessed in this study, however we think that arthroscopic biopsy is not the best reference method because the most important thing we want to know in this study is the load of the inflammation, which cannot be assessed using biopsy. Another limitation is that the scan time of qDESS sequence is around 5 minutes. The acquisition takes this long, due to the multiple echoes that are required for the diffusivity, and also the very large FOV used in this study played a

role. However, this version of qDESS can also be used to assess the T2 relaxation times and apparent diffusion coefficient of cartilage.[18,19] However, as there is no need for a contrast agent, total examination time is shorter than CE-MRI. Finally, we did not externally validate our results in an independent cohort, which we consider an essential next step in the evaluation of qDESS in follow-up research. As a further consideration, the optimal unenhanced MRI technique to depict synovitis is not yet known and future research should continue to investigate the different unenhanced MRI techniques and compare with qDESS MRI.

CONCLUSIONS

In conclusion, synovitis detection is possible without the need for an intravenous contrast agent by using hybrid images created using qDESS MRI. Redefinition of cut-off values is needed for this scoring, because qDESS consistently shows slight underdetection compared to CE-MRI.

ACKNOWLEDGEMENTS

We would like to thank the Dutch Arthritis Society for the funding provided for this study.

REFERENCES

1. Zhang Y, Jordan JM. Epidemiology of osteoarthritis. *Clin Geriatr Med*. 2010;26(3):355-369. doi:10.1016/j.cger.2010.03.001
2. Sellam J, Berenbaum F. The role of synovitis in pathophysiology and clinical symptoms of osteoarthritis. *Nat Rev Rheumatol*. 2010;6(11):625-635. doi:10.1038/nrrheum.2010.159
3. Benito MJ, Veale DJ, FitzGerald O, Van Den Berg WB, Bresnihan B. Synovial tissue inflammation in early and late osteoarthritis. *Ann Rheum Dis*. 2005;64(9):1263-1267. doi:10.1136/ard.2004.025270
4. de Lange-Brokaar BJE, Ioan-Facsinay A, Yusuf E, *et al.* Association of pain in knee osteoarthritis with distinct patterns of synovitis. *Arthritis Rheumatol (Hoboken, NJ)*. 2015;67(3):733-740. doi:10.1002/art.38965
5. Yusuf E, Kortekaas MC, Watt I, Huizinga TWJ, Kloppenburg M. Do knee abnormalities visualised on MRI explain knee pain in knee osteoarthritis? A systematic review. *Ann Rheum Dis*. 2011;70(1):60-67. doi:10.1136/ard.2010.131904
6. Atukorala I, Kwoh CK, Guermazi A, *et al.* Synovitis in knee osteoarthritis: A precursor of disease? *Ann Rheum Dis*. 2016;75(2):390-395. doi:10.1136/annrheumdis-2014-205894
7. Ashraf S, Radhi M, Gowler P, *et al.* The polyadenylation inhibitor cordycepin reduces pain, inflammation and joint pathology in rodent models of osteoarthritis. *Sci Rep*. 2019;9(1):4696. doi:10.1038/s41598-019-41140-1
8. Ayral X, Pickering EH, Woodworth TG, Mackillop N, Dougados M. Synovitis: A potential predictive factor of structural progression of medial tibiofemoral knee osteoarthritis - Results of a 1 year longitudinal arthroscopic study in 422 patients. *Osteoarthr Cartil*. 2005;13(5):361-367. doi:10.1016/j.joca.2005.01.005
9. De Lange-Brokaar BJE, Ioan-Facsinay A, Yusuf E, *et al.* Degree of synovitis on MRI by comprehensive whole knee semi-quantitative scoring method correlates with histologic and macroscopic features of synovial tissue inflammation in knee osteoarthritis. *Osteoarthr Cartil*. 2014;22(10):1606-1613. doi:10.1016/j.joca.2013.12.013
10. Loeuille D, Sauliere N, Champigneulle J, Rat AC, Blum A, Chary-Valckenaere I. Comparing non-enhanced and enhanced sequences in the assessment of effusion and synovitis in knee OA: Associations with clinical, macroscopic and microscopic features. *Osteoarthr Cartil*. 2011;19(12):1433-1439. doi:10.1016/j.joca.2011.08.010
11. Hayashi D, Roemer FW, Katur A, *et al.* Imaging of synovitis in osteoarthritis: current status and outlook. *Semin Arthritis Rheum*. 2011;41(2):116-130. doi:10.1016/j.semarthrit.2010.12.003
12. Guo BJ, Yang ZL, Zhang LJ. Gadolinium Deposition in Brain: Current Scientific Evidence and Future Perspectives. *Front Mol Neurosci*. 2018;11:335. doi:10.3389/fnmol.2018.00335
13. Chaudhari AS, Black MS, Eijgenraam S, *et al.* Five-minute knee MRI for simultaneous morphometry and T 2 relaxometry of cartilage and meniscus and for semiquantitative radiological assessment using double-echo in steady-state at 3T. *J Magn Reson Imaging*. 2018;47(5):1328-1341. doi:10.1002/jmri.25883
14. Redpath TW, Jones RA. FADE–A new fast imaging sequence. *Magn Reson Med*. 1988;6(2):224-234. doi:10.1002/mrm.1910060211
15. Lee SY, Cho ZH. Fast SSFP gradient echo sequence for simultaneous acquisitions of FID and echo signals. *Magn Reson Med*. 1988;8(2):142-150. doi:10.1002/mrm.1910080204
16. Redpath TW, Jones RA. FADE-A new fast imaging sequence. *Magn Reson Med*. 1988;6(2):224-234. doi:10.1002/mrm.1910060211

17. Welsch GH, Scheffler K, Mamisch TC, *et al.* Rapid estimation of cartilage T2 based on double echo at steady state (DESS) with 3 Tesla. *Magn Reson Med*. 2009;62(2):544-549. doi:10.1002/mrm.22036
18. Staroswiecki E, Granlund KL, Alley MT, Gold GE, Hargreaves BA. Simultaneous Estimation of T2 and ADC in Human Articular Cartilage In Vivo with a Modified 3D DESS Sequence at 3 T. *Magn Reson Med*. 2012;67(4):1086-1096. doi:10.1016/j.pestbp.2011.02.012.Investigations
19. Bieri O, Ganter C, Scheffler K. Quantitative in vivo diffusion imaging of cartilage using double echo steady-state free precession. *Magn Reson Med*. 2012;68(3):720-729. doi:10.1002/mrm.23275
20. McWalter EJ, Sveinsson B, Oei EHG, Robinson WH, Genovese MC, Gold GE. Non-contrast diffusion-weighted MRI for detection of synovitis using DESS. In: Milan, Italy: 22nd Int Soc Magn Reson Med Annu Meet Milan; 2014.
21. Kellgren JH, Lawrence JS. Radiological assessment of osteo-arthrosis. *Ann Rheum Dis*. 1957;16(4):494-502. doi:10.1136/ard.16.4.494
22. Hennig J, Weigel M, Scheffler K. Calculation of flip angles for echo trains with predefined amplitudes with the extended phase graph (EPG)-algorithm: Principles and applications to hyperecho and TRAPS sequences. *Magn Reson Med*. 2004;51(1):68-80. doi:10.1002/mrm.10658
23. Gold GE, Han E, Stainsby J, Wright G, Brittain J, Beaulieu C. Musculoskeletal MRI at 3.0 T: relaxation times and image contrast. *AJR Am J Roentgenol*. 2004;183(2):343-351. doi:10.2214/ajr.183.2.1830343
24. Guermazi A, Roemer FW, Hayashi D, *et al.* Assessment of synovitis with contrast-enhanced MRI using a whole-joint semiquantitative scoring system in people with, or at high risk of, knee osteoarthritis: the MOST study. *Ann Rheum Dis*. 2011;70(5):805-811. doi:10.1136/ard.2010.139618
25. Youden WJ. Index for rating diagnostic tests. *Cancer*. 1950;3(1):32-35. doi:10.1002/1097-0142(1950)3:1<32::aid-cncr2820030106>3.0.co;2-3
26. Peterfy CG, Guermazi A, Zaim S, *et al.* Whole-Organ Magnetic Resonance Imaging Score (WORMS) of the knee in osteoarthritis. *Osteoarthr Cartil*. 2004;12(3):177-190. doi:10.1016/j.joca.2003.11.003
27. Kornaat PR, Ceulemans RYT, Kroon HM, *et al.* MRI assessment of knee osteoarthritis: Knee Osteoarthritis Scoring System (KOSS)--inter-observer and intra-observer reproducibility of a compartment-based scoring system. *Skeletal Radiol*. 2005;34(2):95-102. doi:10.1007/s00256-004-0828-0
28. Hunter DJ, Lo GH, Gale D, Grainger AJ, Guermazi A, Conaghan PG. The reliability of a new scoring system for knee osteoarthritis MRI and the validity of bone marrow lesion assessment: BLOKS (Boston Leeds Osteoarthritis Knee Score). *Ann Rheum Dis*. 2008;67(2):206-211. doi:10.1136/ard.2006.066183
29. Hunter DJ, Guermazi A, Lo GH, *et al.* Evolution of semi-quantitative whole joint assessment of knee OA: MOAKS (MRI Osteoarthritis Knee Score). *Osteoarthr Cartil*. 2011;19(8):990-1002. doi:10.1016/j.joca.2011.05.004
30. Agarwal V, Kumar M, Singh JK, Rathore RKS, Misra R, Gupta RK. Diffusion tensor anisotropy magnetic resonance imaging: a new tool to assess synovial inflammation. *Rheumatology*. 2009;48(4):378-382. doi:10.1093/rheumatology/ken499
31. Son YN, Jin W, Jahng G-H, *et al.* Efficacy of double inversion recovery magnetic resonance imaging for the evaluation of the synovium in the femoro-patellar joint without contrast enhancement. *Eur Radiol*. 2018;28(2):459-467. doi:10.1007/s00330-017-5017-3

32. Yi J, Lee YH, Song H-T, Suh J-S. Double-inversion recovery with synthetic magnetic resonance: a pilot study for assessing synovitis of the knee joint compared to contrast-enhanced magnetic resonance imaging. *Eur Radiol*. 2019;29(5):2573-2580. doi:10.1007/s00330-018-5800-9
33. Jahng G-H, Jin W, Yang DM, Ryu KN. Optimization of a double inversion recovery sequence for noninvasive synovium imaging of joint effusion in the knee. *Med Phys*. 2011;38(5):2579-2585. doi:10.1118/1.3581060
34. Yoo HJ, Hong SH, Oh HY, *et al.* Diagnostic Accuracy of a Fluid-attenuated Inversion-Recovery Sequence with Fat Suppression for Assessment of Peripatellar Synovitis: Preliminary Results and Comparison with Contrast-enhanced MR Imaging. *Radiology*. 2017;283(3):769-778. doi:10.1148/radiol.2016160155

CHAPTER 7

GENERAL DISCUSSION

DISCUSSION

Knee osteoarthritis (OA) is expected to be characterized by early changes in perfusion due to inflammation. This can be observed by changes in the synovium, infrapatellar fat pad (IPFP), and in the subchondral bone. This thesis focused on imaging, to study the role of inflammation in knee OA. In this chapter, the clinical implications of different imaging techniques are discussed and future perspectives are provided.

PATIENT POPULATIONS

In **Chapter 2** we included patients with varying knee OA grades, however all these patients had unicompartmental knee OA. This population is therefore unique as it allowed us to analyze two knee compartments with different OA severity and biomechanical loading within the same patient. Analyzing differences within the same patient also has advantages for the statistical analysis, since many potentially confounding factors related to patient characteristics are not an issue.

Although in **Chapters 2 to 4** we used different patient populations included in two prospective clinical studies, one case-control study on PFP (Triple-P study) and one observational study on OA, the same MRI scanner and identical DCE-MRI scan parameters were used. This allowed us to directly compare results of the quantitative DCE-MRI analysis from across the two studies and perform an integrative analysis of healthy volunteers, PFP patients and OA patients in **Chapter 4**.

In our most recent study, the Diagnostic Imaging for Knee Osteoarthritis (DISKO) study, we included patients with a wide range of knee OA. This study, described in **Chapters 5 and 6**, was unique as we were able to perform many different imaging techniques. Moreover, we were able to administer two contrast agents, one for MRI and one for ultrasound, during the same day.

DCE-MRI TO INVESTIGATE INFLAMMATION IN KNEE OA

The first part of this thesis focused on investigating features of knee OA that are believed to be associated with inflammation, because the significance of inflammation in the pathogenesis and symptom perception of OA is increasingly understood.[1–3] Increased blood perfusion, which can be evaluated by dynamic contrast-enhanced (DCE) MRI, has been considered a surrogate measure of inflammation for a variety of musculoskeletal tissues.[4–9] Hence, we applied a quantitative DCE-MRI technique to analyze increased blood perfusion in subchondral bone, bone marrow lesions (BMLs), the IPFP as a whole, and $T2_{FS}$ hyperintense IPFP lesions. After applying a pharmacokinetic model to the data, DCE-MRI provides two main robust quantitative outcome parameters, Ktrans and Kep, which describe the local tissue

perfusion.[10] Ktrans reflects the volume transfer constant, which is a measure of the volume transfer constant between blood plasma and extracellular extravascular space (EES)[11], while Kep represents the rate constant from the EES to the vascular component.

In **Chapter 2** we showed that Ktrans and Kep of both epimetaphyseal and subchondral bone were significantly higher in the most affected compartment than in the least affect compartment in patients with predominantly unicompartmental knee OA. In addition, subchondral BMLs were associated with higher Ktrans and Kep compared to subchondral bone regions without BMLs. BMLs were found to likely account for most of the effect of the higher bone perfusion in knee OA.

Since patellofemoral pain (PFP) is seen as a possible precursor of knee OA[12,13], we analyzed blood perfusion also in patients with PFP. In **Chapter 3** we found that infrapatellar fat pad (IPFP) volume, Ktrans and Vp (the vascular fraction) within the whole IPFP were not different between healthy control subjects and patients with PFP. This was in contrast to our initial hypothesis, which was that PFP would also have an inflammatory component manifested in the IPFP. In **Chapter 4**, we found that $T2_{FS}$-hyperintense regions of the IPFP demonstrated higher quantitative DCE-MRI blood perfusion parameters compared to adjacent tissue with normal signal intensity in patients with knee OA. However, in patients with PFP and healthy control subjects, in which such lesions are also commonly found, we did not find increased blood perfusion. This was contrary to our hypothesis and suggests a different underlying mechanism of IPFP $T2_{FS}$-hyperintense regions across patient subgroups, in which an inflammatory pathogenesis is only present in OA.

Altogether, the results of **Chapters 2-4** suggest that in knee OA the blood perfusion within different lesions in the knee are increased, related to inflammation. This increase in perfusion was not seen in knee lesions within patients with PFP.

TECHNICAL CONSIDERATIONS FOR DCE-MRI

The results of our study described in **Chapter 2** were in concordance with the study of Budzik *et al.*[14], who also showed higher perfusion parameters in OA bone than in non-OA bone. However, Budzik used a simplified, model-free, DCE-MRI analysis. In our opinion the use of a pharmacokinetic model, such as we used in our studies in **Chapter 2, Chapter 3,** and **Chapter 4**, is preferred. Using a pharmacokinetic model makes the perfusion analysis quantitative and provides parameters that are more suitable to compare different patients. Aaron *et al.*[15] studied OA bone perfusion in osteoarthritic bone in the human knee with DCE-MRI, using software based on the Brix pharmacokinetic model. However, in the Brix model, no arterial input function (AIF) is used. Even when a pharmacokinetic model is used, we think it is important to make the model more specific for the patient group studied, by

applying an AIF. In a prior study, it has been demonstrated that the Tofts pharmacokinetic model renders better results than Brix.[16] In that same study it was recommended to use a groupwise or an subject specific AIF, and we chose for the latter.

In all of the described studies, we applied the Tofts model by using the DCE-tool in Horos (Osirix based imaging platform).[17] In this DCE-tool we used a subject-specific AIF, since a group-wise AIF is not yet available within the DCE-tool. From a previous study based on the same DCE-MRI acquisition technique, we know that a group wise AIF is slightly favorable over a subject specific AIF.[16] The reason is a risk of missing the arterial bolus when using a subject-specific AIF, related to the temporal resolution of 10 seconds. However, to overcome this problem we visually checked all AIF curves, and thereafter adapted the AIF arterial region, if needed, to capture the bolus peak adequately.

In our studies we could only include a DCE-MR scan acquisition limited to six minutes due to time constraints. The limitation of such a short acquisition is that the contrast plateau might not be reached. In some cases, especially in **Chapter 3** and **Chapter 4,** this plateau was indeed not reached in the IPFP. Although the Kep value will be affected when the plateau is not reached, we still think that this parameter is still valid as an outcome of these studies, because this limitation applies to both groups and we did not perform any longitudinal measures. The Ktrans perfusion parameter is calculated based on the primary inflow, therefore this parameter is more robust than Kep with shorter scan times.

DIAGNOSTIC ACCURACY OF IMAGING TECHNIQUES FOR VISUALIZATION OF SYNOVITIS IN KNEE OA

In this part of the thesis, we assessed the diagnostic accuracy of a wide range of imaging techniques for visualization of synovitis in the knee in the prospective DISKO study where we were able to apply a wide range of imaging techniques in the same patients. We believed that identifying a combination of accurate and feasible imaging techniques is highly relevant because it is known that synovitis, even in the early stages of knee OA, plays an important role in the perception of symptoms and is an important predictor of OA progression.[18,19,20] The most accepted hypothesis is that, once degraded, cartilage fragments come into the joint and in contact with the synovium. The synovium reacts by producing inflammatory mediators, released in the synovial fluid. These mediators increase angiogenesis and can activate chondrocytes, which eventually can lead to the increase in degradation of the cartilage.[21] A vicious cycle follows.

To overcome the limitations of conventional imaging techniques that visualize a combination of the synovial membrane and the synovial fluid, a surrogate measure of synovitis, we

focused on techniques that are able to directly visualize the synovium and offer a more precise assessment of synovitis, using CE-MRI as the reference standard.

In **Chapter 5** we observed that the diagnostic accuracy of grayscale (GSUS), power Doppler (PDUS) and contrast-enhanced ultrasound (CEUS) for detecting synovitis in knee OA, was lower compared to CE-MRI. GSUS showed the highest overall diagnostic performance compared to PDUS and CEUS when analyzed separately.

One previous study by Song *et al.*[22] evaluated GSUS, PDUS and CEUS in comparison with CE-MRI in a population of 41 patients with painful knee OA. Our finding that PDUS has higher sensitivity than GSUS, however with a lower specificity, is in agreement with their study.

We expected that the inflammation within the knee could be seen better using PDUS and CEUS, where these two methods potentially could detect perfusion increases. However, in our study we could not confirm this hypothesis. One possible reason for this would be some of the patients had no 'active' state of synovitis, which is seen most in rheumatoid arthritis.[23]

Even knowing that the diagnostic accuracy of ultrasound is lower than CE-MRI, it remains an attractive alternative. Ultrasound is more readily available, less costly and faster.

In **Chapter 6** we found that synovitis detection is possible without the need for an intravenous contrast agent by using hybrid images created with quantitative dual echo steady state (qDESS) MRI. The fact that qDESS could differentiate between the synovial membrane and joint effusion, showing 'real synovitis', is very promising. Still, the contrast between the synovial fluid and membrane for the qDESS synovitis images is visually not as good as for the contrast-enhanced T1-weighted images on which the synovial membrane is more clearly distinguishable.

For both studies we used a semiquantitative scoring method for synovitis as described by Guermazi *et al.*[24], which was designed as a specific scoring tool for directly visualized synovium on CE-MRI. Because qDESS consistently showed slight underestimation of synovitis degree compared to CE-MRI, redefinition of cut-off values is needed for synovitis scoring on qDESS. Other scoring methods for synovitis have been integrated in various semi-quantitative scoring systems that assess many knee OA features in different tissues. Examples of these are Whole-Organ Magnetic Resonance Imaging Score (WORMS)[25], Knee Osteoarthritis Scoring System (KOSS)[26], Boston Leeds Osteoarthritis Knee Score (BLOKS)[27], and MRI Osteoarthritis Knee Score (MOAKS)[28]. Since these scoring methods are all based on non-contrast MRI, they all score synovitis indirectly based on a combination of both joint effusion and synovial hypertrophy assessed on T2- and proton density weighted images.

In **Chapter 5** and **Chapter 6** we included only patients with clinical palpable effusion synovitis, however still some of these patients did not have any thickened synovium or even effusion on imaging. A possible explanation may be the fluctuating pattern of inflammatory OA manifestations like effusion and synovial hypertrophy, leading to so-called, 'flares', a sudden and temporary increase in joint pain and other symptoms.[29] Because of the delay between clinical examination and imaging in our study, we might not have captured the flare at the time of imaging, whereas the clinical examination may have corresponded more closely to clinical symptoms of inflammation. Still we think that the effects of these flares on our results are limited, because the compared techniques were performed on the same day within the same patient. Therefore, the amount of synovitis should theoretically not have any influence on our diagnostic performance results.

GOLD STANDARD FOR SYNOVITIS ASSESSMENT

This thesis mainly focused on imaging synovitis, although in the literature histological assessment of the synovial tissue is still considered as the 'gold standard' for the diagnosis of synovitis. Microscopical assessment of synovial tissue is documented in several studies, using different techniques. The synovial biopsies can be stained with hematoxylin, eosin or VIII (immunohistochemistry) before microscopic analysis. Inflammatory cell infiltrates, synovial lining layer thickness, fibrosis and degree of vascularity are features that can be scored. The biopsies can also be examined with immune reagents, using monoclonal antibodies binding T cells (CD2), T helper cells (CD4), T suppressor cells (CD8), B cells (CD19), DR positive cells (I3), and macrophage subset (RM3/1). Histology of synovium as a comparator for imaging techniques in knee OA is not often used.[30–37] While histology has many advantages, it has one major drawback, as it is an invasive technique. Therefore, it is not feasible to perform histological analysis in large studies and in clinical care, and imaging remains the most important tool for assessment of synovitis.

CLINICAL IMPLICATIONS

Inflammatory lesions, seen as altered perfusion regions, described in **Chapters 2-4**, should get more attention within the clinical practice, as they are closely related to inflammation and OA progression.

In situations where a MRI or CE-MRI is not directly indicated, ultrasound could still be useful to detect synovitis in knee OA. According to recent insights, identifying patients with synovitis through imaging is crucial in order to initiate targeted anti-inflammatory therapy and prevent progression of OA.[38]

We believe that when qDESS or a comparable imaging technique is added to existing knee MRI protocols, this will yield important additional information allowing radiologists to de-

scribe the OA status more comprehensively. With this information, treating physicians will be able to tailor therapies more towards the individual patient in a personalized medicine approach, e.g. focused on anti-inflammatory treatment in patients with OA characterized by synovitis demonstrated with qDESS MRI who are at risk for rapid OA progression.

CONCLUSIONS

In conclusion, this thesis contributes to the knowledge of perfusion imaging in patients with knee OA. Perfusion can be quantified using both conventional contrast-enhanced MRI and with a novel, non-contrast-enhanced, MRI sequence. Significant differences in perfusion between patients with and without knee OA were observed. The clinical implications of these findings should be investigated in future studies.

FUTURE RESEARCH

Using a cross-sectional study design, we found higher perfusion within BMLs in **Chapter 2** and higher perfusion within $T2_{FS}$-hyperintense IPFP lesions in **Chapter 4**. In future research, to explore the utility of DCE-MRI for clinical practice, it would be very interesting to evaluate the predictive value of highly perfused BMLs and $T2_{FS}$ hyperintense lesions in the IPFP for progression of OA. Given the fact that inflammation is presumed to be an important factor in OA progression, these lesions may be associated with structural OA changes, and with higher rates of cartilage degeneration over time in the overlying cartilage layer. Also it would be interesting to examine the perfusion of BMLs and $T2_{FS}$-hyperintense IPFP lesions in a population with a wider range of clinical OA severity, to evaluate the diagnostic value of both BMLs and $T2_{FS}$-hyperintense lesions and their perfusion characteristics in classifying patients with unknown OA status, and to study the relationship of perfusion parameters with clinical symptoms.

In our DISKO study described in **Chapter 5** and **Chapter 6** we not only performed ultrasound and CE-MRI, but also DCE-MRI. However, DCE-MRI data have not yet been analyzed. Hopefully in the near future this can still be performed, as we used a new DCE-MRI sequence, the DIfferential Subsampling with Cartesian Ordering (DISCO) sequence[39], which offers images with high spatial resolution scans combined with a high temporal resolution. We included a variety of different knee OA grade, which makes this study particularly suitable to study the DCE-MRI derived perfusion parameters across the range of OA grades.

Inflammation in knee OA is accompanied by angiogenesis, leading to increased perfusion visible on imaging. From animal studies it is known that targeting this angiogenesis induces a reduction in inflammation, cartilage damage, and pain.[40] In future research it would be very interesting to analyze the effects of targeting angiogenesis, as now performed in the

NEO study, where neovascularization around the knee is embolized. Hypothetically this will reduce pain and synovitis.

Nuclear imaging techniques offer useful functional imaging tools to assess for the detection of inflammatory OA features and the prediction of progression of OA. It can be used for the detection of synovitis in patients with chronic knee pain.[41] Scintigraphy is a more sensitive method than physical examination in detecting histologically documented synovitis.[41–43] Using positron emission tomography (PET), 18F-FDG uptake in painful knees is significantly higher than in controls, and the SUVmax has also been demonstrated to be higher in patients with knee pain in the synovium in most cases.[44] The disadvantage of many nuclear techniques is that the findings are less specific for localized inflammation, as it provides an assessment of a larger area and there are multiple processes that can lead to increased radiotracer activity. For instance, FDG-PET reflects the glucose metabolism of target tissues, which is not only determined by inflammation. In addition, no accurate spatial correlation, or correlation with structural abnormalities can be obtained with most common nuclear techniques. It would be interesting to investigate the possibilities of the combination of nuclear imaging and MRI imaging to study inflammation in knee OA, which is now possible by means of the hybrid PET-MRI technique, which combines simultaneously acquired high resolution morphological information with functional information in a single examination.

REFERENCES

1. Scanzello CR, Loeser RF. Editorial: Inflammatory activity in symptomatic knee osteoarthritis: Not all inflammation is local. *Arthritis Rheumatol*. 2015;67(11):2797-2800. doi:10.1002/art.39304
2. Shabestari M, Vik J, Reseland JE, Eriksen EF. Bone marrow lesions in hip osteoarthritis are characterized by increased bone turnover and enhanced angiogenesis. *Osteoarthr Cartil*. 2016;24(10):1745-1752. doi:10.1016/j.joca.2016.05.009
3. Henrotin Y, Pesesse L, Lambert C. Targeting the synovial angiogenesis as a novel treatment approach to osteoarthritis. *Ther Adv Musculoskelet Dis*. 2014;6(1):20-34. doi:10.1177/1759720X13514669
4. Boesen M, Kubassova O, Bouert R, *et al.* Correlation between computer-aided dynamic gadolinium-enhanced MRI assessment of inflammation and semi-quantitative synovitis and bone marrow oedema scores of the wrist in patients with rheumatoid arthritis--a cohort study. *Rheumatol*. 2012;51(1):134-143. doi:10.1093/rheumatology/ker220
5. Axelsen MB, Stoltenberg M, Poggenborg RP, *et al.* Dynamic gadolinium-enhanced magnetic resonance imaging allows accurate assessment of the synovial inflammatory activity in rheumatoid arthritis knee joints: a comparison with synovial histology. *Scand J Rheumatol*. 2012;41(2):89-94. doi:10.3109/03009742.2011.608375
6. Boesen M, Kubassova O, Sudol-Szopinska I, *et al.* MR Imaging of Joint Infection and Inflammation with Emphasis on Dynamic Contrast-Enhanced MR Imaging. *PET Clin*. 2018;13(4):523-550. doi:10.1016/j.cpet.2018.05.007
7. Riis RG, Gudbergsen H, Henriksen M, *et al.* Synovitis assessed on static and dynamic contrast-enhanced magnetic resonance imaging and its association with pain in knee osteoarthritis: A cross-sectional study. *Eur J Radiol*. 2016;85(6):1099-1108. doi:10.1016/j.ejrad.2016.03.017
8. Riis RG, Gudbergsen H, Simonsen O, *et al.* The association between histological, macroscopic and magnetic resonance imaging assessed synovitis in end-stage knee osteoarthritis: a cross-sectional study. *Osteoarthr Cartil*. 2017;25(2):272-280. doi:10.1016/j.joca.2016.10.006
9. Ballegaard C, Riis RG, Bliddal H, *et al.* Knee pain and inflammation in the infrapatellar fat pad estimated by conventional and dynamic contrast-enhanced magnetic resonance imaging in obese patients with osteoarthritis: a cross-sectional study. *Osteoarthr Cartil*. 2014;22(7):933-940. doi:10.1016/j.joca.2014.04.018
10. Zwick S, Kopp-schneider A. Simulation-based comparison of two approaches frequently used for dynamic contrast-enhanced MRI. 2010:432-442. doi:10.1007/s00330-009-1556-6
11. Chikui T, Obara M, Simonetti AW, *et al.* The principal of dynamic contrast enhanced MRI, the method of pharmacokinetic analysis, and its application in the head and neck region. *Int J Dent*. 2012;2012. doi:10.1155/2012/480659
12. Eijkenboom JFA, Waarsing JH, Oei EHG, Bierma-Zeinstra SMA, van Middelkoop M. Is patellofemoral pain a precursor to osteoarthritis? *Bone Joint Res*. 2018. doi:10.1302/2046-3758.79.bjr-2018-0112.r1
13. Thomas MJ, Wood L, Selfe J, Peat G. Anterior knee pain in younger adults as a precursor to subsequent patellofemoral osteoarthritis: A systematic review. *BMC Musculoskelet Disord*. 2010. doi:10.1186/1471-2474-11-201
14. Budzik J-F, Ding J, Norberciak L, *et al.* Perfusion of subchondral bone marrow in knee osteoarthritis: A dynamic contrast-enhanced magnetic resonance imaging preliminary study. *Eur J Radiol*. 2017;88:129-134. doi:10.1016/j.ejrad.2016.12.023
15. Aaron RK, Racine JR, Voisinet A, Evangelista P, Dyke JP. Subchondral bone circulation in osteoarthritis of the human knee. *Osteoarthr Cartil*. May 2018. doi:10.1016/j.joca.2018.04.003

16. Poot DHJ, van der Heijden RA, van Middelkoop M, Oei EHG, Klein S. Dynamic contrast-enhanced MRI of the patellar bone: How to quantify perfusion. *J Magn Reson Imaging*. 2018;47(3):848-858. doi:10.1002/jmri.25817
17. K. S. DCE Tool. http://kyungs.bol.ucla.edu/software/DCE_tool/DCE_tool.html. Published 2015. Accessed May 23, 2018.
18. Sellam J, Berenbaum F. The role of synovitis in pathophysiology and clinical symptoms of osteoarthritis. *Nat Rev Rheumatol*. 2010;6(11):625-635. doi:10.1038/nrrheum.2010.159
19. Rushton MD, Reynard LN, Barter MJ, *et al.* Characterization of the cartilage DNA methylome in knee and hip osteoarthritis. *Arthritis Rheumatol*. 2014;66(9):2450-2460. doi:10.1002/art.38713
20. Hill CL, Hunter DJ, Niu J, *et al.* Synovitis detected on magnetic resonance imaging and its relation to pain and cartilage loss in knee osteoarthritis. *Ann Rheum Dis*. 2007;66(12):1599-1603. doi:10.1136/ard.2006.067470
21. Berenbaum F. Osteoarthritis as an inflammatory disease (osteoarthritis is not osteoarthrosis!). *Osteoarthr Cartil*. 2013;21(1):16-21. doi:10.1016/j.joca.2012.11.012
22. Song IH, Burmester GR, Backhaus M, *et al.* Knee osteoarthritis. Efficacy of a new method of contrast-enhanced musculoskeletal ultrasonography in detection of synovitis in patients with knee osteoarthritis in comparison with magnetic resonance imaging. *Ann Rheum Dis*. 2008;67(1):19-25. doi:10.1136/ard.2006.067462
23. Rednic N, Tamas M, Fodor D, *et al.* Contrast-Enhanced Ultrasound in Knee Joint Synovitis Measurement (Abstract). In: ESSR Congress; 2012. doi:10.1594/essr2012/P-0063
24. Guermazi A, Roemer FW, Hayashi D, *et al.* Assessment of synovitis with contrast-enhanced MRI using a whole-joint semiquantitative scoring system in people with, or at high risk of, knee osteoarthritis: the MOST study. *Ann Rheum Dis*. 2011;70(5):805-811. doi:10.1136/ard.2010.139618
25. Peterfy CG, Guermazi A, Zaim S, *et al.* Whole-Organ Magnetic Resonance Imaging Score (WORMS) of the knee in osteoarthritis. *Osteoarthr Cartil*. 2004;12(3):177-190. doi:10.1016/j.joca.2003.11.003
26. Kornaat PR, Ceulemans RYT, Kroon HM, *et al.* MRI assessment of knee osteoarthritis: Knee Osteoarthritis Scoring System (KOSS)--inter-observer and intra-observer reproducibility of a compartment-based scoring system. *Skeletal Radiol*. 2005;34(2):95-102. doi:10.1007/s00256-004-0828-0
27. Hunter DJ, Lo GH, Gale D, Grainger AJ, Guermazi A, Conaghan PG. The reliability of a new scoring system for knee osteoarthritis MRI and the validity of bone marrow lesion assessment: BLOKS (Boston Leeds Osteoarthritis Knee Score). *Ann Rheum Dis*. 2008;67(2):206-211. doi:10.1136/ard.2006.066183
28. Hunter DJ, Guermazi A, Lo GH, *et al.* Evolution of semi-quantitative whole joint assessment of knee OA: MOAKS (MRI Osteoarthritis Knee Score). *Osteoarthr Cartil*. 2011;19(8):990-1002. doi:10.1016/j.joca.2011.05.004
29. Parry EL, Thomas MJ, Peat G. Defining acute flares in knee osteoarthritis: a systematic review. *BMJ Open*. 2018;8(7):e019804. doi:10.1136/bmjopen-2017-019804
30. Liu L, Ishijima M, Futami I, *et al.* Correlation between synovitis detected on enhanced-magnetic resonance imaging and a histological analysis with a patient-oriented outcome measure for Japanese patients with end-stage knee osteoarthritis receiving joint replacement surgery. *Clin Rheumatol*. 2010;29(10):1185-1190. doi:10.1007/s10067-010-1522-3
31. Loeuille D, Chary-Valckenaere I, Champigneulle J, *et al.* Macroscopic and microscopic features of synovial membrane inflammation in the osteoarthritic knee: correlating magnetic resonance

imaging findings with disease severity. *Arthritis Rheum*. 2005;52(11):3492-3501. doi:10.1002/art.21373

32. De Lange-Brokaar BJE, Ioan-Facsinay A, Yusuf E, *et al.* Degree of synovitis on MRI by comprehensive whole knee semi-quantitative scoring method correlates with histologic and macroscopic features of synovial tissue inflammation in knee osteoarthritis. *Osteoarthr Cartil*. 2014;22(10):1606-1613. doi:10.1016/j.joca.2013.12.013
33. Fernandez-Madrid F, Karvonen RL, Teitge RA, Miller PR, An T, Negendank WG. Synovial thickening detected by MR imaging in osteoarthritis of the knee confirmed by biopsy as synovitis. *Magn Reson Imaging*. 1995;13(2):177-183. doi:10.1016/0730-725x(94)00119-n
34. Loeuille D, Sauliere N, Champigneulle J, Rat AC, Blum A, Chary-Valckenaere I. Comparing non-enhanced and enhanced sequences in the assessment of effusion and synovitis in knee OA: Associations with clinical, macroscopic and microscopic features. *Osteoarthr Cartil*. 2011;19(12):1433-1439. doi:10.1016/j.joca.2011.08.010
35. Takase K, Ohno S, Takeno M, *et al.* Simultaneous evaluation of long-lasting knee synovitis in patients undergoing arthroplasty by power Doppler ultrasonography and contrast-enhanced MRI in comparison with histopathology. *Clin Exp Rheumatol*. 30(1):85-92. http://www.ncbi.nlm.nih.gov/pubmed/22325923.
36. Loeuille D, Rat A-C, Goebel J-C, *et al.* Magnetic resonance imaging in osteoarthritis: which method best reflects synovial membrane inflammation? Correlations with clinical, macroscopic and microscopic features. *Osteoarthr Cartil*. 2009;17(9):1186-1192. doi:10.1016/j.joca.2009.03.006
37. Schmidt WA, Völker L, Zacher J, Schläfke M, Ruhnke M, Gromnica-Ihle E. Colour Doppler ultrasonography to detect pannus in knee joint synovitis. *Clin Exp Rheumatol*. 18(4):439-444. http://www.ncbi.nlm.nih.gov/pubmed/10949717.
38. Philp AM, Davis ET, Jones SW. Developing anti-inflammatory therapeutics for patients with osteoarthritis. *Rheumatology (Oxford)*. 2017;56(6):869-881. doi:10.1093/rheumatology/kew278
39. Saranathan M, Rettmann DW, Hargreaves BA, Clarke SE, Vasanawala SS. DIfferential subsampling with cartesian ordering (DISCO): A high spatio-temporal resolution dixon imaging sequence for multiphasic contrast enhanced abdominal imaging. *J Magn Reson Imaging*. 2012;35(6):1484-1492. doi:10.1002/jmri.23602
40. Ashraf S, Mapp PI, Walsh DA. Contributions of angiogenesis to inflammation, joint damage, and pain in a rat model of osteoarthritis. *Arthritis Rheum*. 2011;63(9):2700-2710. doi:10.1002/art.30422
41. Collier BD, Johnson RP, Carrera GF, *et al.* Chronic knee pain assessed by SPECT: comparison with other modalities. *Radiology*. 1985;157(3):795-802. doi:10.1148/radiology.157.3.3877315
42. de Bois MH, Arndt JW, van der Velde EA, Pauwels EK, Breedveld FC. Joint scintigraphy for quantification of synovitis with 99mTc-labelled human immunoglobulin G compared to late phase scintigraphy with 99mTc-labelled diphosphonate. *Br J Rheumatol*. 1994;33(1):67-73. doi:10.1093/rheumatology/33.1.67
43. de Bois MH, Tak PP, Arndt JW, Kluin PM, Pauwels EK, Breedveld FC. Joint scintigraphy for quantification of synovitis with 99mTc-labelled human immunoglobulin G compared to histological examination. *Clin Exp Rheumatol*. 13(2):155-159. http://www.ncbi.nlm.nih.gov/pubmed/7656461.
44. Parsons MA, Moghbel M, Saboury B, *et al.* Increased 18F-FDG uptake suggests synovial inflammatory reaction with osteoarthritis: preliminary in-vivo results in humans. *Nucl Med Commun*. 2015;36(12):1215-1219. doi:10.1097/MNM.0000000000000376

APPENDICES

APPENDIX

SUMMARY

Knee osteoarthritis (OA) is a complex, whole organ disease with significant disability for patients. To date, the only effective treatment for knee OA is knee arthroplasty. The number of patients with knee OA is likely to increase in the future due to the increasing life expectancy. It is therefore important to understand the pathophysiology of knee OA and to optimize ways to diagnose the disease in an early stage. In this way, early diagnosis could further enable new therapies to counteract OA. This thesis focused on two main research topics; 1) the assessment of quantitative perfusion parameters within different tissues of the knee, and 2) the evaluation of the diagnostic accuracy of imaging techniques for visualization of synovitis in the knee.

QUANTITATIVE MRI PERFUSION PARAMETERS WITHIN DIFFERENT TISSUES OF THE KNEE

Nowadays knee OA is seen as a whole joint disease, in which beside cartilage also (subchondral) bone, synovium, menisci and the infrapatellar fat pad (IPFP) are affected. Changes in subchondral bone could be a marker of altered fluid dynamics, which is thought to affect the excretion of cytokines that regulate and accelerate bone remodeling and cartilage degeneration. In order to compare the perfusion in osteoarthritic bone with the surrounding bone, perfusion parameters within the subchondral bone were measured using quantitative dynamic contrast-enhanced (DCE) MRI in patients with unicompartmental knee OA in **Chapter 2**. The DCE parameters Ktrans and Kep, representing perfusion, of both epimetaphyseal and subchondral bone were significantly higher in the most affected compared to the least affect compartment. In addition, subchondral bone marrow lesions (BMLs) were associated with higher Ktrans and Kep compared to subchondral bone regions without BMLs. The conclusion of this chapter was that BMLs likely account for most of the effect of the higher bone perfusion in knee OA.

Patellofemoral pain (PFP) is a common knee condition and possible precursor of knee osteoarthritis. Inflammation or increased volume of the IPFP may induce knee pain. DCE-MRI perfusion parameters can be used as surrogate measure of inflammation. In **Chapter 3**, kinetic DCE-MRI parameters within the whole IPFP were evaluated in PFP patients and healthy controls. It was assessed if there is a relation between the volume of the IPFP compared to the DCE-MRI perfusion parameters. We also looked at two other parameters, edema in the IPFP and the amount of joint effusion. We concluded that DCE-MRI perfusion parameters and larger volumes of the IPFP were not associated with PFP, but patient's knees with effusion showed higher perfusion, pointing towards inflammation.

In **Chapter 4,** quantitative blood perfusion parameters within $T2_{FS}$-hyperintense regions in the IPFP, based on DCE-MRI, were evaluated between patients with OA, patients with PFP, and control subjects. $T2_{FS}$-hyperintense regions of the IPFP demonstrated higher quantitative DCE-MRI blood perfusion parameters compared to adjacent tissue with normal signal intensity in patients with knee OA. However, no such difference was observed between patients with PFP and healthy control subjects. This suggests different pathophysiology of IPFP $T2_{FS}$-hyperintense regions across patient subgroups, in which an inflammatory pathogenesis is only present in OA.

DIAGNOSTIC ACCURACY OF IMAGING TECHNIQUES FOR VISUALIZATION OF SYNOVITIS IN KNEE OSTEOARTHRITIS

Joint inflammation, characterized by swelling of the synovium and joint effusion, is a key process in knee OA. The accepted reference standard for visualizing synovitis is MRI after intravenous administration of a contrast agent, also referred to as contrast-enhanced MRI (CE-MRI).

Despite the many advantages of MRI for a comprehensive evaluation of the osteoarthritic joint, ultrasound (US) is a suitable alternative to image the soft tissues of the knee. With the most commonly used US-method, grayscale ultrasound (GSUS), it is difficult to differentiate synovium from joint fluid. Other US-methods could be more suitable for this purpose, for example power Doppler ultrasound (PDUS) to visualize the extent of vascularization, which is expected to be increased in synovitis. In addition, contrast-enhanced ultrasound (CEUS) can be used, a relatively novel tool for imaging synovitis. CEUS uses contrast agents composed of microbubbles that allow assessment of perfusion, based on enhanced ultrasound reflections in tissues where blood flow is increased. In **Chapter 5**, CE-MRI was compared with GSUS, PDUS, and CEUS for the visualization of synovitis in knee OA. This study demonstrated that, even under optimized conditions, the combination of GSUS, PDUS, and CEUS shows only limited overall diagnostic accuracy for the assessment of synovitis compared to CE-MRI as the golden standard. Of the evaluated US-methods, GSUS showed the highest overall diagnostic performance. Combining US methods resulted in slightly higher performance in diagnosing moderate or higher degree of synovitis. From a practical perspective, GSUS is most feasibly combined with PDUS, whereas CEUS is less likely to be useful in most clinical practices due to the required contrast agent.

Dual echo steady state (DESS) MRI is an increasingly applied technique in the diagnosis of knee OA, but little is known about DESS used for synovitis scoring. With a modified DESS sequence, rapid diffusion weighted imaging can be performed to acquire two diffusion im-

ages to improve synovitis visualization, referred to as quantitative DESS (qDESS) MRI. A linear combination of the two qDESS images can be used to create an image that displays contrast between synovium and the synovial fluid. Therefore, qDESS does not require contrast agents, and it has a higher resolution than conventional diffusion weighted techniques. In **Chapter 6**, synovitis severity as detected on both CE-MRI and a qDESS sequence were compared. qDESS MRI showed to be accurate in detecting synovitis in patients with knee OA compared to CE-MRI, however with an underestimation of severity. In addition, the qDESS images can differentiate between the synovial membrane and joint effusion, with high diagnostic accuracy for mild and moderate synovitis. As qDESS does not need a contrast agent, this method could be a valuable addition to the existing MRI techniques.

CONCLUSION

In **Chapter 7**, the main findings and future perspectives are discussed. Concluding, it can be said that this thesis contributes to the knowledge of perfusion imaging in patients with knee OA. Perfusion in various joint tissues involved in OA can be quantified using both conventional contrast-enhanced MRI and with a novel, non-contrast-enhanced, MRI sequence. On this novel qDESS MRI sequence, synovitis can be diagnosed. Significant differences in inflammatory changes, assessed with advanced imaging techniques, were observed between patients with and without knee OA. The clinical implications of these findings should be investigated in future studies.

APPENDIX

SAMENVATTING

Knieartrose is een complexe ziekte, die het gehele orgaan aangaat. De ziekte heeft een zeer grote impact voor patiënten. Tot op heden is knieartroplastiek de enige effectieve behandeling voor knieartrose. Het aantal patiënten met knieartrose zal in de toekomst waarschijnlijk toenemen als gevolg van de toenemende levensverwachting. Het is daarom belangrijk om de pathofysiologie van knieartrose te begrijpen en om methoden te optimaliseren die de ziekte in een vroeg stadium kunnen diagnosticeren. Op deze manier kan een vroege diagnose nieuwe therapieën mogelijk maken om artrose tegen te gaan. Dit proefschrift richtte zich op twee belangrijke onderzoeksthema's; 1) de beoordeling van kwantitatieve perfusieparameters binnen verschillende weefsels van de knie, en 2) de evaluatie van de diagnostische nauwkeurigheid van beeldvormende technieken voor visualisatie van synovitis in de knie.

KWANTITATIEVE MRI PERFUSIEPARAMETERS BINNEN VERSCHILLENDE WEEFSELS VAN DE KNIE

Tegenwoordig wordt knieartrose gezien als een aandoening van het gehele gewricht, waarbij naast kraakbeen ook (subchondraal) bot, synovium, menisci en het infrapatellaire vetkussen (IPFP) worden aangetast. Veranderingen in het subchondrale bot zouden een marker kunnen zijn van veranderde vloeistofdynamica, waarvan wordt aangenomen dat het de uitscheiding van cytokines beïnvloedt die botremodellering en kraakbeendegeneratie reguleren en versnellen. Om de perfusie in artrotisch bot te vergelijken met het omliggende bot, werden de perfusieparameters in het subchondrale bot gemeten met behulp van kwantitatieve dynamische contrast-enhanced (DCE) MRI bij patiënten met unicompartimentele knieartrose in **Hoofdstuk 2**. De DCE-parameters Ktrans en Kep, welke perfusie meten van zowel epimetafysair als subchondraal bot, waren significant hoger in het meest aangetaste compartiment in vergelijking met het minst aangetaste compartiment. Bovendien waren subchondrale beenmerglaesies (BML's) geassocieerd met hogere Ktrans en Kep vergeleken met subchondrale gebieden zonder BML's. De conclusie van dit hoofdstuk was dat BMLs waarschijnlijk verantwoordelijk zijn voor het grootste deel van de hogere botperfusie bij knieartrose.

Patellofemoraal pijnsyndroom (PFP) is een veel voorkomende knieaandoening en mogelijke voorloper van artrose in de knie. Ontsteking of toegenomen volume van de IPFP kan kniepijn veroorzaken. DCE-MRI perfusieparameters kunnen worden gebruikt als surrogaat maatstaf voor de ontsteking. In **Hoofdstuk 3** werden kinetische DCE-MRI-parameters binnen de gehele IPFP geëvalueerd bij PFP-patiënten en gezonde controles. Er werd beoordeeld of er een verband bestaat tussen het volume van de IPFP in vergelijking met de DCE-MRI perfusieparameters. We keken ook naar twee andere parameters, oedeem in de IPFP en de hoeveelheid gewrichtseffusie. We concludeerden dat DCE-MRI perfusieparameters en

grotere volumes van de IPFP niet geassocieerd waren met PFP, maar de knieën van patiënten met effusie vertoonden een hogere perfusie, wat duidt op een ontsteking.

In **Hoofdstuk 4** werden kwantitatieve DCE-MRI bloedperfusieparameters, binnen $T2_{FS}$-hyperintense regio's in de IPFP, geëvalueerd tussen patiënten met artrose, patiënten met PFP en gezonde controle patiënten. $T2_{FS}$-hyperintense regio's van de IPFP vertoonden hogere kwantitatieve DCE-MRI bloedperfusieparameters in vergelijking met aangrenzend weefsel met normale signaalintensiteit bij patiënten met knieartrose. Een dergelijk verschil werd echter niet waargenomen tussen patiënten met PFP en gezonde controles. Dit suggereert verschillende pathofysiologieën van de IPFP $T2_{FS}$-hyperintense regio's in subgroepen van patiënten, waarin de inflammatoire pathogenese alleen aanwezig is in artrose.

DIAGNOSTISCHE NAUWKEURIGHEID VAN BEELDTECHNIEKEN VOOR VISUALISATIE VAN SYNOVITIS IN KNIEARTROSE

Gewrichtsontsteking, gekenmerkt door zwelling van het synovium en gewrichtseffusie, is een sleutelproces bij knieartrose. De geaccepteerde referentiestandaard voor het visualiseren van synovitis is MRI na intraveneuze toediening van een contrastmiddel, ook wel contrast-enhanced MRI (CE-MRI) genoemd.

Ondanks de vele voordelen van MRI voor een uitgebreide evaluatie van het artrotisch gewricht, is echografie een geschikt alternatief om het zachte weefsel van de knie in beeld te brengen. Met de meest gebruikte echo methode, grayscale-echografie (GSUS), is het moeilijk om het synoviale weefsel te onderscheiden van gewrichtsvloeistof. Andere echo methoden zouden voor dit doel beter geschikt kunnen zijn, bijvoorbeeld power Doppler-echografie (PDUS) om de mate van vascularisatie te visualiseren, die naar verwachting zal toenemen bij synovitis. Daarnaast kan ook nog contrast-enhanced echografie (CEUS) worden gebruikt, een relatief nieuwe methode voor beeldvorming van synovitis. CEUS maakt gebruik van een contrastmiddel dat is samengesteld uit microbubbels waarmee de doorbloeding kan worden gevisualiseerd, dit contrastmiddel werkt doordat de bubbels verbeterde ultrasone geluidsreflecties geven in weefsels waar de bloedstroom hoog is. In **Hoofdstuk 5** werd CE-MRI vergeleken met GSUS, PDUS en CEUS voor de visualisatie van synovitis bij knieartrose. Deze studie toonde aan dat, zelfs onder geoptimaliseerde omstandigheden, de combinatie van GSUS, PDUS en CEUS slechts een beperkte diagnostische nauwkeurigheid vertoont voor de beoordeling van synovitis in vergelijking met CE-MRI als de referentiestandaard. Van de geëvalueerde echo methoden vertoonde GSUS de hoogste algemene diagnostische prestaties. Het combineren van echo methoden resulteerde in iets betere prestaties bij het diagnosticeren van ten minste matige óf hogere mate van synovitis. Vanuit praktisch oog-

punt is GSUS het meest haalbaar in combinatie met PDUS, terwijl CEUS minder waarschijnlijk gebruikt kan worden in de meeste klinische praktijken, vanwege het vereiste contrastmiddel.

Dual echo steady state (DESS) MRI is een steeds meer toegepaste techniek bij de diagnose van knieartrose, maar er is weinig bekend over DESS welke wordt gebruikt voor het scoren van synovitis. Met een gemodificeerde DESS-sequentie kan snelle diffusie-gewogen beeldvorming worden uitgevoerd. Hiermee worden twee diffusiebeelden verkregen om de visualisatie van synovitis te verbeteren, ook wel kwantitatieve DESS (qDESS) MRI genoemd. Een lineaire combinatie van de twee qDESS-afbeeldingen kan worden gebruikt om een afbeelding te maken die contrast weergeeft tussen het synovium en de synoviale vloeistof. qDESS heeft daarom geen contrastmiddelen nodig en heeft ook een hogere resolutie dan conventionele diffusie-gewogen technieken. In **Hoofdstuk 6** werd de ernst van synovitis vergeleken, zoals gedetecteerd op zowel CE-MRI als met een qDESS sequentie. qDESS MRI bleek accuraat te zijn in het detecteren van synovitis bij patiënten met knieartrose in vergelijking met CE-MRI, maar met een onderschatting van de ernst ervan. Bovendien kunnen de qDESS-afbeeldingen onderscheid maken tussen het synoviale membraan en de synoviale vloeistof, met een hoge diagnostische nauwkeurigheid voor milde en matige synovitis. Omdat qDESS geen contrastmiddel nodig heeft, kan deze methode een waardevolle aanvulling zijn op de bestaande MRI-technieken.

CONCLUSIE

In **Hoofdstuk 7**, worden de belangrijkste bevindingen en de toekomstperspectieven bediscussieerd. Concluderend kan gezegd worden dat dit proefschrift bijdraagt aan de kennis van perfusiebeeldvorming in patiënten met knieartrose. Perfusie in verschillende gewrichtsweefsels die bij artrose zijn betrokken, kan worden gekwantificeerd met behulp van zowel DCE-MRI als met een nieuwe sequentie, welke geen contrast nodig heeft. Met deze nieuwe MRI-sequentie, qDESS, kan synovitis ook worden gediagnosticeerd. Significante verschillen in ontstekingsveranderingen, beoordeeld met geavanceerde beeldvormende technieken, werden waargenomen tussen patiënten met en zonder knieartrose. De klinische implicaties van deze bevindingen zullen in toekomstige studies nog moeten worden onderzocht.

APPENDIX

LIST OF ABBREVIATIONS

3D	Three-dimensional
95% CI	95% confidence interval
AIF	Arterial input function
AUC	Area under the curve
BMI	Body mass index
BML	Bone marrow lesion
CE	Contrast-enhanced
CEUS	Contrast-enhanced ultrasound
CI	Confidence interval
DCE-MRI	Dynamic contrast-enhanced MRI
DIR	Double inversion recovery
DTI	Diffusion Tensor Imaging
EES	Extracellular extravascular space
EPG	Extended phase graph
FA	Fractional anisotropy
FLAIR	Fluid attenuation inversion recovery
FOV	Field-of-view
FSE	Fast spin echo
FSPGR	Fast spoiled gradient echo
GFR	Glomerular filtration rate
GSUS	Grayscale ultrasound
IPFP	Infrapatellar fat pad or Hoffa's fat pad
IQR	Interquartile range
Kep	Rate constant from the EES to the vascular component
KL	Kellgren & Lawrence grading system
KOOS	Knee injury and Osteoarthritis Outcome Score
Ktrans	Volume transfer constant
MOAKS	MRI Osteoarthritis Knee Score
MRI	Magnetic resonance imaging
NPV	Negative predictive value
NRS	Numerical rating score
OA	Osteoarthritis
PDUS	Power Doppler ultrasound
PFP	Patellofemoral pain
PPV	Positive predictive value
qDESS	Quantitative double-echo in steady-state
ROC	Receiver operating characteristic
ROI	Region of Interest
SPGR	Spoiled gradient-echo sequence

SD	Standard deviation
3T	3 Tesla
TR	Repetition time
VAS	Visual analog scale
VOI	Volume of interest

APPENDIX

PHD PORTFOLIO

Name PhD student: B.A. de Vries
Erasmus MC Department: Radiology & Nuclear Medicine
PhD period: 01-04-2016 – 31-12-2019
Promotor: Prof. dr. G.P. Krestin
Daily supervisor: Dr. E.H.G. Oei

General courses and workshops	Year	Workload (ECTS)
– Basiscursus Regelgeving en Organisatie voor Klinisch onderzoekers (NFU)	2015	2
– MRI Scannen in de Praktijk	2016	0.5
– School of MRI 2016: eLearning (ESMRMB)	2016	2
– PhD-day 2017	2017	0.5
– Introduction to data analysis (NIHES)	2016	1.9
– GE Gebruikersdag Echografie	2017	0.5
– Principles of Research in Medicine and Epidemiology (NIHES)	2017	0.7
– Research Integrity	2017	0.3
– CC02AB - Biostatistical Methods I: basic principles (NIHES)	2018	5.7
– Radiologie & Nucleaire Geneeskunde … het heden en de toekomst (symposium)	2018	0.5
– (Bi)weekly ADMIRE research meetings	2016-2019	5
– Personal Leadership	2019	0.3
– Employability outside academia course (PCDI)	2019	2
– Imaging Research on the Move meetings (Radiology & Nuclear Imaging department, Erasmus MC)	2017-2019	2
– Biomedical English Writing and Communication	2019	3

(Inter)national conferences	Year	Workload (ECTS)
– Technical Innovations in Medicine congress (NvvTG)	2016	0.5
– Symposium Quantification in Medical and Preclinical Imaging: state of the art and future developments (UMCG)	2016	2
– Technical Innovations in Medicine congress – Care to create opportunities (NvvTG)	2018	0.5
– Technical Innovations in Medicine congress (NvvTG)	2019	0.5

(Inter)national oral presentations	Year	Workload (ECTS)
– Nordic Cartilage Imaging Meeting, Båstad (Zweden)	2017	2
– European Congress of Radiology, Vienna (Austria)	2018	2
– Annual Meeting of the Radiological Society of North America, Chicago (USA)	2018	3
– Annual Scientific Meeting of the European Society for Magnetic Resonance in Medicine and Biology, Rotterdam (Netherlands)	2019	2

(Inter)national poster presentations	Year	Workload (ECTS)
– Annual Scientific Meeting of the International Society for Magnetic Resonance in Medicine, Paris (France)	2018	2

Teaching activities	Year	Workload (ECTS)
– Lecturing clinical technology students	2018	1
– MRI scan training of fellow PhD Students	2017-2019	1
– Ultrasound hands on course medical students	2019	0.5
– MRI course medical students	2019	0.5
Total	**Total workload (ECTS)**	**44.4**

APPENDIX

LIST OF PUBLICATIONS

This thesis:

Quantitative subchondral bone perfusion imaging in knee osteoarthritis using dynamic contrast-enhanced MRI. **B.A. de Vries**, R.A. van der Heijden, J. Verschueren, P.K. Bos, D.H.J. Poot, J. van Tiel, G. Kotek, G.P. Krestin, E.H.G Oei. *Seminars in Arthritis and Rheumatism* 2020 April; 50(2):177-182. https://doi.org/10.1016/j.semarthrit.2019.07.013

Quantitative volume and dynamic contrast-enhanced MRI derived perfusion of the infrapatellar fat pad in patellofemoral pain. **B.A. de Vries***, R.A. van der Heijden*, D.H.J. Poot, M. van Middelkoop, S.M.A. Bierma-Zeinstra, G.P. Krestin, E.H.G Oei. (*shared first authorship). *Quantitative Imaging in Medicine and Surgery* 2021 January; 11(1):133-142. https://doi.org/10.21037/qims-20-441

Quantitative DCE-MRI demonstrates increased blood perfusion in Hoffa's fat pad signal abnormalities in knee osteoarthritis, but not in patellofemoral pain. **B.A. de Vries***, R.A. van der Heijden*, D.H.J. Poot, M. van Middelkoop, D.E. Meuffels, G.P. Krestin, E.H.G Oei. (*shared first authorship). *European Radiology* 2020 June; 30(6):3401-3408. https://doi.org/10.1007/s00330-020-06671-6

Diagnostic accuracy of grayscale, power Doppler and contrast-enhanced ultrasound compared with contrast-enhanced MRI in the visualization of synovitis in knee osteoarthritis. **B.A. de Vries**, S.J. Breda, D.E. Meuffels, D.F. Hanff, M.G.M Hunink, G.P. Krestin, E.H.G. Oei. *European Journal of Radiology* 2020 December; 133. https://doi.org/10.1016/j.ejrad.2020.109392

Detection of knee synovitis using non-contrast-enhanced qDESS compared with contrast-enhanced MRI. **B.A. de Vries**, S.J. Breda, B. Sveinsson, E.J. McWalter, D.E. Meuffels, G.P. Krestin, B.A. Hargreaves, G.E. Gold, E.H.G. Oei. *Arthritis Research & Therapy* 2021 February; 23(55). https://doi.org/10.1186/s13075-021-02436-8

Other:

Tissue-Specific T2* Biomarkers in Patellar Tendinopathy by Subregional Quantification using 3D Ultra-short Echo Time MRI. S.J. Breda, D.H.J. Poot, D. Papp, **B.A. de Vries**, G. Kotek, G.P. Krestin, J.A. Hernandéz-Tamames, R.J. de Vos, E.H.G. Oei. *Journal of Magnetic Resonance Imaging* 2020 Feb; 52(2):420–430. https://doi.org/10.1002/jmri.27108

Validation of a New Methodology to Determine 3-Dimensional Endograft Apposition, Position, and Expansion in the Aortic Neck After Endovascular Aneurysm Repair. R.C.L. Schuurmann, S.P. Overeem, K van Noort, **B.A. de Vries**, C.H. Slump, J.P.M. de Vries. *Journal Endovascular Theraphy* 2018 June; 25(3):358-365. https://doi.org/10.1177/1526602818764413

URIKA, continuous ultrasound monitoring for the detection of a full bladder in children with dysfunctional voiding: a feasibility study. P.G. van Leuteren, **B.A. de Vries**, G.C.J. de Joode-Smink, B. ten Haken, T.P.V.M. de Jong, P. Dik. *Biomedical Physics & Engineering Express* 2017 February; 3(1). https://doi.org/10.1088/2057-1976/aa589f

APPENDIX

DANKWOORD

Het dankwoord, een leuk en belangrijk deel van dit proefschrift. Op het moment van schrijven ben ik erg enthousiast dat ik hier nu de mensen mag bedanken voor al hun bijdragen, want zoals vele weten, promoveren doe je niet alleen!

Ten eerste wil ik alle patiënten bedanken die het voor mij mogelijk hebben gemaakt om het onderzoek uit te kunnen voeren binnen het Erasmus MC.

Prof. dr. Gabriel Krestin. Geachte prof. Krestin, uw supervisie en sturing hebben het proefschrift gemaakt tot wat het nu is.

Mijn co-promotor dr. Edwin Oei. Beste Edwin, ontzettend bedankt voor al je hulp en inspiratie, je betrokkenheid bij onze onderzoeken de afgelopen jaren, en jouw waardevolle input bij manuscripten.

Geachte leden van de leescommissie, prof. dr. G. Kloppenburg, prof. dr. J.A.N. Verhaar, dr. ir. T. van Walsum, uiteraard is mijn dank aan jullie groot. Bedankt dat jullie de tijd en moeite hebben genomen om mijn proefschrift kritisch onder de loep te nemen. Ook de overige commissieleden, hartelijk dank dat jullie wilden plaatsnemen in mijn commissie. Ik kijk ernaar uit om met jullie van gedachten te kunnen wisselen over dit proefschrift.

Natuurlijk niet te vergeten zijn mijn paranimfen, mijn lieve kamergenootjes, Stephan en Desiree. Desiree, je kwam een jaartje later de onderzoeksgroep binnen. Eigenlijk al vanaf het begin was je betrokken. We hebben een super leuke tijd gehad, met een aantal hele mooie dagen in Chicago. Stephan, maatje, waar moet ik beginnen. Wat heb ik ontzettend veel steun aan jou gehad, een PhD kent pieken en dalen. Beide heb ik met jou kunnen delen. En wat een super toffe tijden hebben we samen meegemaakt op kantoor, in Wenen, in ons veel te luxe appartement in Chicago, en natuurlijk ook met de kerstfeesten. Je bent zelfs gaan motorrijden, met een gezamenlijke trip naar de Eifel als resultaat.

Radiologie staf, secretaresses, bedankt. Laboranten Radiologie, ontzettend bedankt voor al jullie hulp en ideeën tijdens het scannen met de MRI.

Duncan en Max, dank voor de inspiratie en de hulp bij de DISKO studie! Orthopedie staf, aios, onderzoeksmedewerkers, en secretaresses, dank voor alle hulp en input voor de DISKO studie. Ook wil ik Pieter Bakx in het Maasstad ziekenhuis bedanken voor de samenwerking.

I want to thank the people from the BIGR group, Dirk, Stefan, but also, Piotr, Paul, and Juan from the MR physics group, for all your help and support. Ghassan, thanks for our enjoyable moments at the office!

Sita, Myriam, bedankt voor jullie hulp en input bij de studies die we gedaan hebben. Erik, Nicole en Niamh, dank voor al jullie hulp in het lab en voor het analyseren van de bloedmonsters en het synovium weefsel. Yvonne, dank voor je hulp en input bij de lab-projecten. Gerjo, dank voor de mogelijkheid om onderzoek te kunnen doen in het lab en voor uw waardevolle input bij projecten.

Kantoorbuurtjes van NA-25 en NA-26, Dianne, Fatih, Nikki, bedankt voor jullie gezelligheid en luisterend oor. We konden altijd even binnenkomen voor een leuk gesprek of een bakkie. Kars, bedankt voor super gezellige tijd, avonturen, ballentent etentjes, Wenen en feestjes. Die feestjes zorgden altijd voor mooie tijden, aansluitend met wilde fietstochten/valpartijen op de Erasmusbrug.

Susanne, dank voor al je hulp, en bedankt voor de gezelligheid tijdens de radiologie parties en leuke tijden in Wenen. Rianne, bedankt voor je hulp en input en interesse. Samen hebben we leuke onderzoeken uitgedacht en opgeschreven. Andere collega's van de Admire groep, Fjorda, Jukka, Marleen, Tijmen, Tong, Joost, Jasper, dank voor al jullie input tijdens de meetings en daarbuiten en alle gezelligheid.

Natuurlijk wil ik iedereen van het Trialbureau radiologie ontzettend bedanken voor al jullie hulp met het opzetten en het doorlopen van de DISKO studie.

Dear colleges from the US, Garry, Brian, Bragi and Emily, thank you for sharing your valuable knowledge and experience. It was an honor to work with you all. Unfortunately, I have not been able to meet you in person. However, I would like to thank you for your willingness to provide data and feedback whenever needed.

Dear Masimo colleagues, from the first day I started working at Masimo, you all have been supportive to finish my PhD. It is a pleasure working with you. Thank you!

Pieter Dik, nogmaals dank voor het begeleiden en hulp bij mijn master thesis, jouw enthousiasme heeft er mede voor gezorgd dat ik met onderzoek ben doorgegaan.

Ook vrienden hebben in deze tijd een belangrijke rol gespeeld. Onno, ik mis zo nu en dan onze gesprekken die we vroeger, toen we nog naast elkaar woonden, met elkaar hadden op de schommels. Met jou kan ik alles delen, positieve en negatieve dingen. Ook onze vele game avondjes hebben mij goed gedaan! Dennis, tof dat we nog steeds contact hebben. Samen eten, borrelen en ook vele filosofische gedachten en levensgesprekken zijn voorbij gekomen. Thanks daarvoor! Hanneke, ik ben super dankbaar dat ik jou al zo lang ken, je bent een super waardevolle vriendin! Berend en Merlijn, ik ben erg blij met jullie als buurtjes,

heel erg bedankt voor je hulp in de periode dat ik op zoek was naar een volgende baan. Klim/boulder groep, onze Bleau weekendjes waren onvergetelijk! En natuurlijk de rest van de vrienden plus partners, bedankt voor jullie steun en begrip!

Eric, Ellen en Julien, jullie steunden niet alleen Daphne, maar ook mij met alle liefde in de afgelopen jaren. Met onze gezamenlijke vakanties konden we even alles loslaten en genieten.

Mam, bedankt voor je onvoorwaardelijke steun en liefde, jij had er altijd vertrouwen in, vertelde mij vaak dat ik gewoon moest doorzetten. Hugo, dank voor je interesse en je hulp, ook onze gezamenlijke vakanties zorgden voor ontspanning tijdens de PhD periode. Jan, lieve papa, wat mis ik jou! Zeker op dit soort momenten, die ik graag met je had willen delen. Mijn keuzes die ik gemaakt heb de afgelopen jaren, om technische geneeskunde te gaan studeren en daarna ook nog een promotietraject te starten. Met jouw PhD en je biologie opleiding wist je wat dat betekende, ik hoop dat je trots naar beneden kijkt.

Daphne, lieffie, jij hebt onlangs zelf ook je PhD afgerond. Ik ben super trots op je! We weten beiden uit ervaring wat het betekent om dit traject te doorlopen. Ik ben heel erg blij dat jij mij hebt kunnen steunen tijdens dit traject, je voelde goed aan wat ik nodig had en samen kunnen wij de wereld aan. Zonder jou was dit nooit gelukt, wat ben ik blij dat ik je ken! Dit jaar is ons jaar, ik zie uit naar onze dag en onze volgende reisjes die we hopelijk snel weer kunnen maken.

APPENDIX

ABOUT THE AUTHOR

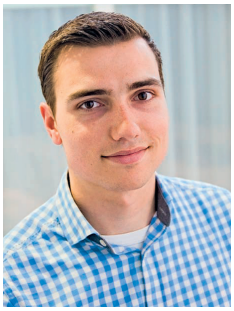

Bastiaan Alexander de Vries was born on February 21st, 1991 in Haarlem, the Netherlands. In 2009, Bas graduated from high school at the Atheneum College Hageveld in Heemstede. In that same year, he started studying Technical Medicine at the University of Twente in Enschede. After graduating for his bachelor's degree, he paused his studies to travel in South-East-Asia and India for five months.

After that, he continued his studies with the Technical Medicine master's program Medical Imaging and Interventions. In the second year of the master's study, he performed multiple internships. During these internships he worked on software to calculate 3D surface areas of the aorta before stent placement, adaptive radiotherapy in the pelvic region, flow displacement artefacts on 7T MRI, and renal microstructure visualization using MR diffusion tensor imaging.

The goal of his graduation internship was to find a technical solution to alarm patients with urinary incontinence and urinary retention, when they have a full bladder and need to void. This research was performed at the Pediatric Urology department in the University Medical Center in Utrecht. After successfully finishing his master's, he started his PhD research at the department of Radiology & Nuclear Medicine in the Erasmus Medical Center in Rotterdam, which resulted in this thesis.

Since October 2020, he works at Masimo, a global medical technology company that develops and manufactures innovative noninvasive patient monitoring technologies. At Masimo, he works as a Clinical Support Specialist in a technical clinical team, and supports clinicians with a technical perspective. Bas lives in Haarlem, together with Daphne.